

Textile Technology for Soft Robotic and Autonomous Garments

Vanessa Sanchez,* Conor J. Walsh, and Robert J. Wood

Textiles have emerged as a promising class of materials for developing wearable robots that move and feel like everyday clothing. Textiles represent a favorable material platform for wearable robots due to their flexibility, low weight, breathability, and soft hand-feel. Textiles also offer a unique level of programmability because of their inherent hierarchical nature, enabling researchers to modify and tune properties at several interdependent material scales. With these advantages and capabilities in mind, roboticists have begun to use textiles, not simply as substrates, but as functional components that program actuation and sensing. In parallel, materials scientists are developing new materials that respond to thermal, electrical, and hygroscopic stimuli by leveraging textile structures for function. Although textiles are one of humankind's oldest technologies, materials scientists and roboticists are just beginning to tap into their potential. This review provides a textile-centric survey of the current state of the art in wearable robotic garments and highlights metrics that will guide materials development. Recent advances in textile materials for robotic components (i.e., as sensors, actuators, and integration components) are described with a focus on how these materials and technologies set the stage for wearable robots programmed at the material level.

1. Introduction

We spend most of our lives in direct contact with textiles, whether in the form of clothing, bed sheets, pillows, bandages, reusable bags, or even face masks used to prevent the spread of disease. Recently, the field of robotics has begun to adopt textiles as materials of choice for wearable robots and devices because of many of the advantages textiles exhibit in these everyday applications. For example, compared to the rigid metals, composites, and plastics used in wearable robotic exoskeletons, textiles—and in turn, robotic garments constructed from them—are lightweight, soft, and flexible, and can improve safety for the wearer and others in the vicinity of the wearable robot. In addition, textiles promote garment comfort: they are inherently breathable because their porous structures permit the transmission of vapor, allowing evaporative heat flow away


from the body.^[1] Textiles are also robust, and they resist abrasion and tear propagation due to the ability of individual yarns to move.^[2] Unique structural and mechanical properties are possible due to the textile structure (Figure 1); for example, knit loops enable stiff and relatively inextensible fibers and yarns to become stretchable metamaterials. Therefore, when traditionally hard components, such as electronic circuits, are integrated into wearable robotic systems, a textile architecture can enable the necessary materials to be a part of a flexible and soft system through its geometry. Last, researchers and designers can create 3D shell structures through knitting, weaving, and sewing that cannot be made easily with many traditional manufacturing methods. And because textiles are commercially available materials, they support the rapid transition of devices from the research lab to medical or consumer products.

The field is undergoing a transition from viewing textiles as substrates—that is, base materials upon which we attach sensors, actuators, and power supplies—to utilizing textiles as programmed active textile systems, in which robots can be formed from the ground up in an integrated manner (Figure 2). Originally, textiles were used as passive substrates, materials that primarily acted as scaffolds to comfortably and conformally fit the body and anchor rigid components (e.g., LEDs, motors, printed circuit boards). In such a configuration, the textile lends little functionality to the wearable robot beyond that provided by everyday clothing. In the early 2010s, researchers began to leverage the unique mechanical properties of textiles in order to design and improve the function of wearable robot components. Engineered actuators with varied textile structures direct forces^[3–5] and define motions,^[6–9] while sensors employ carefully selected and developed textile architectures to increase sensitivity.^[10–13] A majority of this work is done in a discrete manner; generally, sensors and actuators are developed separately and full systems are subsequently built through cut-and-sew techniques, piecing these components together into a robotic garment.^[14–20]

The field is moving towards an approach based on programmed active textiles, which we define as systems wherein a majority of the textile robots' passive (fit, shape, comfort) and active (actuation, sensing, signal lines and integration) functionality can be pre-programmed through textile-structural fabrication processes in an additive, hierarchical manner. Through modification of the scale and placement of components, the textile microstructures, and the materials, a systematic and iterative device development loop will form that will ultimately

V. Sanchez, Prof. C. J. Walsh, Prof. R. J. Wood
John A. Paulson School of Engineering and Applied Sciences
29 Oxford St., Cambridge, MA 02138, USA
E-mail: vsanchez@seas.harvard.edu

V. Sanchez, Prof. C. J. Walsh, Prof. R. J. Wood
Wyss Institute for Biologically Inspired Engineering
3 Blackfan Cir., Boston, MA 02115, USA

 The ORCID identification number(s) for the author(s) of this article can be found under <https://doi.org/10.1002/adfm.202008278>.

DOI: 10.1002/adfm.202008278

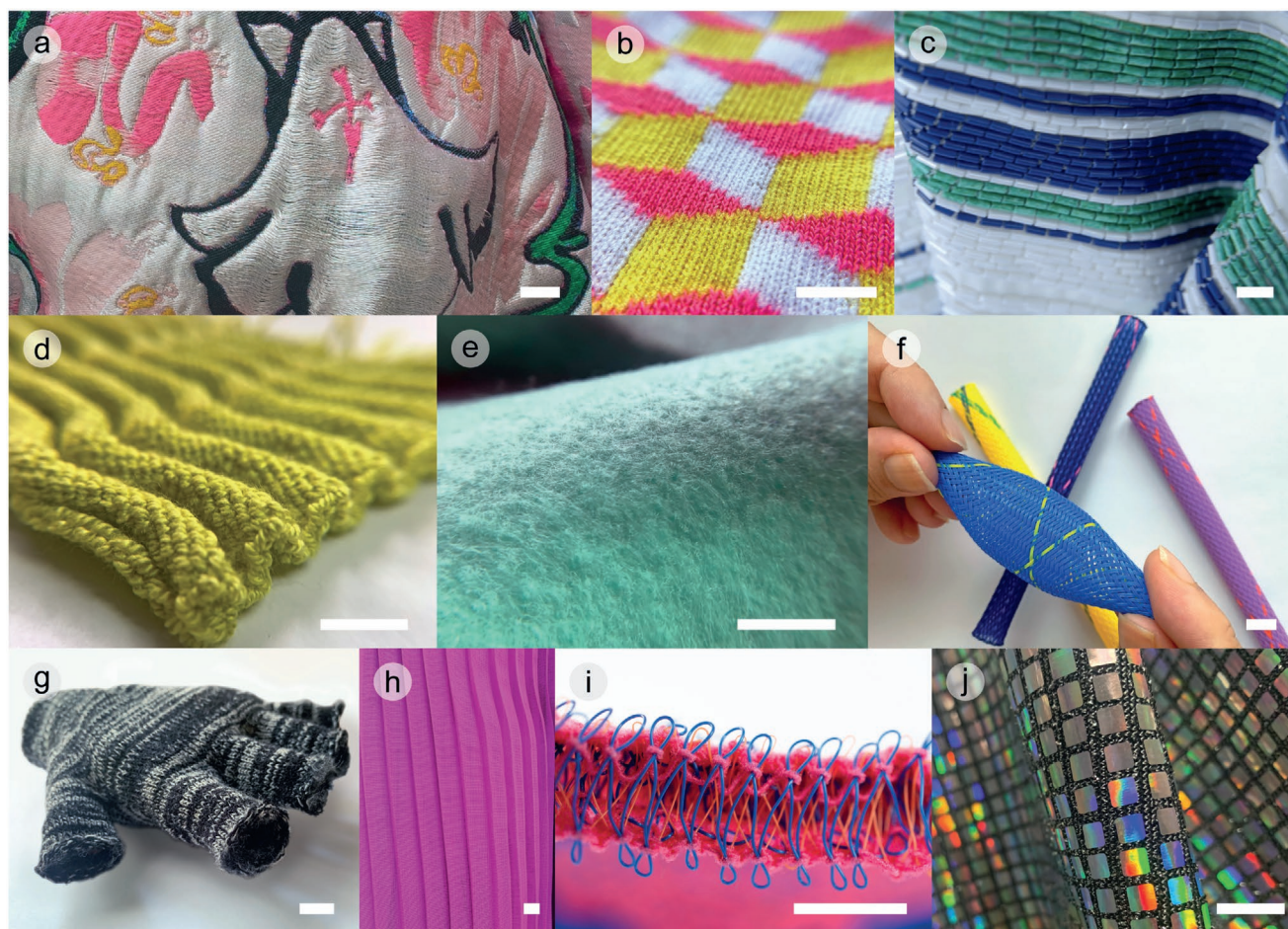


Figure 1. A selection of materials produced through textile structuring and post processing. a) Jacquard weaving enables a variety of materials to be integrated on the front and back of a textile in a programmed manner. Textile designed by Brandon Wen, worn by Ben Adam, and photographed by Oxiea Villamonte. Reproduced with permission. Copyright 2020, the designer and photographer. b) Multi-color, or jacquard, weft knitting patterns multiple yarns into a monolithic structure while providing intrinsic stretchability. c) Sewing enables attachment of many discrete rigid components (here, glass beads), while maintaining material flexibility. Textile designed and photograph provided by Johnathan Hayden. Reproduced with permission. Copyright 2020, the designer and photographer. d) Textile structures program larger scale shaping; here, a combination of knit and purl stitches self-folds into a wrinkled structure. e) Low-cost nonwoven formation processes shape fibers directly into textiles. f) Some textile structuring processes create 3D globally shaped shells: for example, braiding produces tubes that act as springs, while 3D weft knitting can make g) complex shapes like branching tubes. h) Post processing techniques like pleating can modify the mechanical properties of a textile—a relatively stiff woven material can become stretchable. i) Spacer knit textiles have been used to provide padding or as 3D structuring for sensors. A research sample highlights the unique knit construction used to achieve this type of structure. Textile designed by Suzanne Oude Hengel and Milou Voorwinden and photographed by Lieke Biel. Reproduced with permission. Copyright 2020, the designers and photographer. j) Textile finishing processes like lamination create composite materials with textiles and films; here a knit textile is bonded with thermoplastic polyurethane (TPU) films. All scale bars represent 10 mm.

enable full textile robots. The advantages and capabilities of this textile-based approach parallel those offered by 3D printing.

In a programmed active textile formation technique, such as 3D multi-material weft knitting, multiple materials can easily be mechanically coupled together without adhesives, and without the challenges that would be encountered in subtractive processes like computer numerical control (CNC) milling. Analogous to multi-material 3D printing, in which material placement and shaping can be controlled, programmed textile formation is an additive process which enables technical textile structures that are completely unique to the device needs by defining global shaping and placement of varied microstructured areas, as seen in the recently-developed Nike Flyknit sneakers. However, unlike 3D printing, textile formation allows

for structures with more internal open spaces, without the use of support material and with little consideration for the component materials' chemical compatibility. Yarns are predominantly in a solid phase during textile formation, and no inter-material adhesion is typically required to hold structures together. These processes are being used currently at production scale; however, the speeds are slower and the costs are higher than producing yardage of material and using cut-and-sew processes to form simple shapes. As such, this approach is not yet optimized for making basic structures, like a simple T-shirt.

Similar to CNC machining and 3D printing, there is less operator involvement in programmed active textile fabrication processes as compared to cut-and-sew techniques. This automation can reduce variation between samples due to

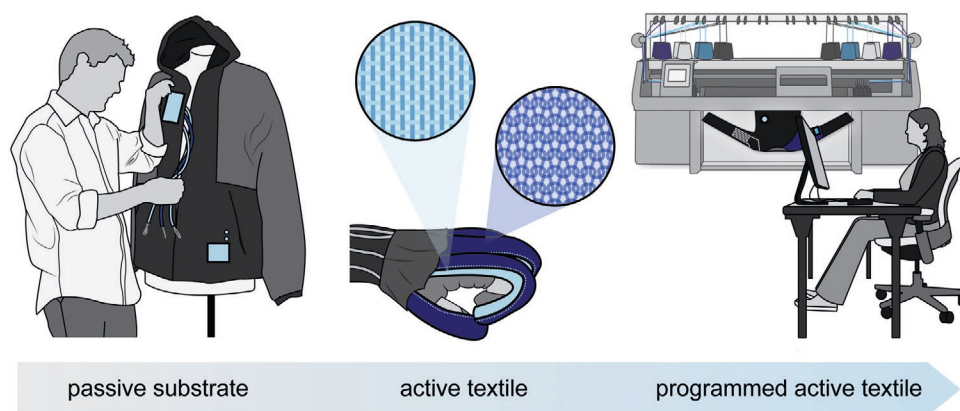


Figure 2. The future of textile-based wearable robotics. Incorporation of textiles in wearable robots has evolved from using textiles as passive substrates to considering them as active materials. Recent developments are paving the way for a future where active textile systems can be pre-programmed and where global garment shaping and distributed sensing and actuation patterns can be created at the time of design.

human variability in fabrication. Additionally, the programming approach enables higher resolution patterning than cut-and-sew; for example, knit stitches on a fine gauge 3D knitting machine can support 72 stitches per centimeter (i.e., each stitch is approximately 1.4 mm in width, not considering pre-strained material effects which will further decrease stitch size when relaxed). Typical minimum tolerances for machine sewn garments made by human operators are in the 3–5 mm range.^[21,22]

A programmed active textile system approach is highly supportive of customizable mass manufacturing. Mass customization is on an uptick for consumer purchases^[23] and supports a more sustainable apparel manufacturing route because excess fabric scraps are not generated, as opposed to cut-and-sew processes. Wearable robotic systems can be produced as needed, limiting excess inventory of raw materials. Additionally, in the field of functional apparel, experts on size and fit have argued that there is no universal sizing standard to accommodate the broad range of human body types; statistical averages used to define size sets result in garments that truly fit “no-one” perfectly, or that consistently leave out less common body types.^[24,25] In addition to cultural traditions and societal norms, our current everyday clothing is worn for modesty, warmth, and aesthetics. Although ill-fitting everyday clothing has limited negative consequences for the wearer, for robotic clothing which incorporates function that is highly dependent on precise placement of components (such as force-paths) on the body, poor fit can reduce performance,^[3] motivating the need for customization.

With this change underway, in this review we have compiled and generalized current findings in the active textile material area and preliminary work in the programmed active textile area of textile robotics research in order to provide a framework on how textile structures are employed in these systems, highlight the lessons learned in the literature, and identify promising areas of future research (Figure 3). We note that, while wearable robots may take many forms, in this review we exclusively focus on wearable robots that function by changing shape or applying force to the wearer, thereby incorporating a clear mechanical actuation component in their operation. Because textile-based robots are so closely linked to their wearable applications, this review first describes several common use cases of textile-based

robotic garments and their generalized system-level needs in Section 2. We then provide a brief overview of textile structures, machinery, and general textile terms for a materials science, engineering, and robotics audience in Section 3. Next, we highlight how the properties of textiles are being leveraged in the constituent components of robotic garments, including: actuators described in Section 4, sensors in Section 5, and integration including signal, power, and fluidic lines in Section 6. We link the performance of these components back to implications for wearable devices, while highlighting gaps and areas for future directions. Last, we conclude this review and discuss the current state of the field and our outlook for the future in Section 7.

2. Applications for Textile-Based Wearable Robots

Research into textile materials as sensors, actuators, and integration lines is largely driven by the needs of applications—wearable robots are the primary application area for this work. Wearable robots require actuators to change garment shape or apply forces to the body, sensors to detect the wearer’s state, determine interaction between the robot and the wearer or their environment, and monitor the robot’s independent state, and integration components to link these constituent parts distributed throughout the garment to processing, power, and control elements.

Textile-based wearable robots have been developed through research efforts in fields including robotics, biomedical engineering, and human-computer interaction. By compiling this research, it is apparent that several classes of wearable robots are emerging, including locomotion assistance, grasping and reaching, shape-change for dressing, thermoregulation, haptics and communication, and therapeutic compression (Figure 4). Even within these classes, the mechanisms of operation and form factors of wearable robots can vary considerably, yet there are clear and distinguishable trends defining these separate application areas. The goal of this section is to describe these textile-based wearable robot application areas, dissect area-dependent performance goals, and compare the performance metrics across areas in order to provide materials scientists defined targets in their development of textile components for wearable robots.

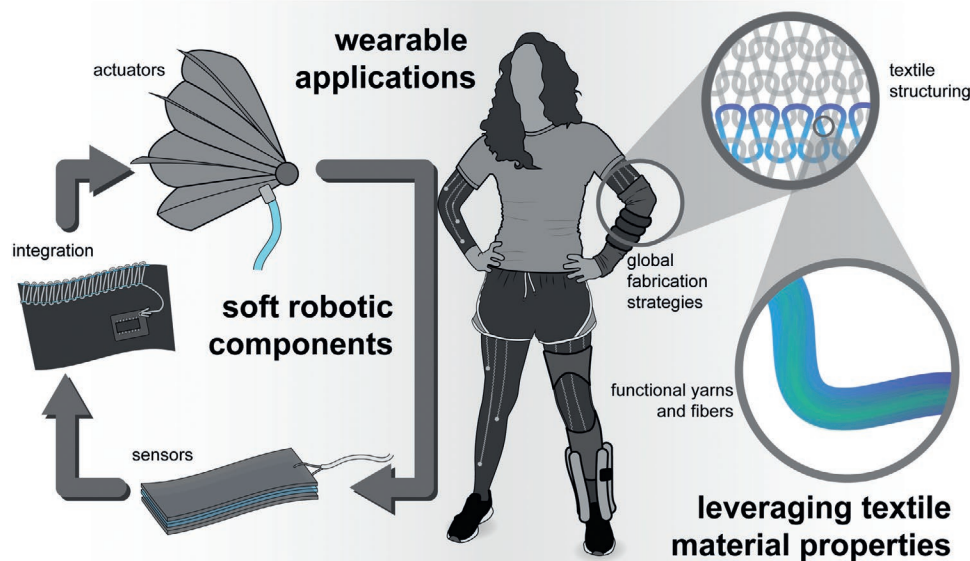


Figure 3. An overview of the contents of this review paper. We identify major application areas for garments with embedded robotic elements and their system-level metrics, driving performance requirements for new materials. We then provide a brief overview of the hierarchical textile structure and summarize how properties unique to textiles are leveraged when developing sensors, actuators, and integration components necessary for soft robotic and autonomous garments.

2.1. Locomotion Assistance

Wearable robots for locomotion augment able-bodied people and assist people with mobility disabilities in activities including

walking,^[26–30] running,^[31] and sit-to-stand motions,^[18,32] which enable the user to begin locomotion. These devices can be used as assistive garments or as training and rehabilitative devices. A majority of these devices do not provide the full forces

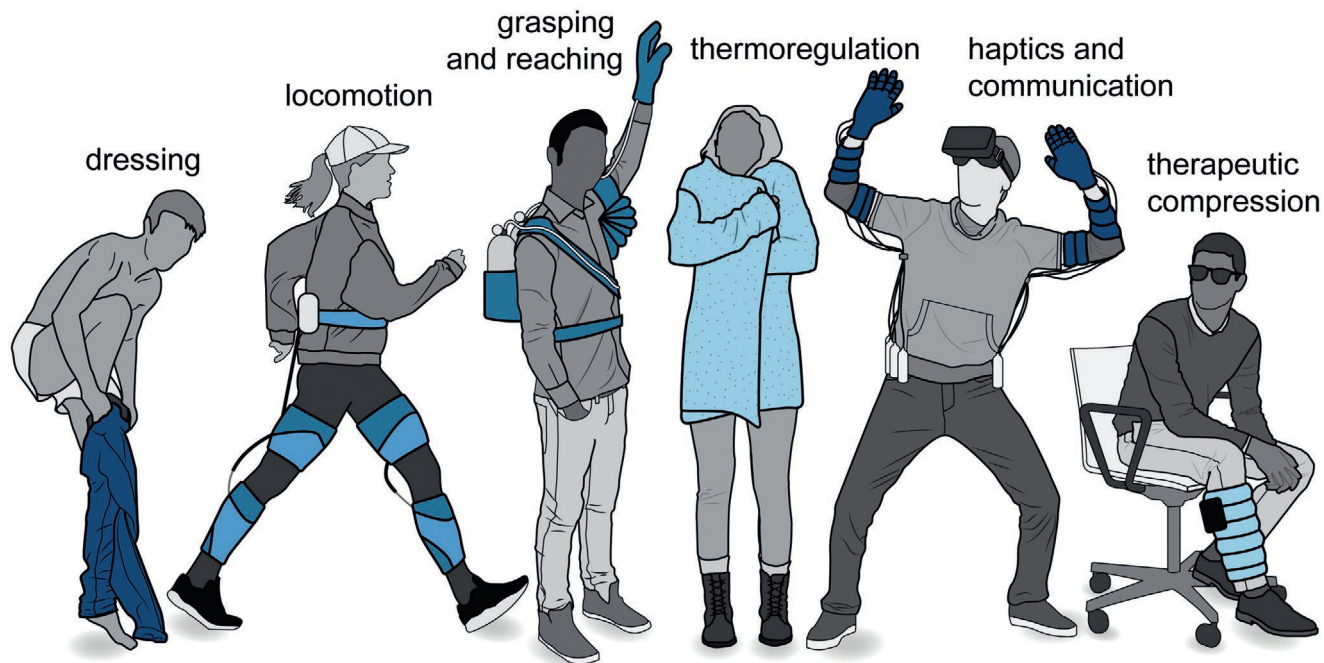


Figure 4. Common use cases for textile-based wearable robots. Autonomously extending and retracting garments assist with dressing. Garments that apply forces to biological muscle aid locomotion while using sensors to detect gait cycle timing and provide support to assist with grasping and reaching while determining arm and hand motion through sensing. Dynamic thermoregulation assistance through shape-change alters garment coverage area or modifies textile porosity. Garments provide physical cues for haptic feedback and communication while obtaining information about the wearer's posture and motion. Compression wearables assist with rehabilitation and therapy while gaining sensor information to provide correct pressure doses.

necessary for locomotion and instead work in parallel with the wearer's biological muscle. For example, when used to assist walking, these robots actuate along with the user's step, as opposed to the robot providing all of the force to walk and support the wearer. This approach is possible because research has shown that relatively low levels of assistive force can enable significant reductions in metabolic cost, although these reductions scale with the magnitude of assistance.^[33] The use of textiles improves comfort, enables devices to fit more users, and allows these devices to reduce mass around distal components and concentrate it in a central location to increase efficiency.^[33,34]

Commonly, textile-based robotic garments for locomotion employ actuators that contract or use displacement mechanisms (e.g., pulleys) to pull across a joint (typically the ankle, knee, or hip) to assist with extension or flexion, similar to the contraction of biological muscles. These actuation profiles are achieved in textiles through cable driven systems that use separate electric motors and mechanical linkages,^[18,27,35] or textile-based pneumatic artificial muscles,^[7,28,29,36] which require a compressor or compressed fluid tank in addition to a power supply. In addition to fibrous cables and textile pneumatic artificial muscles, textile materials find function in passive areas of these wearable robots. Fabrics with high tensile stiffness are designed into the garment structure as anchoring points for actuators so that the forces may be efficiently transferred through the system, reducing losses due to stretching the material.^[33,37] In addition, textile-based foam composites and meshes dampen the applied forces for wearer comfort.^[31] The fluidic actuation approach implements global patterning of woven textile pouches with high tensile stiffness (described in more detail in Section 4.2) to create tailored fluidic actuators that can assist with flexion at a joint,^[17] extend at a joint,^[30,32] provide support through a change in material stiffness,^[7,29] or implement a combination of these strategies. Few instances of "shape-changing-material-based" wearable robots for locomotion have been demonstrated to date, and those developed employ few textile-based components.^[38,39]

These wearable robots require sensors in order to estimate the position of the wearer, determine the force the actuators are applying to the body, establish the position of actuators, and obtain information used to estimate timing in the gait cycle. Commercially available load cells have been integrated into cable driven implementations of these robots because they can accurately determine the force of the cable; however, they remain rigid and bulky.^[27,31,35,37] MEMS-based inertial measurement units (IMUs) are commonly employed to determine wearer joint angles^[31,36,40] and to estimate gait timing measurements because they provide multi-axis data and are commercially available at a low cost. However, these sensors are rigid, often bulky, and typically not fully integrated into the textile garments to allow for maintenance including washing. Alternatively, softer film-based force sensors,^[29] pressure sensors,^[40] and switches^[28,37,41] implemented in insoles or shoes can help estimate gait cycle timing by mapping the amount of contact between the wearer's foot and the ground,^[38] signaling the heel-strike and toe-off times,^[41] or potentially by determining the center of mass. In addition to film-based composites,^[29] textile-based implementations have demonstrated utility as soft sensors. Soft textile-based sensors have been employed to

characterize the pressure profiles delivered by textile robots; however, these sensors are not integrated into the garments.^[3] Although less commonly used in full wearable robotic systems, soft strain sensors for joint angle determination^[36] and gait measurement have been proposed^[42] and highlight a potential approach for creating fully textile-based wearable locomotion assistance robots. While not typically used in textile based garments for locomotion outside of evaluation, electromyography (EMG) is another potential strategy in determining wearer intent.^[43] Sensor drift has been identified as an issue in these systems,^[40] and can affect all types of sensors, signifying the importance of developing and characterizing sensors that are robust to continuous and cyclic use in variable environments.

The requirements for wearable robots that assist with locomotion vary based on the targeted user population (e.g., people who have experienced a stroke compared to able-bodied users), the joint being assisted, and the type of locomotive activity (e.g., walking, running, sit-to-stand). Speed requirements for wearable robots change with the desired speed of locomotion—when people run or walk at faster speeds, their stride time typically decreases, meaning that the gait cycle bandwidth increases. In one experiment on running, an average gait cycle bandwidth per leg for a speed of 4.1 m s⁻¹ was 1.44 Hz, while at 3.1 m s⁻¹ bandwidth dropped to 1.38 Hz.^[44] In another study focused on walking, gait cycles per leg ranged from 0.56 Hz at a walking speed of 0.53 m s⁻¹ to 1.25 Hz at 2.1 m s⁻¹ walking speed.^[45] These speeds guide requirements for textile-based robots, but because assistance can be most effective when applied at specific timings during the gait cycle, often with actuation cycles taking 50% or less of the stride period, locomotion assistance robots must be faster.^[17,28,31,46,47] Generally, textile robots for populations with mobility disabilities operate at slower speeds and apply lower forces than those made for able-bodied populations.^[7,27,31,47] Assistive forces provided by the wearable robot can be scaled in proportion to those provided by the body, and scaling must also take speed into account. Peak torques generated by muscle motion can vary based on speed, as seen with the torque of the knee flexor, where one study reported a maximum torque of approximately 45 Nm at a walking speed of 5 mph and a minimum of approximately 11 Nm at 0.5 mph.^[48] When assistance magnitude was scaled to body mass for a locomotion assistance textile-based robot for able-bodied wearers, higher forces provided a higher metabolic reduction.^[33] Sit-to-stand motions can require higher torques than those in a typical gait; in one study, the average joint torque was determined to be approximately 180 Nm per leg for extension of the knee, 120 Nm per leg for dorsiflexion at the ankle, and 80 Nm for flexion at the hip for a "fast sit to stand motion."^[49] Many of these values are affected by the weight and anthropometric measurements of the person, and additionally often only enlist male participants, meaning women may have different requirements.

2.2. Grasping and Reaching Assistance

In a typical day, people reach for, grasp, lift, and manipulate a variety of objects in order to interact with their environment for tasks like opening doors, eating meals, or taking showers.

Textile-based wearable robots that assist and rehabilitate users with grasping, reaching, and lifting actions enable users with upper extremity mobility disabilities to be empowered and independently interact with their environment,^[5,16,50–52] and to reduce fatigue or increase power of able-bodied wearers.^[22,53] Here, textiles offer similar capabilities in terms of comfort, safety, and lighter weight to those seen in robotic locomotion assistance. The “transparent” nature of textiles has additionally enabled these robots to be magnetic resonance imaging-compatible for simultaneous rehabilitation and imaging exercises.^[54,55] Because of the lighter weight of the upper extremities compared to the legs, more robots used for grasping and reaching assistance have been developed to fully support motion, but those used in parallel with biological muscle are still common.

Grasping and reaching assistance robots use actuators that either flex or extend the joints of the fingers,^[14,56] the wrist,^[57,58] the elbow,^[22,59] or the shoulder.^[16,59,60] Strategies to support abduction of the shoulder, provide a scaffold to support the limb, or a combination of these methods are also common.^[61–63] Cable driven systems are commonly employed and use textiles to define and route anchoring points across the body.^[19,51,61,64] Fluidic textile actuators are frequently used to “push” and create temporary supporting structures to cradle the body.^[22,62] In addition to global shaping of textile fluidic actuators,^[16,22,60,65] seen in locomotion assistance robots, multi material textile actuators consisting of combinations of knits and wovens have been employed to create motions such as bending to match those of the body.^[6,20,66–68] The lesser forces required in some applications may enable the use of these stretchable knit materials.

Many of these robots have been developed with control systems that consider the state of actuators (e.g., position, pressure, force) but do not include the state of the wearer and their environment in their controller. This is potentially a consequence of the added uncertainty and complexity involved with grasping, reaching, and lifting tasks compared to the relatively consistent motions seen in walking and running. In addition to the force or pressure sensors used to determine the force of a cable or pressure of a fluid within a textile pouch, researchers have begun to employ additional sensors to estimate the position of the limb,^[14,20,69,70] acquire environmental cues,^[5] obtain wearer inputs,^[53,71] and detect intent.^[20,72,73] For these applications, textiles have been used as a substrate to hold IMUs to obtain the position of the arm.^[61,69] EMG sensors help detect user intent and may include traditional adhesive electrodes that are not part of the wearable robot,^[20,74] or can employ garment-integrated textile electrodes.^[75,76] Textile-based strain and pressure sensors can determine assistive glove position and grasping force.^[14,67] Recently, textile-based strain sensors have been used to estimate the position of the shoulder, which is particularly complex due to its multi degree-of-freedom (DOF) motions.^[15]

Depending on the device use case, joints assisted, and ratio of user to robot effort, the metrics of these robots vary accordingly (e.g., a robot built to help warehouse workers lift boxes would require higher forces than a robot built to assist a person who has a spinal cord injury lift their food on a fork). Considering interactions with the objects encountered during

activities of daily living (ADL), baseline metrics can be determined. For grasping, the bulk of the objects encountered in everyday life weigh 1.5 kg or less.^[77] Experimental data on pinch force requirements for a variety of daily living tasks were determined to range from 1.4 to 31.4 N, with a majority of tasks requiring 10.4 N or less.^[78] Maximum grip strength of healthy young adults may be more than an order of magnitude higher than these forces.^[79] Forces and moments for the elbow can be higher than those of the hand during ADLs, with maximums reported as high as 25 N along the humeral longitudinal axis and 5.8 Nm for elbow flexion when raising an object to head height and lowering it to a shelf.^[80] For reaching with the shoulder, Rosen and colleagues found the highest torque required for ADLs to be 10 Nm.^[81] The bandwidth for both sensors and actuators can be dictated by the motions of the human body. Hand speeds and movements can be quite fast, with a maximum range of 6–12 Hz and movements >2 Hz often utilized during ADLs,^[82] while most motions of the body are <10 Hz.^[83] However, when considering a rehabilitation approach, these speed requirements may be slower. For example, in assistive gloves, typical rehabilitation exercises for fingers are performed at <0.5 Hz.^[84,85]

2.3. Shape-Change for Dressing

Dressing is an ADL which approximately 4% of non-institutionalized Americans over 65 and approximately 79% of institutionalized Americans over 65 have required help from another person to perform.^[86] And, paradoxically, while dressing is the most burdensome ADL on assistive staff, dressing has seen the most limited use of assistive technologies.^[87] While several groups have proposed at-home robotic systems (typically containing rigid robotic arms) to aid with dressing, self-fitting and assistive dressing garments may potentially enable the wearer to dress and undress throughout the day regardless of location. Self-fitting garments may also alter their fit (i.e., varying their shape and compression on the body) for functional support or aesthetics, which holds promise for light compression garments in particular, as they can be difficult to don and doff.

For self-fitting and assistive-dressing garments, multiple approaches can be taken; the garment may dynamically expand and contract (either by simply modifying its amount of “ease,”^[88,89] or by expanding into a structure into which the user may enter^[90]) so the user may put on the garment, or vary its compression force over time to alter “fit.”^[91] Oftentimes shape-changing materials, such as SMAs^[92] or coiled polymer actuators,^[91] integrated into textile garments have been employed because high forces and speeds are not as critical. Fluidic actuation systems have also been used.^[89,90] In these systems, the shape-change is reversible over many cycles, as opposed to one-time shape-changing garments that are permanently “tailored” for the body.^[93]

Most of these garments have not yet incorporated sensors or closed-loop control schemes; however, one could envision the potential of sensors in these systems. Force and pressure sensors can ensure that safe, prescribed levels of compression could be implemented in garments that apply light levels

of compression for fit, while strain sensors could be used to optimize the amount of expansion and prevent unnecessary over-stretching to save the user time.

Garment “fit,” the end goal of a dressing action, is a challenging metric to quantify and measure because the body itself changes shape during motion, and thus fit can vary immensely.^[25] A general takeaway is that these garments require large amounts of expansion. For example, 50% strain is noted as a textile requirement for use in activewear, which is assumed to include the needs for donning and doffing.^[25] When considering compressive fit of standard garments, one may note that estimates of the maximum comfortable normal pressure of orthoses are typically around 5 kPa,^[94] while other sources indicate that blood flow drops but remains stable at 30 mmHg (≈ 3.9 kPa);^[95] additionally, others have selected values below those reported for medical compression (<2.4 kPa).^[88,96] As for speeds, providing someone the ability to dress themselves may not have as strict time constraints, and actuation cycles that last several minutes may be acceptable.

2.4. Thermoregulation

Standard thermal comfort is defined quantitatively as a balance between the metabolic heat generated by a person and the heat loss to the environment.^[97,98] Garments play a role in this relationship because they dictate the body's interactions with moisture, heat, and light. By dynamically altering the properties of their constituent materials, robotic garments may actively assist in wearer thermoregulation.

Robotic and autonomous textile systems for thermoregulation actuate and change their shape to alter the coverage area of the garment^[99] or change the textile on a microstructural level to modify porosity or radiation blocking properties.^[100] In these systems, reversible, cyclical shape-change is achieved without any user actuation, unlike semi-passive systems including phase change garments in which the user must manually put the garment into a cold environment to solidify a liquid^[101,102] or replenish fluid that has evaporated^[103] to maintain the effect. Although there are other approaches to develop responsive garments for thermoregulation, including integrated fluidic cooling systems^[104,105] and textile-based Joule heating wearables,^[106–108] because there is no mechanical actuation directly associated with the textiles used in these systems, these areas will not be considered in the scope of this review. For a detailed review on smart textile-based systems for thermoregulation, beyond robotics, we recommend the article by Tabor and colleagues.^[109]

Typically, shape-changing materials are integrated into textiles to actuate and change structure on a garment level to alter garment breathability,^[99,110] and thus its heat transfer and moisture management properties, allowing for more sophisticated temperature regulation than simple passive protection from the elements. Going deeper, some garments incorporate structural changes on the yarn scale (described further in Section 3) to modify IR properties of the textile.^[100] These systems most often respond to a stimulus through self-sensing, or have not yet had an electronic closed-loop controller accounting for the state of the environment and the wearer. Additional sensing

elements could be incorporated into devices that use non-environmentally actuated shape-change for dynamic temperature and humidity-regulated electronic feedback control.

General formalized metrics have not yet been reported for robotic garments developed in this field. As changing the garment shape is the goal of these devices, forces are not typically measured, and indicators of success include lower temperatures between the garment and skin or less IR transfer through the garment when compared to a control garment.^[99,100] As many of these robotic textiles require distributed active material networks to open large numbers of pores or to work together to change a structure, it may be quite hard to accurately measure and understand the discrete force contributions in the textile structure, opening up some interesting research questions. When considering speeds, relatively slow systems are currently acceptable, with actuation speeds of approximately 0.01 Hz reported.^[100]

Aside from metrics, some design rules should be considered. For thermally driven actuation systems, the actuator material should either be i) minimized to prevent injecting additional heat into the system, unless it can be coupled with a change to increase insulation of the wearer, or ii) optimized to change with ambient temperature. For example, an SMA-driven system, which often requires >100 °C to actuate, may be best actuated when contraction of the fiber results in more insulation, leading to a synergistic heating and insulating effect. Meanwhile a material that contracts upon a temperature differential encountered in the ambient environment may be used without artificially injecting heat into the system, allowing environmental change to drive textile shape-change.^[111]

2.5. Haptics and Communication

Wearable robots for haptics and communication provide a diverse range of functions for the wearer, including user interfaces, navigation cues, movement cueing and guidance, and notifications. While some garments in this area change their shape to communicate visually to others,^[112,113] a large subset of the area of communication and haptics includes tactile feedback wherein several main mechanisms are employed including vibration, point-based pressure, compression, skin stretch, curvature change, temperature change, and impedance (or resistance to wearer motion).^[114–116] Wearables for tactile haptics and communication can take many forms including sleeves,^[114] gloves,^[117] bracelets,^[118] and entire garments.^[119–122] Based on the location of the haptic device, the feedback mechanism used, and the device goal, the component design and performance metrics change.

Haptic systems for tactile feedback apply vibrations and forces to the body^[118,123] or restrict its motion.^[124] Rigid vibration motors, often attached to textile substrates, have been one of the most ubiquitous methods used because they are inexpensive and can reach the higher range of frequencies that skin mechanoreceptors can sense.^[120,125,126] Recently, in order to provide more comfortable, conformable, and soft haptic wearables, textile integrated approaches have been explored using cable driven systems, fluidic systems, and shape-changing materials. Textile-integrated cable driven actuation systems have moved

the torso for drone steering,^[127] textile-integrated elastomer DEAs have provided vibration cues,^[128] and SMA-integrated textile robots have applied compression to the body.^[129–131] One of the most predominant new approaches is the utilization of fluidic textile-integrated actuators,^[116,122,132,133] and often global patterning of woven fabrics has been used to program inflation.^[114,118,121,134]

Many initial haptic devices used closed-loop control to monitor only the actuator state independently. More recently, sensing is increasingly incorporated into many of these devices to detect the state and intent of the user and interactions between the actuators and user. Similar to previous application areas, IMUs placed onto textiles have been used to determine user position^[127] and film-based force sensors have been used in insoles for gait detection.^[132] Flexible-film^[121] and textile-based^[114,134] resistive and capacitive pressure and force sensors have been employed for force control of actuators to ensure desired forces are applied to the wearers' bodies.

Several key metrics determine the materials and development of wearable robots for haptics, including actuation mechanism, feedback stimulus type, DOF, actuator resolution, actuation displacement, and bandwidth. The tactile receptors in the skin are sensitive to varied frequency ranges, spanning approximately from 1 to 1000 Hz,^[116,126,135] driving relevant bandwidths for both actuators and sensors. The spatial resolution of these receptors also varies from 0.5 to >20 mm.^[116,126] And when differentiating between two stimuli, differentiation thresholds vary based on the location on the body. The fingers and lips require lower spacial detection thresholds (<10 mm) compared to the forearm and calf (>40 mm).^[136] When this receptor density and differentiation ability are considered along with the amount of information the robot needs to convey, the materials and viable fabrication strategies with compatible resolutions can be determined. Mechanoreceptors in the skin are not equally sensitive to different feedback mechanisms (e.g., point pressure, skin stretch, compression), which in turn can define which textile actuation mechanisms and materials are practical. For example, fluidic actuation has been used for skin stretch and pressure feedback,^[114] while SMA approaches have been primarily used for compression feedback.^[129–131] Force parameters can define which sensors and actuators are well suited to these systems, and for tactile information, studies have indicated relatively low forces (3–4 N) enable the user to perceive large amounts of information.^[137,138] For more information, we suggest the following resources.^[116,136,138]

2.6. Therapeutic Compression

The clinical use cases for therapeutic compression range from treatment of burns and burn scarring,^[139–142] to sensory-based interventions for children with mental health and developmental disorders such as attention deficit hyperactivity disorder and autism,^[143–145] to treatment and prevention of lymphedema, deep-vein thrombosis, and venous ulcers.^[146–151] Recent evidence has suggested that cyclic mechanical stimulation can also improve regeneration of injured skeletal muscle when compared to no intervention.^[152]

Passive pressure garments have been used clinically; however, a large amount of customization is required to create garments that impart the required pressures,^[142] intermittent compression cannot be achieved, and in some applications, such as developmental disorder intervention, users become acclimated to sustained pressure over time.^[143] To overcome these challenges, wearable robots for therapeutic compression have been developed to apply cyclic and reprogrammable sustained pressures, with the caveat of requiring power sources. Unlike the compression seen in dressing applications, these garments typically operate at higher pressures and for longer functional activation time frames (e.g., >20 h of continuous pressure per day has been suggested to treat lymphedema and burns^[139,146] vs a few minutes of actuation needed to don and doff the garment in dressing activities). By incorporating variable compression systems into robotic garments, the cost of treatments can be lowered,^[153] and the dosage of treatment can be increased. These outcomes are made possible by requiring less garment customization to achieve specific pressures (i.e., by using force- and pressure-based feedback control schemes, garments of a set size could potentially apply prescribed pressures to wearers of different body types), which can potentially expand device availability and enable users to remain mobile during treatment.

Robotic garments that deliver therapeutic pressure have incorporated fabric-based actuation systems in cable driven, fluidic, and active shape-changing material configurations. Cable driven fabric sleeves with a hybrid fabric-ABS design have been used to generate pressure for the arm.^[154] Fluidic-based robots incorporating textile-based actuators have been used to apply forces to the limbs while remaining lightweight and compliant.^[155–157] SMA-based wearable robots have been used to apply compression to the torso and limbs,^[158,159] where the fabric acts as a scaffold to support compression and maintains a thermal barrier between the SMA and the skin. An additional consideration includes developing actuation systems for distributed pressure in order to avoid pressure peaks, which are a potential safety hazard.

Sensors can potentially play a key role in wearable robots for therapeutic compression. Although many pressure garments currently used in clinical settings do not offer facile and quick continuous monitoring of pressure applied by the garment, in some cases the dose (e.g., frequency and amount of applied pressure) has been noted as a determining factor in treatment effectiveness.^[140,160] As illustrated in passive pressure garments, the shape of the area of the body the garment is worn on can affect the interfacial pressure applied to the body^[161] and, in fluidic active pressure garments, tissue fluid pressures generated can be lower than the set pressure in the inflated chambers.^[162] Recent therapeutic compression robots with integrated textile pressure sensors measure pressure at the skin-robot interface for force-based feedback control schemes. Using this strategy, the prescribed forces applied to the body were more accurately delivered than when simply monitoring the air pressure delivered to actuators.^[155] Building on this work, fabric-based sensors have been used in control schemes for cable driven compression systems,^[154] while arrayed soft film-based sensors have enabled monitoring and control of multiple chambers in fluidic systems.^[163,164] The variability of the body shape and additional

Table 1. Representative required metrics based on a literature survey.

	Locomotion	Grasping and reaching	Dressing	Thermoregulation	Haptics and communication	Therapeutic compression
Device goal	Apply force to wearer	Apply force to wearer	Change garment shape OR apply force to wearer	Change garment shape	Apply force to wearer OR change garment shape	Apply force to wearer
Duration of use	A few to many hours per day	A few to many hours per day	A few minutes per day	Many hours per day	A few minutes to many hours per day	Many hours per day to several days at a time
Typical required force	High (<500 N)	Moderate (<100 N)	Estimated low (<10 N)	Estimated low (<10 N)	Low to moderate (<50 N)	Low to moderate (<75 N)
Required strain	Low to moderate (<40%)	Moderate (<75%)	Estimated moderate to high (<100%)	Estimated low to moderate (<50%)	Estimated low to moderate (<40%)	Estimated low to moderate (<50%)
Typical required speed relative to human motion	Moderate to slow (<5 Hz)	Moderate to slow (<10 Hz)	Estimated slow (<1 Hz)	Estimated slow (<1 Hz)	Varies (<1000 Hz)	Slow (<1 Hz)

precision offered by monitoring interfacial pressure signifies the need for distributed soft and conformable fabric pressure sensors to map and regulate pressures in these wearable robots.

Recommended amounts of pressure vary based on the application. Recommended pressures to treat hypertrophic scars, which can occur after burns, are between 24 and 44 mmHg (approximately 3.2 to 6.9 kPa),^[139] while prescribed pressures for lymphedema treatment can range between 30–60 mmHg (4–8 kPa),^[146] with some devices offering up to 300 mmHg (40 kPa) of pressure.^[148] Pressures of 45–160 mmHg (6–21.3 kPa) have been reported for the treatment of deep vein thrombosis.^[165,166] Such prescribed pressures are often for the actuator inflation; as discussed, interfacial pressures can vary. Robotic compression garments for autism have been built based on the above specifications.^[158] In some applications such as sensory interventions for autism, sustained pressures are used, and in others, like treatment for lymphedema and deep vein thrombosis, intermittent compression is more common.^[146,148] For example, in the case of lymphedema treatment, reported cyclic actuation speeds range from 0.5 to 0.008 Hz,^[148] while for deep vein thrombosis cycle times up to 0.45 Hz have been reported using rapid inflation (as quick as 0.5 s) and moderate to slow deflation to complete the cycle.^[165,166] While some of the above metrics are currently being applied in clinical settings, experts suggest that more work must be done to determine the optimal effective parameters.^[146–148,167] An upside for materials scientists and roboticists in regards to this challenge is that by using robotic garments in future studies, better control of pressure profiles and doses can be achieved and monitored, and thus these parameters can be more accurately and systematically studied.

2.7. Comparing Metrics Based on Applications

To provide a quantitative set of metrics for materials scientists to refer to as they develop constituent textile materials and components for wearable robots, a survey of 163 textile-based wearable robot device papers was conducted. Maximum forces, speeds, and displacements were tracked based on application

area, with findings described in **Table 1**. Graphical representations of several key metrics are shown in **Figure 5** and **Figure S1**, Supporting Information. More detailed information on these metrics and devices is provided in the Supporting Information. As expected, some of the highest forces are required for locomotion assistance because of the requirement to move the lower extremities. Grasping, lifting, and reaching also had relatively high force requirements, although there is large amount of force variation owing to specific variations in use cases and joints assisted—for example, ranging from assisting a post-stroke patient moving their fingers to assisting the elbow of a warehouse worker lifting heavy boxes. In addition to these quantitative metrics, the actuation strategy for devices in each application was recorded as well as the presence of sensors, as displayed in **Figure 6** along with medians across all metrics for each application area.

Compiling these results provides insights into the metrics that fields choose to characterize and report, and how they vary based on the application. For example, wearable robots for haptics are commonly characterized in terms of pressures and not torques because devices usually apply normal pressure to the body, as opposed to rotating a joint. Additionally, gaps in the field can be identified. For example, based on this survey, few thermoregulation garments have been demonstrated to date, and little characterization of the actuation forces, speeds, and strains for garments used for thermoregulation exists, opening up some interesting research questions: for example, what distributed forces are required? With the synthesis of this information, we hope to provide some specific ranges to target when developing robotic materials.

3. Textile Science and Technology for the Future of Wearable Robots

Textiles are one of humankind's oldest technologies, with human-made cords dating back tens of thousands of years.^[168,169] Although this long history provides a number of techniques to draw from when developing wearable robots, advances in equipment and scientific understanding of textile structures are still made every day.

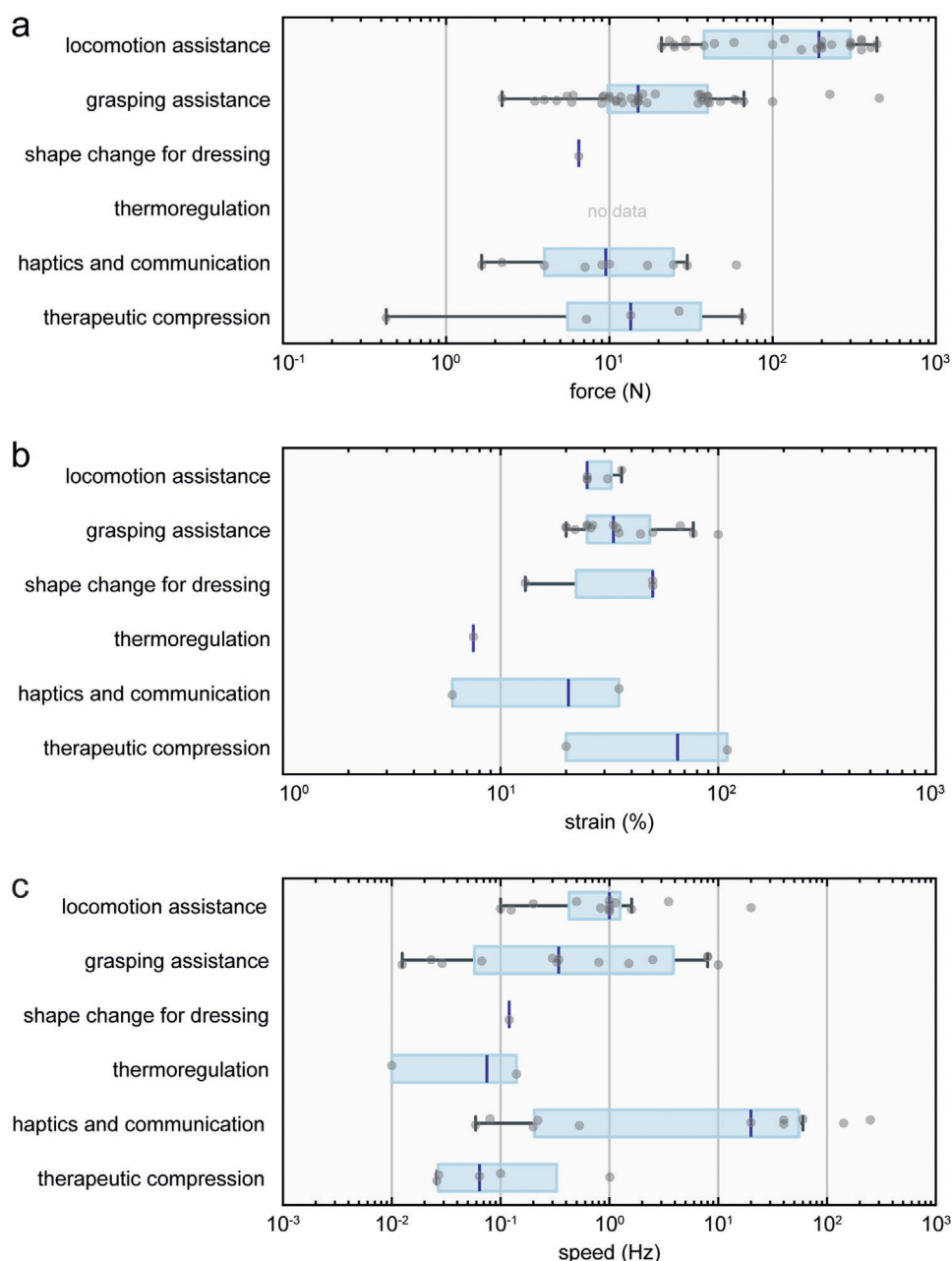


Figure 5. The maximum metrics of a) forces, b) strains, and c) speeds across device applications.

In the simplest sense, textiles are networks of interlacing and inter-looping flexible rods, or yarns, whose length is much greater than their diameter. When incorporated into textile architectures, these seemingly simple yarns can generate complex materials and behaviors, resulting from the inherent hierarchy in their structuring (Figure 7). As such, textile science is a field that follows a geometric and fabrication-focused nomenclature system. The smallest material unit (above the molecular level) when considering textiles is the fiber. Fibers are spun into yarn, commonly encountered as sewing thread or knitting yarn. Yarns are structured into textiles, wherein the structuring parameters can impart unique mechanical properties, including anisotropy and stretchability. Several of these textile

structuring processes support simultaneous global shaping into 3D shell structures. Alternatively, sewing and bonding techniques are used to adhere multiple pieces of textiles into shell shapes in what is known as cut-and-sew processing.

3.1. Fibers, Yarns, and Cords

Fibers are the smallest unit of textiles. Fibers have two classifications: filament fibers, which are functionally infinite continuous strands; and staple fibers, which are short pieces less than several inches in length (Figure 7). Most synthetic fibers are available in filament form, while natural fibers are typically limited

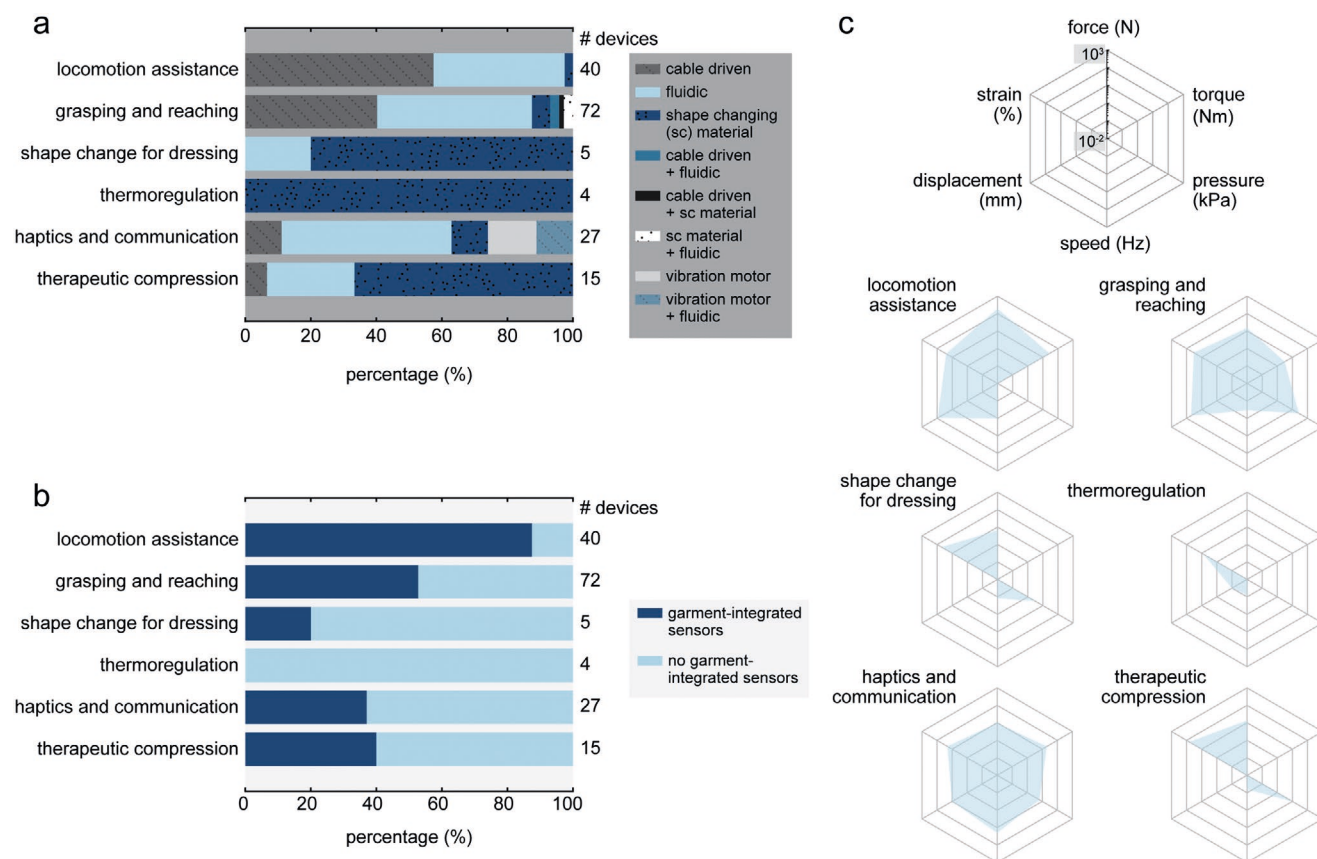


Figure 6. Metrics across textile-based wearable robots based on application. The a) actuation method and b) use of sensors vary based on end application. These variations may be related to the required metrics for the devices. c) Plotting the median maximum values on a logarithmic scale helps visualize these differences in device requirements.

to staple. Synthetic fibers are formed through several processes including melt spinning, thermal drawing, and wet spinning, and resulting fibers can be made of multiple materials and may have complex (non-circular) cross-sections. Multi-material fibers have been employed by materials scientists as actuators,^[111] sensors,^[170] and conductors used as power and signal lines.^[171]

Fibers are then structured, or spun, into yarn, with several yarn constructions illustrated in Figure 7. For staple fibers, this process requires the fibers to be aligned and twisted into shape. While filament fibers can be twisted, they do not require twist insertion or multiple fibers to constitute a final “yarn,” instead inherently functioning as a monofilament yarn without further modification. In addition to these basic yarns, more complex yarn structures are possible; multiple yarns can be twisted together (typically in the opposite direction that the constituent yarns were twisted, e.g., counterclockwise if originally twisted clockwise) into a “plied yarn.” A yarn can be cospun, wherein “cover” fibers or yarns are wrapped around a core yarn; typically this core is an elastomeric monofilament and is covered with non-stretch staple, resulting in a stretch yarn with non-stretch material at its surface. This construction is commonly employed by materials scientists developing strain sensors.^[172–174] “Fancy yarns” are a class of yarns that intentionally introduce defects into the structure, and, although not yet embraced by materials scientists, they offer another promising avenue of imparting anisotropy.^[175,176]

Cords include ropes, filled braids (as opposed to the hollow braided tubes covered later in this section), and fibrous materials with other post-processing techniques including knotting. These materials are less commonly structured into textiles; however, some of the capabilities of these materials find function as materials for textile robots. Unlike common twisted yarns, braids do not twist under load due to their self-balanced enlaced structure, potentially motivating their current use as tendons in cable driven actuation systems. Conductive wires are braided to impart more flexibility as opposed to a solid core wire of the same gauge, and materials researchers have recently structured these wires into knit and woven textiles to be used as signal lines.

3.2. Textile Structural Formation

3.2.1. Wovens

Woven textiles are made by perpendicularly interlacing yarns in a machine called a loom (Figure 7). The yarns held in the longitudinal direction during production are known as the warp, while yarns that are inserted into these warp yarns in overlapping configurations are known as the weft. These directions may define the fabric’s mechanical properties; warp

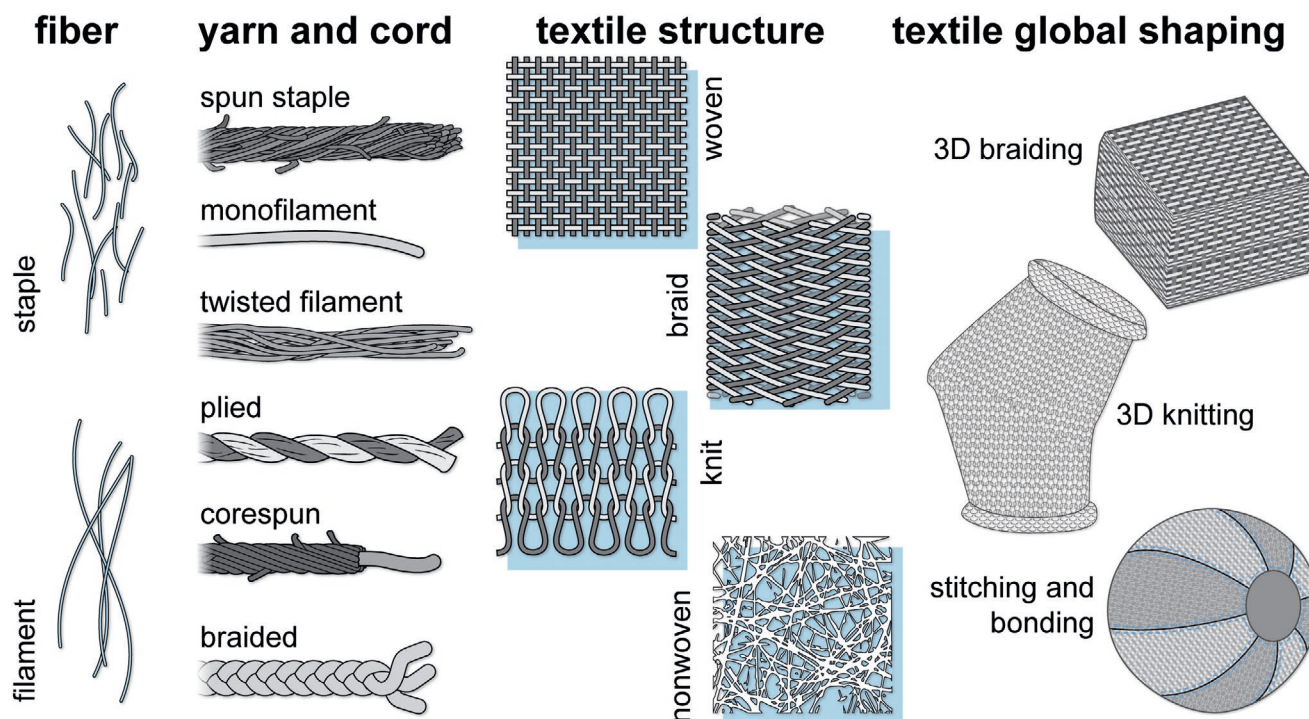


Figure 7. The hierarchy of textiles. Fibers are spun or twisted into simple yarns which in turn may be structured into complex yarns and cords (plied, corespun, braided). These yarns and cords can then be made into textile micro-structures. Some textile formation techniques, such as knitting and braiding, support 3D shaping during structural formation, while others, such as wovens, are typically formed into 3D structures through stitching and bonding.

yarns must be pulled taught for long periods of time in the weaving process, and therefore stiffer yarns are typically used, while thicker yarns are often used as the weft to improve production speed. By varying how the weft yarns pass over or under warp yarns in formation, the weave structure and textile properties change.^[177] Plain weave (a checkerboard pattern) is the most common, while twills impart a diagonal, and satins and sateens have long floats (lengths of yarn without interlacings). Jacquard looms allow for the greatest amount of design complexity in this patterning due to individual warp control (Figure 1a).

Wovens are typically non-stretchable textiles (e.g., a button-down dress shirt or a pair of jeans) unless elastomeric yarns are included in their structure. Wovens are used specifically for their high tensile stiffness in wearable robotics, exemplified by the use of narrow woven seatbelt webbing to distribute force in locomotion assistance robots.^[3,41] However, there is some inherent stretch in wovens. Because woven fabrics are formed with perpendicular 90° interlacings, when a force is applied at a 45° angle, also known as the bias direction, the textile can stretch because there are no yarns in a linear configuration in this direction. Regardless, when elastomeric yarns are incorporated into woven structures, unique mechanical properties can be achieved quite simply; for example, woven waistband elastic typically has a Poisson's ratio of approximately zero.

Machinery variations have enabled the production of more complex woven structures including gauzes that achieve the crossing of multiple adjacent yarns.^[177,178] By using looms with multiple warps, and subsequently cutting the two textile

layers apart, pile weave textiles, wherein additional yarns protrude perpendicularly from the structure, can be produced with increased material surface area (e.g. velvet).^[177] Although weaving perhaps lends itself least easily to the formation of 3D geometries based on standard equipment, multiple warp looms have been further developed and repurposed to produce 3D woven geometries. 3D wovens produced in this manner include solids where multiple layers are interlaced, as well as shell-like 3D spacer fabrics with large air gaps between connected structures, similar to cardboard.^[179,180]

Researchers have recently leveraged simple woven structures to create textiles with even more unique mechanical properties. Auxetic wovens have been formed on basic looms by inserting a combination of elastomeric and non-stretch yarns as the weft and varying the type of woven structure to produce blocks of looser and tighter weaves. Zulifquar and colleagues first demonstrated this principle with uniaxial elastomeric yarn insertion,^[181] while Cai and others translated this concept to woven textiles that could stretch biaxially.^[182,183]

3.2.2. Braids

Braids are familiar textile structures formed with three or more yarns, and typically are structured through machinery with sets of two or more of interlacing yarns, similar to wovens (Figure 7). However, unlike wovens, braids are produced when two or more sets of yarn carriers rotate in circular patterns (one set clockwise, and the other counterclockwise) to intertwine

yarns into a structure.^[184] A third set of yarns fed parallel to the formed length of the braid may be inserted in triaxial braiding.^[185] Braids are commonly produced with yarns at various angles (compared to the 90° angle standard in wovens), described by the “braid angle” between each yarn and an imaginary line parallel to the axial direction of the overall braid structure. This angle has consequences for the mechanical properties of the braid, as seen in McKibben actuators.

Braids easily lend themselves to simple 3D shell shaping. A predominant method of forming braids is maypole braiding, which may be performed by braiding around a circular mandrel^[184] and creating a braided textile that is pre-formed in a tube shape, depicted in Figure 1f; this technique is commonly used for McKibben fluidic actuators. Methods of creating more complex 3D braided shell structures by forming braids over mandrels with additional shaping have been suggested and demonstrated.^[179,186,187] In the fields of braiding and composites, these 3D shell shapes are known as 2D braids (because of the shell nature of the textile). Meanwhile, “true” 3D braids exist, but require additional systems of yarn carriers.^[179] For more information on the braiding process, we suggest these references.^[179,185]

3.2.3. Knits

Knits are systems of interlaced loops of yarns that afford the greatest diversity in terms of mechanical properties among textile structures.^[188] By varying the manner in which yarns interlock, very stiff and very stretchable regions of material can be made in a monolithic manner on one piece of equipment. For example, most people are familiar with the stretchable jersey knit of a T-shirt, but by adding inlay (or weave-in) yarns during the knitting process, taut linear yarns can be incorporated into one direction of the looped structure, forming a material with highly anisotropic stiffness.^[179]

The two automated knit fabrication methods are warp knitting and weft knitting. 3D flatbed weft knitting (or V-flatbed or X-flatbed knitting) can seamlessly produce a wide variety of microstructures and 3D shapes.^[188–190] Industrial 3D weft knitting machines by manufacturers such as Stoll and Shima Seiki are widely available for production manufacturing, and recently, a simplified benchtop version with core capabilities for prototyping has been developed by the company Kniterate (Figure S2, Supporting Information). In a weft knitting machine, rows of knit loops are formed by pulling new loops through previously formed loops in a horizontal, or “weft-wise”, manner, while in warp knitting individual yarns at each needle form loops in a “warp-wise” manner. For both knitting strategies, the rows of loops are called the courses, while columns are known as wales, and these directions typically have anisotropic mechanical stiffness, affecting the behavior of textile components like knit sensors.^[10,13]

The weft knitting process enables users to vary parameters like the loop length and yarn tension while also providing the ability to employ a wide variety of stitch operations.^[190] These stitch operations include knit (a loop), purl (a reverse loop), tuck (a loop made while holding the loop from the previous row(s)), miss (do not form a loop), and transfer (move the loop to a

different needle), which, when used together, alter the geometry and mechanics of the resulting knit material. Machines also enable the direct placement of multiple materials illustrated in Figure 1b through techniques like stripes (where the yarn type is changed at a row), plating (where a machine varies which one of two or more yarns is on the “face” of the knit), or intarsia (which enables discrete material placement within a row). Knitting machines also enable the simultaneous ability to impart global shaping of a material “shell” through operations called short row knitting, transfer-based increases and decreases, or formation of a tube using two separate needle beds. For more detailed explanations of the knitting machine operations and global shaping process, we recommend the following resources.^[113,189–191]

In soft robotics, several programmed material concepts, such as origami^[192,193] and kirigami,^[194] have been leveraged for actuator and sensor development to introduce directed and controlled anisotropy for desired kinematics or structural properties. Researchers working in the area of knit structure development have been able to use knit operations to incorporate similar structuring into knit textiles. Self-folding knits, reminiscent of origami, have been formed through alternating knit and purl loops^[195,196] (Figure 1d), or through varying the number of stitches in adjacent rows, forcing “bubbling” through short row and transfer-based increase and decrease shaping techniques.^[196] Unlike origami, these knit structures have the advantage that they can potentially be made in tubes without added adhesives or connection strategies, enabling complex shell structures like multi-branched tubes (Figure 1g).

Some of the same strategies for self-folding knits can be utilized to form auxetic knit structures. Zigzag blocks of knit and purl stitches^[197,198] as well as alternating horizontal and vertical knit and purl stripes^[199] have been used to form auxetic fabrics on flatbed weft knitting machines. Inspired by the kirigami process, knit structures with integrated holes and “hinges” function as auxetic textiles based on rotations of geometric planes.^[199] Although this section focuses on flatbed weft knitting due to the range of machine functions, other knitting methods such as warp knitting enable the production of unique materials as well; for example, auxetic warp knits have been structured with a hinging technique.^[200] Although not yet used in robotic garments, these programmed materials highlight some of the newest capabilities in knitting structuring and, based on their success in other soft robot implementations, may have potential in programming actuator motion or improving sensor performance.

3D flatbed knitting provides levels of automation not available with manual knitting and enables placement of variable knit microstructures, and thus mechanical properties, in specified areas on 3D shell shapes. However, programming the 3D flatbed knitting machinery is an infamously complex process where each individual needle operation must be controlled, with only a few experts able to produce full knit patterns.^[191,201] The description by McCann and colleagues may explain the process best; programming these machines is akin to “requiring all CNC machine users to write toolpath G-code by hand, or all computer programmers to work in assembly.”^[191] To improve the usability of 3D knitting machines, computer science researchers are developing new computer-aided manufacturing

software to control machine operations using methods for both global 3D shaping procedures as well as local microstructures.

Early work provided knitting patterns (although not machine code) for 3D objects.^[202] McCann and colleagues recreated this concept to translate basic objects to a compiler, providing machine operations based on tube and sheet primitives.^[191] Building on this work, machine instruction algorithms to improve yarn transfer operation planning for flat knitting were developed,^[203] as well as processes to produce knit objects from complex 3D meshes (e.g., STL files commonly used for 3D printing) that maintain the global shape of the object.^[204] This culminated in the development of a visual programming language for knitting machines by Narayanan and colleagues.^[205] Other researchers such as Wu and colleagues developed similar algorithm sets for hand knitting.^[206] Recently, Kaspar and colleagues have incorporated the use of neural networks into their design methodologies to enable weft knitting machine manufacturing instructions to be generated from images of knit fabric structures,^[207] further simplifying the knit design process. These advances parallel those of the 3D printing boom: lower cost equipment coupled with more user-friendly programming methods indicate we could be on the cusp of a knitting revolution.

3.2.4. Nonwovens

Nonwovens are some of the simplest textile structures, formed from fibers that are attached together through mechanical entanglement or chemical adhesion (e.g., glues or thermal bonding), or a mix of both strategies (Figures 1e and 7). Aside from some animal wool felts, these materials are not traditionally used as the main structural component of clothing because of their low flexibility and low durability^[208]; however, they have seen use as interfacing—that is, additional material layers to stiffen fabrics, to build structure, and as thermal and electrical insulation layers.

Generally, the nonwoven structure does not provide recoverable elasticity, but other useful mechanical properties can be achieved. Based on the fabrication strategy, fibers in nonwovens can be randomly distributed or highly aligned,^[208] directing material stiffness. In nonwoven textiles, mechanical anisotropy resulting from fiber alignment has found use in soft robotics to direct motion.^[209,210]

Methods of simultaneously forming nanoscale fibers and structuring them into nonwoven sheets has been of interest to materials researchers due to the fibers' high surface area to volume ratio, high porosity, and high flexibility. Some of these methods, such as pull spinning, enable 3D shaping of

the resulting textile.^[211] The use of fibers at the nanoscale has improved the response time of moisture-driven soft actuators due to high material porosity, while fiber alignment has improved bending range.^[212] Challenges in producing durable nanofiber structures that can be cut-and-sewn into larger structures have led some researchers to explore forming nanofiber nonwovens directly atop other existing macro-scale fabrics as composite materials and subsequently using relatively specialized technology, such as ultrasonic sewing, to bond these materials.^[213]

Although nonwovens can be particularly low-cost materials (stemming from their high production speeds), durability and processability appear to be challenges that transcend scale. Nonwovens have been used as the basis for some textile sensors^[214] and some actuating garments that do not apply forces to the body;^[112] however, these instances are rare. Currently, nonwovens are uncommon as actuation or sensing components in textile wearable robots, regardless of fiber scale. When nonwovens are used, they are often paired with other materials, such as other textiles or elastomers, in a composite structure.

3.2.5. Mechanical Properties across Textile Structures

The textile architecture can play a key role in governing mechanical properties of the material. For a general overview of mechanical behavior, **Table 2** provides experimentally derived mechanical properties of common textile constructions within textile classes. We do note there are some consequences of such generalizations. Different architectures (e.g., a rib knit compared to a jersey for knits, and a twill weave versus a plain weave for wovens) cause variation within these values.^[219,224,240] Even within one stitch architecture, textile design parameters, such as stitch density and knit loop length, can affect the mechanical properties.^[223] The constituent yarn materials and yarn construction may also alter material mechanics; a fabric made with thin wool yarns^[221] will behave quite differently than one made from thick Kevlar yarns within the same plain weave textile architecture.^[241] There is renewed interest in textile modeling in order to estimate these mechanical properties without the need for experimental parametric sweeps, which are lacking in the literature.

3.3. 3D Global Shaping of Textiles and Post-Processing Techniques

Although some textile structural formation techniques afford the ability to form 3D shapes simultaneously during formation

Table 2. Experimentally derived tensile properties for textile classes.

Textile structure class	Young's modulus	Stretchability	Poisson's ratio	Breaking force	Strain at failure	Sources cited
Woven (plain weave)	5–85 MPa, 20 GPD (grams per denier)	1–2%	0.2–0.8	130–800 N	7–40%	[215–221]
Knit (jersey knit)	0.035–0.65 MPa (with spandex) 6–35 MPa (without spandex)	<5–80% (estimated)	0.1–0.5	75–335 N	7–220%	[222–227]
Braided tube	3–80 GPD	1–3%	0.25–1.75	160–420 N	8–150%	[218,227–231]
Nonwoven	4–160 MPa, 0.5–45 GPD	0.5–4%	0.1–4	800–11750 N	1–55%	[232–239]

of the textile (as in 3D braiding and 3D knitting), a majority of clothing is formed through cut-and-sew techniques where pieces of flat textile materials are cut and attached at their edges to form 3D shapes. In addition to these shaping steps, other post processing techniques and “textile finishing” processes can be used to further modify the textiles and alter their mechanical and chemical properties, when developing active textile materials and wearable robots.

Stitching (or sewing) is the most common processes used to form 3D shapes from flat textiles. Stitching enables the mechanical coupling of textile materials without adhesives. In addition to attaching two textile sheets together, stitching can be used in a post-processing technique known as embroidery, where one or multiple threads are joined to a textile in a controlled and patterned manner. Stitched seam architectures vary greatly and can be leveraged for their unique mechanical and structural properties by materials scientists and roboticists.^[242] For example, zigzag stitches have been used to attach fiber-based sensors to base fabrics through a technique called couching,^[243] and overlock stitches have been used to form strain sensors because they stretch readily due to their looping structures.^[244] Additionally, overlock stitches maintain the stretchability of knit fabrics chosen to define fluidic actuation profiles.^[14] Except in the case of embroidery, stitching is predominately performed by human operators and therefore suffers from resolution issues as discussed previously.

To overcome some of the challenges associated with stitching, including limited resolution and speed, lamination and bonding based processes have emerged as fabrication techniques in the development of wearable robots and their components. Adhesives such as liquid glues or thermally activated films have been used to attach components together: glues have been used to create airtight fluidic actuators^[245] and thermal adhesives have been used to connect signal lines to textile sensors, maintaining electronic connections.^[13] Through these lamination-based fabrication processes, entire soft robotic gloves have been formed.^[66] Because adhesives form chemical bonds and not mechanical coupling, more care must be taken in terms of material compatibility to ensure delamination does not occur. An alternative method, ultrasonic sewing, uses high frequency vibrations to create heat and meld polymeric materials together without the use of additional thermal adhesives.

Post-processing, or textile finishing, techniques include dyeing, bleaching, coating, and heat treating. Similar processes are leveraged in the development of textile sensors, actuators, and integration components. Coating polymeric yarns using electroless plating processes has produced conductive yarn as heating elements in actuators,^[246] while processes like dip coating have created sensors.^[172] Heat-based processes are often performed in industry to set structures like pleats (Figure 1h) or ensure the dimensional stability of materials, and have been used to pattern areas of stiffness based on material melting temperatures in robotic garments.^[247]

4. Textile Actuators for Wearable Robots

Actuators in wearable robots exert forces upon the body or change garment shape. There are three main mechanisms

used: cable driven (or tendon driven) actuators, fluidic actuators, and shape-changing-material based actuators. Specifically, in cable driven robots, textiles route forces, anchor to the body and prevent slippage of the device, and improve user comfort with padding and by maintaining the wearer's range of motion. In fluidic textile robots, textiles program the actuation path and the actuator shape upon inflation and provide similar force-routing, anchoring, and comfort properties to those in cable driven systems. In textile robots employing active, shape-changing yarns, mechanisms including electronic, thermal, and swelling-based actuation approaches are incorporated into the fabric. In these mechanisms, the textile microstructure and global shaping directs shape-change. In cable driven and fluidic systems, a compressor or electronic motor is used to drive actuation, while the textile is a passive component used to preset mechanical properties. When shape-changing materials are structured into textile architectures, the textile itself is an active actuation component, but the robot may still require additional power components such as batteries.

4.1. Cable Driven Textile Actuators

Cable (or tendon) driven wearables use a passive, stiff, yet flexible cable that is pulled by an external mechanical actuation system in order to transmit force to the textile (Figure 8a). Devices spanning several application categories use this approach, including garments for reaching and grasping assistance,^[4,5,51,61,64] locomotion,^[26,27,41] haptics,^[127,248] and therapeutic compression^[154] (Figure 8b–d). In these wearables, cables connect to textile-based components that anchor to the body at specific locations to form mechanical linkages. The textile components and the cable are essentially passive transmissions, and a separate mechanical actuation box containing predominantly rigid linkage and gear actuation mechanisms and electric motors is where motion is generated.

The first textile component in these systems is the cable itself. Cables made from metals such as twisted and braided steel^[53,70,249] and polymers including aramid fibers,^[19] ultra-high molecular weight polyethylene cables,^[5,18,127,250] and woven seat belt webbing^[251] have been employed. Material characterization (bending stiffness, friction coefficients between relevant materials, tensile stiffness, etc.) of cables is rarely reported in the literature. This lack of detail is potentially because the materials are off-the-shelf and chosen to be essentially inextensible—for example, one type of webbing used as a cable has a modulus of 2.41 GPa.^[251] A key takeaway is that cable materials have high tensile stiffness and some degree of flexibility.

These cables can be coiled around a mandrel or used in a twisted string architecture,^[252] wherein rotary motion on the cable is directly converted into linear motion by their twisting. Cables are often protected from friction using sheaths (known as Bowden cables). When used in this sheathed configuration, because the sheath cannot change length itself, sheathed areas do not contribute to the actuation displacement. When areas of the cable remain un-sheathed and are routed through textile materials, the friction management between textiles and cables is non-trivial, signifying a need for further materials development in this area.



Figure 8. Cable driven actuators. a) A generalized schematic of a garment with cable driven actuation. b) Cable driven gloves assist with grasping.^[5] Alternative image provided by the authors and reproduced with permission. Copyright 2017, the authors. c) Cable driven locomotion assistance garments aid in walking and running. Adapted with permission.^[31] Copyright 2019, AAAS. d) Cable driven shoulder assistance devices aid with reaching. Adapted under the terms of the CC-BY-4.0 license.^[4] Copyright 2019, the authors. Published by Frontiers. Textiles are used in these robots in several manners: e) High stiffness fabrics, such as webbing, distribute forces. Reproduced with permission.^[3] Copyright 2015, ASME. f) These high stiffness fabrics are typically routed through anchoring points. Adapted with permission.^[31] Copyright 2019, AAAS. g) Textiles also provide padding and high friction to reduce robot slippage and improve wearer comfort. Adapted with permission.^[31] Copyright 2019, AAAS. h) Knitting research illustrates that cables can be routed through garments during the textile fabrication stage resulting in garments with actuating components such as a sweater with actuating sleeve. Adapted with permission.^[113] Copyright 2019, the authors. Published by ACM.

Aside from the cables, textiles are used to route forces on the body while remaining compliant so that the wearer is comfortable and can maintain their range of motion, especially when the robot is not activated. One key requirement of cable driven systems is maximizing the garment's tensile stiffness

to prevent suit slippage, to prevent shear forces acting on the body, and to maximize robot efficiency.^[41,253] Highly engineered textiles, such as woven seat belt webbing, have been used to maximize stiffness because of their high tensile modulus and flexibility^[3,19] (Figure 8e). Traditionally, these stiff textiles

are directly incorporated into anchoring points for the cables, fabricated through cut-and-sew processing (Figure 8f). This routing has a second purpose—it directs the force away from the sole anchoring point to distribute it around the body for wearer comfort.

Cable driven wearable robots are designed to distribute forces in order to minimize the peak normal force on the body.^[37] In addition to using stiff materials, textiles with high-friction coatings and padding layers, such as spacer fabrics, are employed to reduce slippage and dampen forces for comfort^[18,31] (Figure 8g). The design of the textile components also plays a key role. As intuitively expected, garments with larger surface areas and thus higher areas of human-robot contact have higher stiffness and more evenly distributed pressures. The addition of elastic textiles to predominantly woven garments improves pressure distribution at the expense of reduced stiffness.^[3]

In cable driven systems, a majority of the characterization has been done on base materials or in human-robot or test-rig-robot performance studies; however, oftentimes several textile-based manufacturing methods are used to stitch together many materials to form these garments. When using cut-and-sew processes, the continuity of yarns within these materials is destroyed and, in turn, seam strength becomes a major contributor to overall textile robot strength.^[180] The field of textile quality testing provides several methods to evaluate and understand the interactions between materials and garment formation techniques, such as seam strength tests.^[242] Durability of these garments is an area that has not been directly addressed in this field. Rarely are failure modes of textile devices reported, nor are the effects of washability on performance of these devices over time. Materials systems and durability testing could provide key insights into the challenges, and thus research directions, that materials scientists and textile engineers must tackle.

Although cut-and-sew processes are the predominant fabrication strategy for these wearable robots, recent work has explored the use of 3D knitting in developing cable driven actuators. Koerner combined the capabilities of 3D knitting with post processing to form high tensile stiffness areas with integrated anchoring loops for cables in an assistive glove. Two yarn types were initially knit into the structure, where a subsequent stream-treatment step enabled the low melt polyethylene terephthalate (PET) yarn to become more rigid, while selectively maintaining flexibility in the areas formed by high melting temperature yarns.^[247] Computational knitting work by Albaugh and colleagues investigated the direct incorporation of tendons into soft actuators^[113] during the textile formation process. Inlay (or weave-in) programmed course-wise (or horizontal) tendons, while yarn carrier tangling programmed wale wise (or vertical) tendons, and a combination of the two in an alternating pattern created diagonal tendons (Figure 8h). These strategies suggest a programmed material approach could be employed in developing monolithic textile-based cable driven wearable robots in the future, without stitching or bonding techniques.

Cable driven mechanisms can generate high forces—robots that actuate with more than 350 N of force have been reported in devices.^[41,254] These robots are especially good at high-speed actuation (systems with a bandwidth of 20 Hz for force control have been demonstrated),^[37] which represents an advantage over

most fluidic and active textile devices (discussed in detail later). These attributes make cable driven systems well suited for wearable tasks where high forces and high speeds are required, such as locomotion or grasping and reaching. Challenges outside the area of textiles remain, including reducing battery weight while extending battery life and reducing actuator bulk. Yet, when developing new devices using these classical linkage and gear actuation mechanisms, textile materials innovations have potential to further improve these robots' performance. Rapid and integrated methods of forming cable driven soft systems^[113,247] can potentially enable researchers to systematically study cable routing strategies, anchoring point locations, and mechanical properties of the textile for force routing and comfort.

4.2. Fluidic Textile Actuators

In contrast to cable driven systems, where a static tendon is repeatedly coiled through an external pulley system, some wearables change shape at the textile level. Fluidic textile actuators accomplish this shape-change when a textile-based pouch,^[16,255] or several pouches working in unison,^[22,256,257] are inflated by an external liquid or air source, which may traditionally include an air tank, pump, or compressor. Alternative fluidic power sources have been suggested^[258] and recently used in textile-based devices.^[259,260] These actuators either use a textile as a constraining pouch material and contain an oversized internal bladder (currently allowing for a larger design space in terms of textile structure) or are made from composite heat-sealable textile materials—fabrics with an integrated thermoplastic coating or lamination. The heat sealable approach allows for less complex, more streamlined manufacturing procedures and more predictable, less hysteretic behavior, as there are no effects of friction and entanglement between the constraining outer textile and internal bladders.^[245,261,262]

Because fluidic textile actuators rely on expansion of bladders, in addition to “pulling” as seen in cable driven systems, they are able to “push,” and are used to press up the limbs of a wearer as stabilizing structures.^[22,32,60] In these actuators, textile microstructures and textile-based patterning are leveraged to generate a wide array of functional motions for wearable robotics including contraction, extension, and bending. Graduated pressure levels within the same actuator have been used for the actuator to serve as a variable stiffness material.^[29] When approaching robotic garment development from a programmed-systems view, a fluidic approach may be quite promising if a garment requires several types of motions for one or more tasks because many diverse motions can be achieved. Similar to cable driven systems, textiles are used for anchoring to the wearer and providing comfort. To prevent redundancy, this topic will not be covered; instead the use of textile global shaping techniques and local microstructuring to generate actuation will be discussed in detail.

4.2.1. Textile-Based Linear Actuators

Braided textile pneumatic artificial muscles (PAMs) (or McKibben actuators) employ the microstructure of a braided textile

tube to constrain expansion of a stretchable bladder, causing the PAM to expand radially and contract along the axial direction when pressurized^[263] (Figure 9a). Braided PAMs are probably the most ubiquitous textile actuator and have been used in wearable robots since their inception in the 1960s.^[264] These actuators are now employed in many devices with applications ranging from locomotion assistance^[28,36] to elbow and shoulder motion^[265] (Figure 9b,c). As investigated experimentally as well as via modeling, the braid construction has a large effect on actuator behavior.^[262,266,267] During actuation, the braid angle increases from its initial braid angle towards a neutral angle of approximately 54°; afterward, no more contraction and expansion can occur because the forces are balanced.^[262,267,268] Thus, actuators with lower initial braid angles (i.e., closer to 0°) have greater stroke lengths and higher force generation capabilities.^[266] Braids with lower yarn densities (i.e., fewer strands per cm²) and reduced yarn thickness can enable lower braid angles and increase actuation stroke, increase work density, and reduce braid-bladder friction.^[262] However, the lower density of

constraining material means these braids are less able to contain the internal bladder, at times leading to device failure.^[269] Friction between the braid and internal bladder is a major cause of actuator hysteresis.^[261,262] By optimizing the textile-bladder parameters, contractions up to 30–35% strain and high forces >1000 N (dependent on the radius and pressurization) have been achieved.^[269,270] As this is a vast research area in itself, for more information we suggest reviews on these actuators and their modeling.^[267,271]

Knitted PAMs (a.k.a. “Paynter” PAMs) are a textile PAM variation that keeps a similar extensible bladder and replaces the braided textile tube seen in McKibben actuators with a knit tube for increased flexibility in the uninflated state. Because they are more flexible, knitted PAMs may be less restrictive on range of motion and increase comfort in wearables. These actuators were first proposed in a patent by Paynter in 1988.^[274] Ball and colleagues iterated on the design, developing a PAM from a circular weft knitted jersey tube made of ultra-high molecular weight polyethylene (chosen for its high stiffness and low

fluidic linear actuators

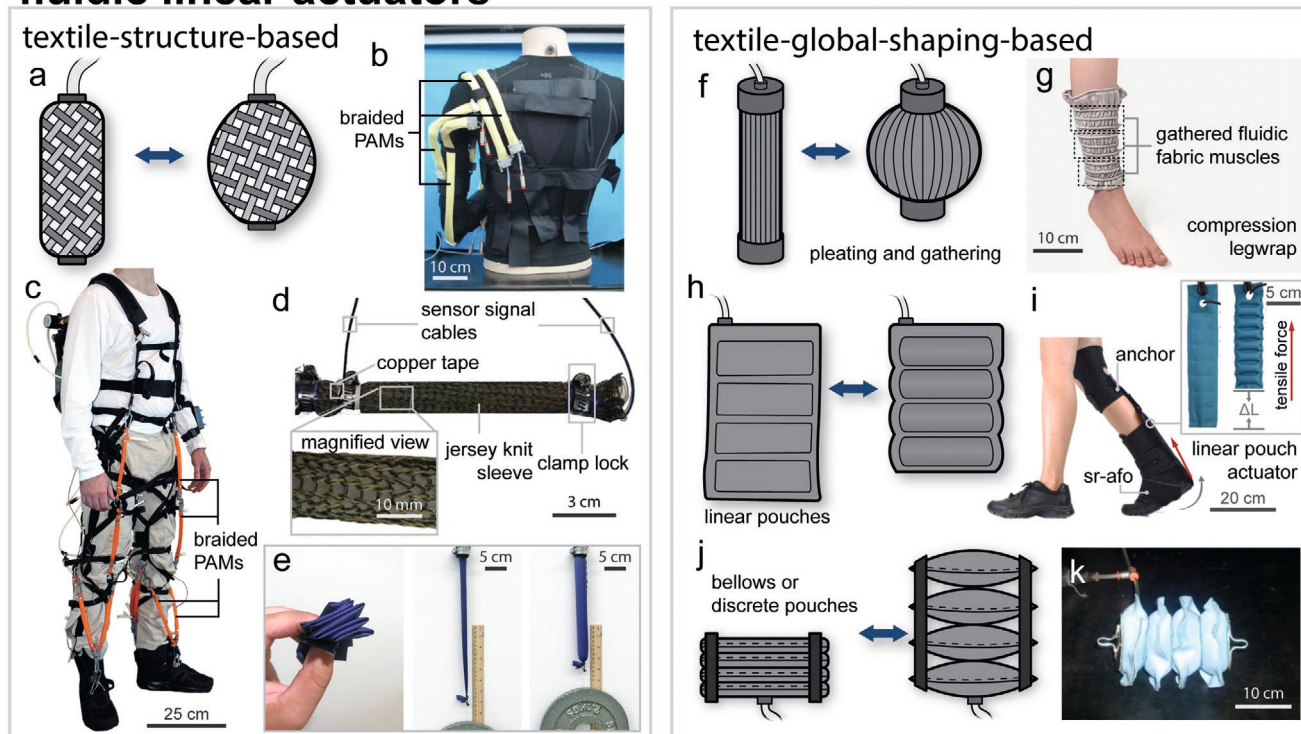


Figure 9. Textile-based fluidic linear actuators. a) Schematic of a braided textile actuator: a representative actuator that primarily employs the textile microstructure to create linear motion. b) Multiple braided textile actuators used to assist in shoulder motion. Reproduced with permission.^[265] Copyright 2017, Taylor and Francis. c) Assistive locomotion suit based on McKibben actuators.^[28] Alternative Figure provided by the authors and reproduced with permission. Copyright 2013, the authors. d) Knitting linear actuators from conductive fibers enables integrated strain sensing. Reproduced under the terms of the CC-BY-4.0 license.^[272] Copyright 2019, the authors. Published by IEEE. e) Heat-sealable wovens enable linear actuators to be flexible and hysteresis-free.^[245] Alternative images provided by the authors and reproduced with permission. Copyright 2020, the authors. Global shaping techniques are also used to form textile linear actuators. f) A representative schematic of a pleated textile actuator. g) Gathering enables woven textile sheets with integrated elastic tubing to behave as textile IPAMs.^[157] Alternative images provided by the authors and reproduced with permission. Copyright 2020, the authors. h) Representative schematic of linear multi-chamber actuators or inflatable servos. i) A multi-chamber actuator is used in an ankle orthosis to assist in plantar flexion, while remaining compliant and low profile.^[7] Alternative image provided by the authors and reproduced with permission. Copyright 2020, the authors. j) Textile-based bellows enable linear expansion. k) Textile bellows are formed with global patterning strategies. Reproduced with permission.^[273] Copyright 2014, Taylor and Francis.

coefficient of friction) containing a polyethylene bladder,^[255] and developed a model to predict actuation behavior. Due to the stretch of the knit structure, a shorter knitted PAM is able to produce the same stroke length as a longer braided PAM. Knitted PAMs have an expected trade-off; knitted PAMs achieve lower maximum force and lower energy output per stroke than their braided counterparts. Belforte and colleagues explored knitted PAMs further by first stitching off-the-shelf knits into PAM based tubes,^[275] and, in subsequent studies, compared them to stitched off-the-shelf wovens.^[276] Confirming the results of Ball and colleagues, they observed that a knitted fabric PAM had contracted more than a woven PAM upon inflation with increased hysteresis. Similar to the characterization in cable driven systems, no comments on the addition of seams and their effects were reported. Jamil and colleagues built upon this concept by knitting conductive yarns into jersey and rib microstructures to simultaneously act as the PAM constraining layer and displacement sensing component^[272,277] (Figure 9d).

Interestingly, researchers have only developed knitted PAMs in basic jersey and 1 × 1 rib knit constructions with single materials, opening up a multitude of research directions. One may wonder if other knit constructions (e.g., including self-folding structures or those with highly anisotropic stiffness) can overcome some of the force and hysteresis challenges.

Building on the increased flexibility goal, woven structures have been used as textile PAMs. Recently, Naclerio and Hawkes sought to develop textile PAMs that remained in a relatively planar geometry when uninflated while reducing the PAM hysteresis by using a woven heat-sealable textile (HST) in a bladder-free architecture.^[245] By aligning the woven materials such that their bias direction falls on the lengthwise axis of the actuator, a similar mechanism to braided PAMs can be achieved (with maximum contraction ratios of about 30%); however, because the textile is a precoated woven sheet, it is relatively flat, and bladder-textile friction is no longer present, reducing hysteresis (Figure 9e).

In addition to contracting actuators that require pressurization in their contracted state, expanding linear actuators may be required in robotic garments. For example, these actuators have found use in wearable robots for dressing, as the garment is required to be in the expanded state (needed for dressing) for a much shorter time than it is contracted (needed during wear), enabling it to be worn passively and actuated only during donning and doffing activities.^[89] Inverse pneumatic artificial muscles (IPAMs) expand axially in the inflated state (and are named to differentiate themselves from the majority of PAMs, which contract upon inflation),^[278] returning to their contracted state when deflated. Recently, elastomer-based IPAM implementations that rely on integrated fibers have been developed and implemented in wearables.^[89,279,280]

Fully textile-based implementations of IPAMs are also feasible. Braided McKibben actuators once more find relevance in this area. Although braided actuators are primarily known for their contraction, when the initial braid angle is larger than 54°, these actuators will extend in length and contract radially when pressurized,^[268] acting as inverse PAMs. The braid angle decreases until the 54° braid angle is reached, and larger initial braid angles (i.e., closer to 90°) will increase extension strains. The IPAM principle relies on material properties for strain

recovery (as opposed to a counteracting weight or pre-load in a contracting PAM), requiring highly stretchable and stiff materials to be employed for the IPAM to successfully return to its original reduced length. These material considerations may explain why elastomer-based IPAMs have been favored in wearable devices as opposed to textile-based implementations.

Textile linear actuators do not need to rely only upon the textile microstructure—global shaping techniques have been used to build and improve textile PAMs. Daerden improved PAM performance by pleating coated woven textiles (Figure 9f). This pleated PAM did not rely upon bladder and textile deformation, but instead unfolded to contract.^[261] Because there is no inter-yarn motion and membrane-braid friction, hysteresis is reduced. The pleated design enabled this actuator to achieve a stroke of about 41%, and modeling results suggest that increasing the number of pleats would further improve performance. Zhu and colleagues used another global shaping technique—wrinkling, also known as gathering—to produce textile IPAM sheets (Figure 9g). Woven textile sheets are stitched together, elastic tubing is inserted with a snug fit, and the fabric is pushed into a gathered (or wrinkled) configuration. When not pressurized, the elastic nature of the tube causes the fabric to return to a gathered form and contract. When pressurized, the elastic tube is constrained radially by the stitching and thus expands axially with strains over 100%.^[157] Other fabric integrated tubing configurations that did not include gathered structuring or a snug fit of tubing experienced lower actuation strains (in a contraction sense), highlighting the importance of the gathered structure architecture.^[281]

When developing global-shaping based textile linear actuators, planar implementations remain a design goal for low profile and flexibility. In a multi-pouch textile PAM, known as an “inflatable servo” in its first implementation in the 1960s,^[282] several pouches are linearly connected such that, upon inflation, the pouches change shape from flat to curved, causing contraction^[282,283] (Figure 9h). These multi-pouch PAMs have been used in wearables such as forearm sleeves^[284] and locomotive orthoses^[7] in place of cables for the same contraction motions (Figure 9i). Because of the planar design, automated systems to form multiple pouches onto one sheet have been proposed.^[284] In addition to coated textiles, plastic films have been used to successfully form these actuators,^[283] but a textile offers more resistance to tear propagation; however, coated textiles required to form an airtight bladder are slightly less robust than their uncoated counterparts due to the coating's hindrance of yarn motion.^[285] In order to maximize the contraction, the textile used should have minimal bending stiffness for the pouches to easily transition from flat to curved, as well as a relatively high tensile stiffness so that, upon inflation, energy is not used for elastic deformation of the material structure. Past textile-based systems have employed medium weight (70 Denier) heat-sealable wovens to accomplish this with a Young's modulus of 224 MPa.^[29,286] When considering other fabric constructions, a similar stiffness may be acceptable.

Globally patterned textile bellows expand from planar to 3D upon inflation, with similar behavior to IPAMs, in a single patterned actuator^[273] or in discrete multi-pouch architectures^[286] (Figure 9j,k). Unlike elastomeric IPAMs, these textile actuators can be pulled into a more open state if loaded and

are not typically used to lift hanging loads unless actuated by vacuum.^[273] Instead they act as “pushers” up until a point (after which they will buckle without any constraining support around their edges).

4.2.2. Programming Fluidic Textile Actuators for Bending and Complex Topographies

Aside from linear actuation, wearable devices often require complex motions, like bending, or the deployment of structures that are tailored to support the body. Some of the same strategies used to create linear actuators have been translated and refined in order to create bending, rotational, and lifting structures.

Similar to textile bellows, as illustrated in **Figure 10a**, multi-pouch actuation techniques rely on discrete pouches with relatively simple architectures attached at a hinge point to create torsional motion upon inflation. Thalman and colleagues attached these actuators to a textile base to be used in an elbow assistance device^[22] and used rigid retainers to ensure bending motion (**Figure 10b**). Nguyen and colleagues used three separate arrays of these textile actuator pouches in a wearable soft continuum limb that had arbitrary kinematics resulting from the inflation of specific pouches.^[287] Natividad and colleagues implemented this multi chamber actuation by having all textile actuators connect to a flexible elastomer base “spine” which enabled re-configurable quick connections (**Figure 10c**). The actuation profile could be arbitrarily changed by swapping the size and location of textile pouch actuators.^[257,288] Modular actuator approaches could face challenges in requiring the fabrication of many pouches to operate, but because of the pouch simplicity, researchers have automated the fabrication process using CNC methods to seal heat-sealable textiles into pouch modules.^[287] Additionally, because these modular actuators are primarily coupled through mechanical methods, this approach enables users to easily swap out failed modules with new ones.

At times, a modular, multi-pouch approach is not preferred in order to reduce device complexity, and thus reduce the number of potential failure points and minimize the number of fluidic lines required for actuation. Stitching- and bonding-based techniques have been used as global patterning strategies to create singular actuators with complex topographies in order to form structures to support the body (**Figure 10d**). O'Neill and colleagues used sewing to create woven constraining layers for a multi-chamber actuator and later a bifurcated bending actuator to fit under a wearer's arm for shoulder motion assistance and stabilization.^[16,60] Depicted in **Figure 10e**, their bifurcated design enables the arm to be “cradled and held in place.” In other instances, engineered actuator shapes are used to improve device mechanical performance. Sridar and colleagues illustrated that an “I” shaped actuator (akin to an I-beam used in construction) applied higher forces to the knee during actuation compared to an “O” shaped actuator when inflated to the same internal pressure.^[30] Global shaping strategies can also enable additional DOFs to be integrated into a system. Liang and colleagues first bonded a single piece of fabric in a tube-like manner to create a soft arm and subsequently bonded internal points on this tube to itself in different orientations

to create two joints for two DOFs.^[291] Khin and colleagues used a v-shaped inner fold to form a single actuator that could generate bending motions.^[292] Fang and colleagues stacked heat-sealable textile layers and bonded at the edges to form an accordion geometry for torsional actuation^[289] (**Figure 10f**). This accordion actuator was integrated into a knee-mounted device and provided torques as high as 25 Nm when inflated with 40 kPa of air pressure.

Simple global patterning strategies such as pleating and gathering modify the properties of a single piece of fabric or a simple actuator to direct unfolding upon inflation (**Figure 10g**). Two-actuator structures are common where a second, longer actuator can be attached to the first, shorter actuator in a buckled, pleated architecture, allowing bending and extension motions based on selective inflation.^[52,68,293] Yap has translated this principle of attaching a pleated linear actuator to a strain limiting layer for actuators used in soft gloves for finger bending assistance^[52] (**Figure 10h**). Pleating can be applied to one fabric sheet in a two layer actuator to cause unfolding for bending motions^[50,294] (**Figure 10i**). Zhou, Correia, and colleagues replaced pleating with selective gathering of a layer of fabric in two-layer bending actuators for the fingers. The gathering process simplified fabrication, while the selective location enabled actuator articulation for joint-like bending in assistive gloves.^[67,157]

Others used a combination of tendons and fluidic chambers to program and reprogram bending in inflatable actuators, leveraging the flexible nature of textiles to temporarily pleat or gather the structures. Stilli demonstrated this principle using three tendons routed through a textile-based sleeve that held a latex bladder for pneumatic actuation.^[295] Maghooa and colleagues built on this principle, adding more segments into their actuator.^[296] More recently, Nassour and colleagues placed a textile-TPU composite bladder within a textile housing that contained routed tendons.^[297,298] By pulling the tendons and thus modifying the housing length selectively through pleating, different bending, twisting, and elongating behaviors could be achieved by the actuators.

Recent work has reduced the number of actuators and complexity of actuator fabrication in wearables by leveraging diverse textile microstructures, programming variable areas of stiffness through cut-and-sew stitching and bonding techniques (**Figure 10j**). Wearables with one geometrically simple fluidic actuator have been exhibited for some motions, like ankle plantar flexion,^[17] but many fluidic-based wearables commonly incorporate several separate actuators,^[7,28] rely on one pouch with complex global shaping achieved through sewing,^[60] or employ multiple textile pouches in unison as one actuator in order to program motion.^[22,62] Such systems can take advantage of these textile microstructural techniques. Kadowaki and colleagues potentially initiated this direction in 2011 by inserting a rubber bladder between a stiff woven rubber fabric and a more stretchable textile, the structure of which is not described. The material mismatch created a bending motion upon inflation. By maintaining the configuration of the woven rubber and incorporating the stretchable fabric at an angle, a bending and twisting motion was achieved.^[20] Al-Fahaam and colleagues modified a braided IPAM actuator by reinforcing one side through stitching in order to constrain expansion, leading to bending,^[299] and used these actuators in an assistive

fluidic bending and complex motions

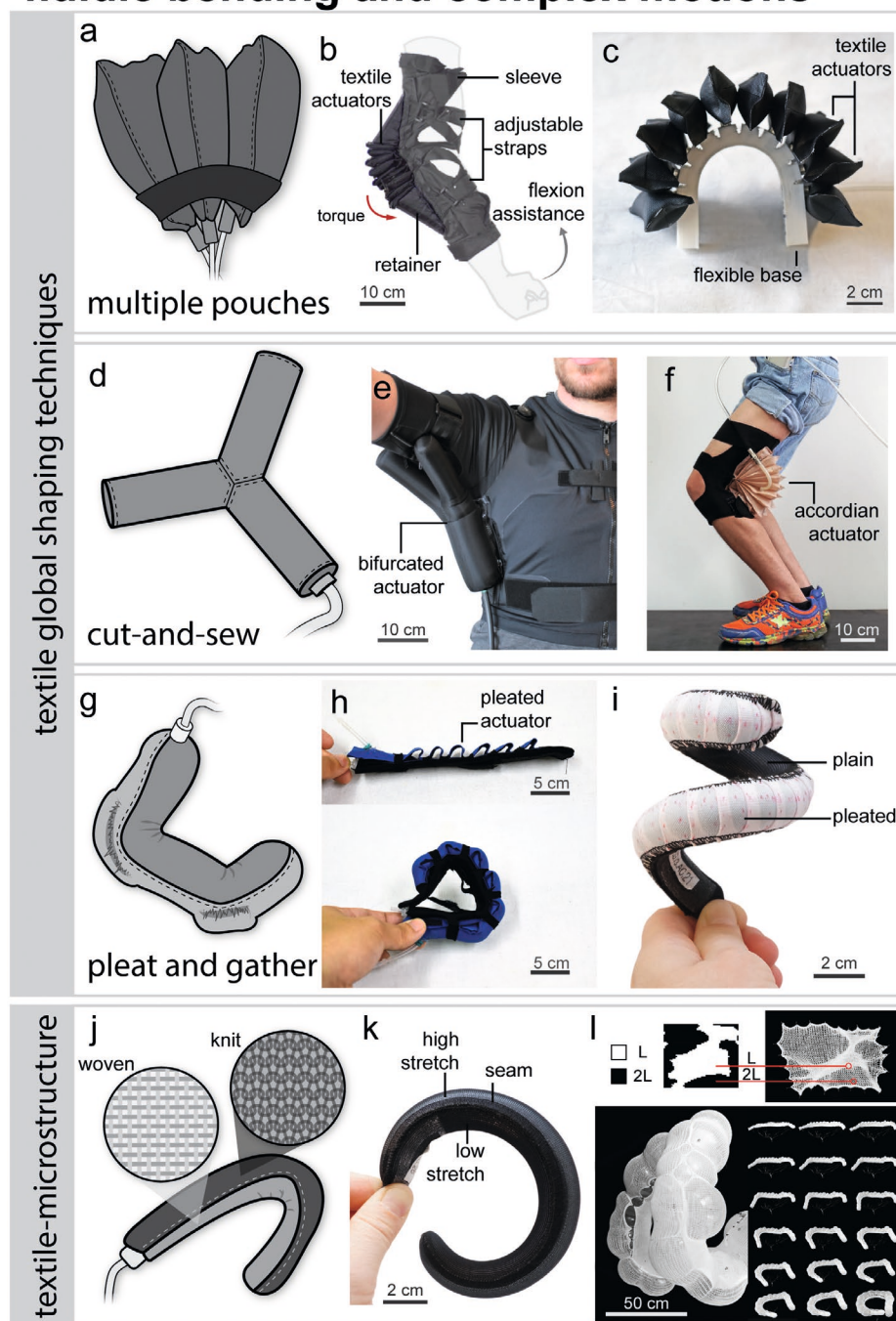


Figure 10. Textile-based fluidic actuators for bending and complex shaping. a) In a multi-pouch approach, actuators are asymmetrically constrained to induce bending. b) Attaching multiple actuators to a fabric substrate generated torques for elbow assistance.^[22] Alternative figure provided by the authors and reproduced with permission. Copyright 2018, the authors. c) Multi-pouch textile actuators can be selectively attached to a flexible base for a reconfigurable bending profile.^[257,288] Alternative image provided by the authors and reproduced with permission. Copyright 2017, the authors. d) Cut-and-sew processes attach several pieces of fabric to make actuators with complex shapes. e) A bifurcated cut-and-sew actuator cradles the shoulder to stabilize it in an assistive robot. Reproduced with permission.^[16] Copyright 2020, IEEE. f) Layers of heat-sealable textiles bonded selectively enable an accordion-shaped actuator to provide torsional assistance to the knee.^[289] Alternative image provided by the authors and reproduced with permission. Copyright 2020, the authors. g) Gathering and pleating adds more material fullness for motions such as articulated bending. h) Constrained pleating of a tube-shaped actuator creates a bending motion.^[52] Alternative photographs provided by the authors and reproduced with permission. Copyright 2017, the authors. i) Pleating on a knit pneumatic actuator creates bending when paired with a stiffer un-pleated material.^[6] Alternative photo provided by the authors and reproduced with permission. Copyright 2018, the authors. j) Leveraging the mechanical properties of varied textile structures can program actuation. k) A stretchable knit and a flexible, yet inextensible woven create a bending motion in fluidic actuators.^[6] Alternative photo provided by the authors and reproduced with permission. Copyright 2018, the authors. l) Jersey knit stitches of length l and $2l$ have different mechanical stiffness and program expansion upon on inflation. Adapted with permission.^[290] Copyright 2016, eCAADe.

glove for grasping.^[300] Cappello and colleagues built upon this work and developed an actuator by stitching together an effectively inextensible plain weave fabric and a relatively uniaxially stretchable warp-knitted raschel into a two sided pouch containing a bladder^[6] (Figure 10k). Further iterations employed bonding with TPU films to remove the bladder to reduce hysteresis and speed up fabrication,^[66] while Ge and colleagues employed rib knits as the second layer as opposed to a warp knit.^[68] Because of the balanced nature of the rib structure, the curling that is exhibited in other knits is minimized, making fabrication easier.

Multitudes of structuring strategies enable off-the-shelf textiles to program motion in inflatable actuators, and several strategies are oftentimes used simultaneously. Global shaping and multiple actuators has made devices for shoulder assistance,^[62] and gathering paired with textile microstructural programming have resulted in bending actuators for the fingers.^[6,14] Challenges remain regarding the extensive amount of operator involvement in fabrication. Researchers predominantly in the field of architecture have begun to explore knitting as a method to directly preprogram fluidic actuators. Baranovskaya employed a technique using the jersey stitch and varying the stitch lengths, L and $2L$, in a binary manner to program bending (Figure 10l);^[290] stitches of length $2L$ enabled more expansion upon inflation. Stitch density plays a key role in actuator behavior; in samples that incorporated the same ratios of L and $2L$ stitches overall, those with a higher spatial density of $2L$ stitches underwent more extreme bending upon inflation. Ahlquist and colleagues also investigated programming inflatable actuators through knit patterning by incorporating relatively inextensible “miss stitches” to create stiffer regions^[301] and by employing multi-gauge knitting. In multi-gauge knitting, the stitch length is altered, similar to Baranovskaya’s method, but this change in stitch length is accomplished by alternating knitting on every needle (making a stretchable region) versus knitting only on every other needle (creating a stiffer region).^[302]

4.2.3. Textile Jamming

Although most fluidic textile actuators fill with a liquid or gas to operate, others have used vacuum jamming to create variable stiffness materials that can support the body dynamically when needed. Jamming offers some key advantages—leaks can be less detrimental to actuator operation because the actuator can potentially self-seal, and flexible materials can be transformed to stiff materials while maintaining a low profile. However, there are trade-offs; because only an absolute amount of vacuum can be pulled and stored in a tank (i.e., up to 1 atm), compared to the nearly-unlimited potential for storage of a pressurized gas in a tank, it may be less practical to use a tank-based system in a wearable device, and a pump might be required for operation, increasing bulk and weight.

In order to create textile-based vacuum actuators, similar approaches to pressurized actuators have been used. Mitsuda investigated using stacked knit sheets in a vacuum

layer jamming approach and highlighted that the knit textile orientation (warp-wise, weft-wise, or alternating both directions) affected the jammed materials stiffness.^[117] By integrating the sheets into a glove, a wearable force display was realized. Li and colleagues used heat sealable textile pouches to encapsulate foam and plastic origami skeletons. Foam and plastic directed motion for artificial muscle actuators when vacuum was applied.^[193] Sadeghi and colleagues performed a preliminary feasibility study on further integrated textile jamming.^[303] They used a woven cotton fabric covered with plastic beads contained within a pouch. The beads acted as an interlocking mechanism when vacuum was pulled to improve the frictional contact, while the textile in an unjammed state remained flexible. The resulting stiffness of the jammed material scaled with bead size. Non-textile-based wearables with vacuum jamming have been used to provide resistance in haptic interfaces for training, games, and rehabilitation exercises.^[304] As this is a relatively new approach in the wearables space, this may be a topic to follow for new methods of using textile structures and other new wearable robot applications, such as variable stiffness protective sports gear.

4.2.4. Conclusions for Fluidic Textile Actuators

Volumetric expansion strains of textile fluidic actuators can be considered infinite—planar fabric pouches inflate to 3D structures—while strains of 41% and >100% have been realized for uniaxial contraction and expansion, respectively.^[157,261] Forces for fluidic actuators can be high: >1000 N is achievable^[269] and interaction forces of 450 N between a fluidic actuator and the body have been demonstrated.^[62] Actuation speed remains a challenge and bandwidth is dependent upon the chosen inflation pressure, which in turn can dictate the resulting forces. For example, a representative bandwidth of a braided PAM or McKibben system is 2.4 Hz.^[305] To overcome this issue, there may be some potential in carefully redesigning the actuator and system. The total volume of actuators in a system has been shown to affect the bandwidth exponentially,^[288] suggesting fabrication strategies, such as braiding and 3D knitting, may find function in developing global actuator shapes that can maximize force at lower volumes. Most fluidic actuators that use gas (CO_2 , N_2 , air) as a fluid simply vent to the environment to deflate, but researchers have looked to improve this process. These researchers include Teh, Goetz, and their colleagues, who sped up the emptying rate by including a vacuum chamber in their fluidic systems.^[122,306]

Several failure modes have been reported in these actuators. When using heat sealable textile laminates, pouch leakage and disconnections from fluidic tubing and fittings have occurred when over-pressurized.^[245,288] Some of these actuators have been successfully cycled up to 100 000 times with minimal performance changes.^[245] Delamination is less of a problem in cut-and-sew actuators with separate bladders, but these face different issues. Stitched actuators containing a separate bladder are afflicted by stitch failure, bladder “ballooning,” and fabric tearing at stitch interfaces.^[157] Monolithic textile constraining

layers (braids, 3D knits) can mitigate stitch-based failures, but ballooning of the bladder can still occur, especially when yarn density is low.^[269] Indicating these failure modes is a step in the right direction—work can be directed towards solving these problems, but there remains much work to be done in further studying the effects of long term cyclic actuation as well as device washability.

Because of the ease of production and large diversity of actuation profiles achieved using this method, spanning from artificial muscles, to bending actuators, to linear “pushers,” device-level implementations for many wearable robotic tasks include trousers for ease of doffing clothing,^[89] McKibben leg wraps to assist with ankle motion,^[307] and pouch-driven devices to improve range of motion of the shoulder.^[60] The diversity of achievable motions is promising as a path towards multifunctional devices with distributed actuators with specific programmed motions. A large frontier of opportunities in this area is related to efficiently and systematically designing these actuators, by pre-programming motion through textile structural design, as opposed to empirically developing such devices, relying on time-consuming prototyping and iteration cycles.

4.3. Active Yarn-Based Textile Actuators

Actuation utilizing active or shape-changing yarns enables electronic, thermal, and mass transfer (or absorption) based

actuation mechanisms to be employed for wearable robots. In the purest sense, these materials are shape-changing in the yarn state, and subsequently structured into textiles; however, “shape-changing yarns” have been used to describe actuators where an active yarn is subsequently structured into a textile actuator (**Figure 11a**) or when an existing textile structure is functionalized in order to actuate. The effects of the fabrication pathway on performance have not been quantitatively evaluated in scenarios where both strategies are possible (e.g., coating a yarn with carbon nanotube (CNT) particles before knitting and after knitting), and their differences may affect actuator behavior. For example, while coating a material in the textile structure, overlapping yarns may prevent uniform coating on each individual yarn; on the other hand, the high mechanical stresses and frictions induced during textile structuring could cause coatings to flake off, and both scenarios could potentially affect how well an actuator performs. In this section, we include both fabrication strategies to reduce redundancy, and we note that more work on investigation of the fabrication effects may be informative.

There are relatively few examples of full robotic garments using these shape-changing yarn strategies compared to the prior two approaches, and these garments are typically actuated through shape memory alloy (SMAs),^[88] fluidic,^[59] and environmental absorption-based approaches.^[99] Most of these devices have been actuation-focused and do not include closed-loop feedback control. We speculate that the

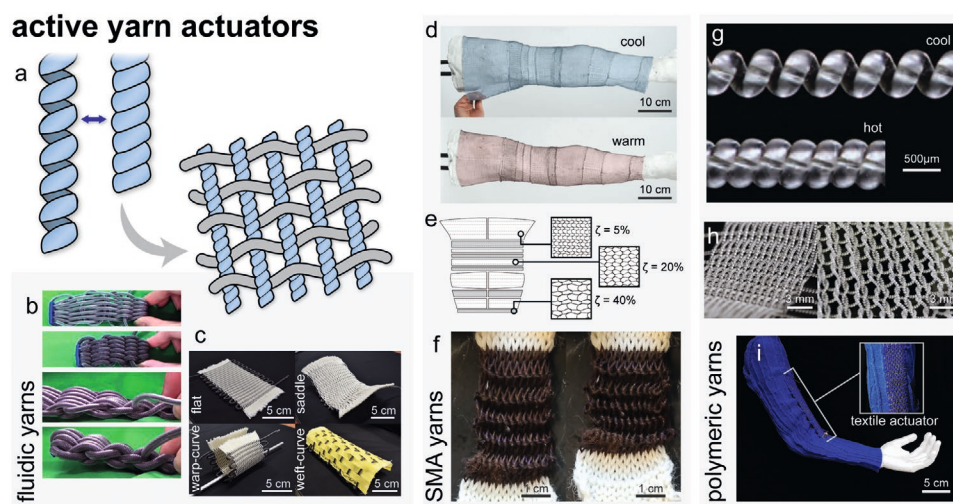


Figure 11. Active yarn actuators. a) Thin fluidic actuators, SMAs, and thermally responsive polymers act as active yarns and are integrated into larger textile structures. b) A woven fluidic yarn actuator undergoes greater contraction strains than those of the constituent yarns.^[59] Alternative photographs provided by the authors and reproduced with permission. Copyright 2019, the authors. c) By modifying the geometry and mechanical properties of passive weft yarns woven with fluidic actuating yarns, the actuation deformations in an unconstrained state can vary.^[9] Alternative photograph provided by the authors and reproduced with permission. Copyright 2019, the authors. d) Optimizing the knit loop geometry and SMA wire diameter enables variable contraction ratios in SMA knits for body topography matching in self-fitting garments. e) Indicative knit structures. Adapted with permission.^[88] Copyright 2019, Wiley. f) Drawing SMAs into microfibers and spinning them into yarn produces softer and more “knittable” materials while maintaining shape memory effects. Reproduced with permission.^[312] Copyright 2020, Wiley. g) Coiling is a common strategy to amplify contractile actuation of polymeric yarns, like nylon depicted here. Adapted with permission.^[313] Copyright 2014, AAAS. h) Coiled monofilament yarns have been woven (left) and knit (right) into textile architectures to amplify actuation forces and strains. Reproduced with permission under the PNAS license to publish.^[314] Copyright 2016, National Academy of Sciences. i) Spandex coiled actuating yarns woven into a textile, with conducting yarns for heating, assist arm lifting.^[315] Alternative photographs provided by Prof. Choi on behalf of the authors. Copyright 2018, the authors.

lack of full devices is because the research field is focused primarily on the materials themselves. Stemming from the materials focus: i) There are more stages to system development when compared to using off-the-shelf materials (i.e., textile yarns and fabric sheets), and with more stages come more possibilities to propagate failures from material to full wearable system. ii) The need to fabricate large amounts of material, and potentially structure it, is not feasible in terms of cost, time, and quality control using laboratory-scale setups. iii) The development of these materials is performed by a different community of researchers, wherein the material performance is the end-goal itself and devices are mainly proof-of-concept demonstrations.

4.3.1. Fluidic Active Yarn Actuators

Unlike fluidic actuators discussed previously in Section 4.2, fluidic active yarn actuators employ fluidic yarns that are in turn structured into textiles to program actuation. These yarns are typically braided PAMs (whose operation is described in Section 4.2.1) forming “Russian Doll actuators” through textile structure stacking. Similar to fluidic actuators, they have been integrated into wearables, sometimes in parallel with their development, such as in haptic posturing garments^[308] and arm-lifting assistive devices.^[59]

Funabara “wove” extremely thin (1.3 mm diameter) braided PAMs into a larger structure.^[308] The “woven” structure is a pseudo-textile because yarn friction did not cause the yarns to remain in place; rather, rigid polymeric junction clamps kept the structure together. Yet this proof-of-concept highlighted the value of textile structures. By controlling two sets of yarn (one on the face and one on the back) in both the warp and weft directions, the fabric “sheet” could bend and twist—realizing 3D motions from yarn contraction. Funabara later modified their fabric design to create a true textile and wove a plain weave structure from Lycra spandex and threaded braided PAMs through this textile at off axis angles (approximately 15° from the warp yarns).^[309] By folding the textile in half, these actuators appeared both on the face and back of the device and could realize forward to backwards and side-to-side bending motions as well as twisting motions.

In addition to creating out-of-plane motions, textile structures can improve PAM contraction ratios. Koizumi and colleagues discovered that by structuring braided PAMs into larger braids they could enhance the contraction ratio—their braided PAMs contracted 37% when braided compared to the 25% ratio of their constituent PAM yarns. However, the contraction force was reduced and this reduction scaled with braiding angle of the larger braid.^[310,311] In 2019 Abe and colleagues wove braided PAMs into a larger modified plain weave structure wherein two crossing braided PAM weft yarns were threaded through at each pass as depicted in Figure 11b. This structure resulted in an increase of the PAM contraction ratio by about 19%.^[59] They highlight that, even when only actuating the warp, the actuator saw increased contraction and they hypothesized that the rigidity of the braid maintains the woven structure and prevents out of plane

deformation during contraction, leading to this improved displacement. Hiramitsu and colleagues explored the effects of plain weaving a braided PAM as the weft and using yarns of different geometries and mechanical properties as the warp.^[9] Because the PAMs expand radially, they push the passive warp yarns into more exaggerated undulating paths, causing textile contraction. Based on their results, they suggest passive warp yarns should be flat with high bending stiffness, but not greater than that of the braided PAM in order to maximize contraction force. They also anecdotally illustrate the different effects of passive yarn geometry upon textile shape-change (Figure 11c), suggesting this area may benefit from further research.

Because of the material simplicity (i.e., off the shelf braids and elastic tubing), a fluidic active yarn approach may provide an excellent testbed to understand geometric and mechanical actuation effects of contracting and extending yarns. Aside from some of the previously discussed challenges in fluidic actuators, one issue in this approach is that the braids of different yarns may potentially interfere with each other through frictional effects or “clogging” during operation. Koizumi and colleagues observed that structures with more intersections between their constituent PAM “yarns” had more hysteresis and lower contraction force and hypothesized this clogging interaction was the cause.^[310] More work may need to be conducted on developing yarn systems that isolate the PAM yarns from each other while preserving their intra-yarn braid motion, which causes contraction in the first place.

4.3.2. Shape Memory Alloy Yarn Actuators

In shape memory alloys or SMAs, the actuation is generated from different crystalline phases that are favored at different temperatures. In the martensite phase, the material takes on an orthorhombic or monoclinic twinned crystal structure, while heating up to the austenite phase transforms the material to a cubic structure. Under adequate stresses, the crystal structure in the twinned martensite phase allows the material to become detwinned and elongate. Leveraging these phase changes, SMAs can be used as linear actuators by “preprogramming” the material at high temperature, cooling down the material to its martensite phase in which it elongates when a load is applied, and subsequently reheating back to the austenite phase where it contracts to the programmed shape. Subsequent loaded cycles between both phases through heating and cooling enable repeated actuation. SMAs represent one of the most mature fields in the area of active textile materials, and several devices have been developed. Textile-based wearable devices for self-fitting^[316] and active compression^[88,317] using knits made fully from active SMA materials, active compression garments consisting of discrete SMA fibers,^[158,318] active orthotics in which SMAs are patterned into a textile substrate,^[39] and shape-changing garments for visual communication using SMAs incorporated in a felted textile^[112] have been demonstrated.

Because SMAs are conductive, they can be used as a self-contained actuation system by directly connecting a power

source to the ends of the SMA, applying a current to heat the SMA, and conversely removing the applied current to allow the SMA to cool. These materials have relatively low actuation strains (4–8%) in their native monofilament state,^[319,320] so methods of amplification have been used in textile actuators including coiling the SMA, which can lead to strains of $\approx 50\%$ with 0.25 N of force^[321] before integrating into a textile through interlacing,^[322] sewing,^[323] or discretely connecting SMA yarns.^[130,158,159,318] Textile structuring, namely knitting the SMA “yarns,” can also enable increased actuation strains. In one study, knitting enabled strains of $\approx 51\%$ at moderate forces (1.22 N) or strains of $\approx 4\%$ with enhanced forces (12 N).^[324]

Knit textile structuring can direct contraction and out of plane motion for SMAs. Because a rib knit self-folds into a waved architecture, Abel leveraged this property and illustrated that a 2×2 rib stitch could be used as a lifting actuator able to displace up to 6.3 mm at a force of approximately 20 N, with its maximum work achieved when displacing approximately 60 N of load over 4 mm.^[319] Using knit structures, Abel and colleagues illustrated that 3D pre-programmed shape-changes of SMA textiles could be achieved^[8,325] by varying the ratio and location of knit and purl loops, which changes the localized balance of the microstructured material, and by including transfer stitches. Achievable motions included folding, rolling, and localized torques. Eschen and Abel defined the simplest set of geometric parameters to describe SMA knit loop geometry as the knit index, a function of loop length and wire diameter.^[326] Knit actuator performance is a function of wire diameter and knit index; for example, the maximum percent contraction of an active knit scales with the knit index. A design tool for knit actuators was created using these findings. Granberry and colleagues leveraged these design guidelines and, along with 3D anthropometric scan data, were able to develop SMA knit structures that initially enable ease for garment donning and subsequently use body heat to contract to accurately match the topographical shapes of the wearer’s limb^[88] (Figure 11d,e). In addition to the knit and purl stitches used in these studies, more complex knit structures including needle lace with buttonhole stitches and needle lace with ceylon stitches can create SMA textiles that deform in an auxetic manner as well as shear during actuation.^[327] This research is indicative of a rich area that can benefit from continued knit stitch exploration.

Woven architectures have also been used with SMA yarns to direct bending actuation and multiply actuation force. Han illustrated deformation programmability by weaving SMAs into varying woven structures along with additional nylon warps and glass fibers as the weft. They subsequently formed composites with these textiles and additional layers of plain woven glass fiber fabrics using polydimethylsiloxane (PDMS) as an adhesive and recovering spring. The woven structure affected the bending behavior of their actuator—a plain weave created a higher bending deformation than a satin weave.^[328] Weaving enables multiple SMA wire “yarns” to be incorporated into a larger structure to multiply the force of singular yarns without generating the high bending rigidity observed in sheet metal. Skalitisky and colleagues wove SMAs with a modified narrow fabric loom in a plain weave process with a binder yarn at the edges. They illustrated that an SMA woven fabric

behaves like a collection of SMA wires in terms of stress, but had a lower axial stiffness (78% of that of unstructured wires).^[329,330]

The SMA yarn structure and textile-integration method must be compatible with each other. When coiled SMA yarns were stitched onto fabrics, the stitch length was set equal to the coil circumference so that the SMA could coil fully, and thus contract fully.^[323] Before integrating SMAs into textile structures, other groups modified the SMA “yarn” to incorporate additional functional properties: Han and Ahn reproduced the knit structures developed by Abel and first corespun their SMA (Figure 7) to prevent shorting between knit yarns and to increase friction to reduce slippage within their shape-morphing device.^[331] Yuen and colleagues included SMP sheaths and an external conductor on their yarns to set and hold actuation-induced stiffness.^[332] Weinberg and colleagues created NiTi microfilaments through a novel drawing method and utilized yarn spinning techniques to spin these microfilament bundles into twisted plied yarns (Figure 7) in order to produce SMA yarns with reduced bending stiffness when compared to filament wires of the same diameter.^[312] These yarns are more “knittable” because of their reduced bending stiffness, enabling textiles with higher yarn densities and improved wearability while maintaining similar shape memory effects to those seen in monofilament SMA knits (Figure 11f).

SMA actuators are promising: they are often formed from commercially engineered materials, they can be successfully integrated into textile structures using several techniques, and they achieve relatively high strains and forces through textile hierarchy with rapid contraction rates relative to body motions. However, there are several key challenges in implementing SMAs in wearables: i) SMA textile actuators overall have a fast contraction speed, but their expansion is quite slow because the wire must cool to the environment. ii) The temperatures required to heat many SMA actuators are non-trivial, reaching over 100 °C.^[333] For such devices to be safely worn on or close to the body, they need additional insulating layers, but as these layers prevent heat from escaping, they may further slow the cooling rate. iii) As most SMA actuators are made from metal filaments, they may cause wearer discomfort due to weight and stiffness, although recent efforts show promise in mitigating this issue.^[312]

4.3.3. Thermally Induced Polymeric Yarn Actuators

Shape memory polymers (SMPs) are able to actuate in a thermally-induced manner, similar to SMAs, but SMPs can possess higher intrinsic recoverable elastic deformations than SMAs (up to 800% compared to $<8\%$), have lower densities ($0.9\text{--}1.1\text{ g cm}^{-3}$ compared to $6\text{--}8\text{ g cm}^{-3}$), and are less expensive ($<\$10\text{ lb}^{-1}$ vs $\approx \$250\text{ lb}^{-1}$).^[334] However, there are trade-offs: recovery speeds are slower than SMAs and stresses generated are two orders of magnitude lower than those of SMAs.^[334] In addition to a thermal stimulus, SMPs have been developed to be responsive to other stimuli as well, including pH and light.^[335] SMPs are beginning to see incorporation in robotic garments, including those for dressing^[91] and arm lifting assistance.^[315] In a typical SMP cycle, the polymer is deformed at

a temperature higher than its SMP transition temperature, then it is subsequently cooled (below the transition state), and the load is removed, freezing the polymer in this new shape with minimal recovery. When the polymer is heated once more above the transition temperature (in an unloaded state), the polymer chains become mobile, stored strain energy is recovered, and the polymer returns to its initial shape.

In coiled polymer yarn actuators, this process is slightly different: 1) in an actuator, the load is not typically removed during operation, and 2) the actuator is usually not frozen or set in place, although some textile applications have used this feature of SMPs to freeze other fabric actuators in place^[332,336] or to create variable stiffness fabrics.^[337] Instead, a mechanism slightly more nuanced for semi-crystalline monofilaments drives actuation. Although typical thermoplastic monofilament yarns are engineered to have highly aligned polymer chains through thermal drawing, creating crystalline microdomains, aligned yet semi-amorphous regions still exist within many of these polymers. These amorphous regions are where the majority of motion occurs. The amorphous regions link crystalline domains in a highly extended low volume fraction state (meaning they are stretched out linearly but are not closely packed). When heated, these molecules' moduli increase due to the thermodynamics of rubber elasticity pulling upon the crystalline domains, thus contracting the monofilament axially.^[313]

Similar to SMAs, in order to improve actuation stroke, coils and twist are incorporated into these yarns. As illustrated by Haines and colleagues, the tensile stroke of heating-induced contraction is amplified,^[313] enabling substantial contraction strains of up to 49% for nylon yarns (Figure 11g). Actuation frequently requires high temperatures (often ≈ 100 °C or more depending on the polymer),^[313] and using higher actuation temperatures has been reported as a method to reduce hysteresis.^[338] Integrated conductors used for resistive heating enable heat to be directly applied to the polymer, reducing heat transfer requirements and enabling these active yarns to be self-contained systems. Haines implemented twisted CNT fibers as the conductor, and other researchers later employed simpler, potentially less hazardous, and lower cost implementations, including using silver paint on nylon fibers,^[339] plating through lab-prepared electroless silver plating processes on PET yarns,^[246] and simply using off-the-shelf conductive silver-plated nylon yarns as the base for coiled actuators.^[340]

Polymeric material innovations have also led to improved performance. To improve the strain performance over long-term cyclic use, Yang and colleagues used a less crystalline polymer, spandex, in the same coiled architecture and saw improved long-term actuator repeatability.^[341] Fan and Li incorporated a cross-linked poly(ethylene-co-vinyl acetate) into the coiled structure because they argued chemical crosslinked shape memory polymers ensure a stable network and enable tunable actuator behavior through modifying the degree of cross-linking. Actuation strains of up to 68% at a temperature range from 20 to 67 °C (a change of 47 °C) were achieved,^[342] much lower than those observed in nylons. Minimizing the required actuation temperature remains a research goal, especially in a wearables context in order to maintain wearer safety without requiring additional insulation layers. Kanik and colleagues took a multi-material approach and formed a coiled actuating yarn with a bimorph

fiber formed from high density polyethylene and a cyclic olefin copolymer elastomer through thermal drawing.^[111] They chose these materials for compatibility with thermal drawing, driven by viscosity matching, and to maximize the difference in negative thermal expansion between the materials, which they believed further reduced the temperature to drive actuation. This strategy proved effective; for example, a 50% contraction strain with a temperature change of only 14 °C was possible.

Another approach is to use a different class of materials—Roach and colleagues leveraged liquid crystal elastomers (LCEs), which undergo shape-change by a transition between nematic and isotropic states upon a stimulus, achieving rapid shape-change.^[343] By using a custom fabrication process, lengths of LCE relevant for textiles were produced and strained, thereby aligning the LCE mesogens as required for operation. By transitioning from -20 to 120 °C (a change of 140 °C), an actuation strain of 51% was achieved. Although the temperatures required here are high, LCE yarns have not been explored in detail, potentially because of alignment challenges, highlighting an important first step. Although heating elements are not typically included in these materials' chemistry innovations, they should not be ignored because they must meet the strain and adhesion requirements of the yarns.

Polymeric actuating yarns have been integrated into textiles. Roach and colleagues incorporated LCE yarns as threads by sewing them through woven and knit structures to create actuation directed by passive textile structuring. Knit tubes contracted and expanded radially, and sewn knits with mountain and valley seams folded upon heating of the LCE yarn.^[343] Haines and colleagues structured piled coiled actuating nylon yarns into braids. When the braid was kept radially constrained (i.e., wrapped over a rigid tube), it lifted a 630 g load by a 16.4% contraction strain. An additional effect was that pores between yarns decreased by 20.6%. Although the temperatures used to actuate were quite high (93 °C), the shape-change suggests potential for thermoregulation wearables.^[313]

Haines also explored woven textiles by plain weaving coiled polymeric nylon yarn actuators in the warp direction with spun yarns and silver-plated nylon conductors in the weft as structural insulating layers and heating elements, respectively. The woven actuators were able to provide 12% reversible contraction for a 2 kg load.^[313] Steele and colleagues wove the artificial muscle fibers developed by Haines into a textile using cotton and silver yarns as the weft for stability and integrated heating, respectively.^[91] Intuitively, more actuating yarns in parallel amplify actuator force, and they were able to generate a maximum of 6.5 N of force with their woven structure at 135 °C after 3.9 min of heating, compared to ≈ 0.7 N achieved by a single yarn (although the single yarn was only heated to 80 °C). Yang and colleagues used five of their coiled spandex yarns^[341] as warp yarns in plain weave flat and cylindrical woven structures with silver-plated nylon conductive fibers and acrylic fibers as the wefts.^[315] The cylindrical textile had a 32.7% contraction with a 10.3 N load, while the planar fabric contracted 34.3% with a 4.91 N load. By integrating a 12-yarn version of this actuator into a sweater, they assisted motion of a mannequin arm (Figure 11i).

Haines additionally formed their active nylon yarns into a jersey knit architecture through machine knitting (Figure 11h,

right), illustrating that the bending stiffness of these yarns is low enough to be compatible with knitting machinery; however, they provided no characterization of knit actuator textile performance.^[314] An additional variation in which coiling was not performed saw a CNT coated spandex polymer integrated into a knit textile by Foroughi and colleagues in a circular knitting machine (forming a knit tube).^[344] Here, the contraction mechanism remains the same, but there was no amplification step through coiling because the spandex exhibited high actuation strains on its own. Contraction strains of the knit textile were found to be up to 16.5%, when prestrained to 100% through loading, after heating to 70 °C.

Polymeric yarn actuators offer a lower cost option to produce actuating textiles when compared to their SMA counterparts. These materials offer high strains (>50% strains have been achieved in yarns without textile structuring)^[111,343] and are inherently lighter in weight than SMAs. Speed remains a major challenge, and actuation temperatures have been highlighted as an issue specifically for wearables^[315]; however, new materials improvements are beginning to alleviate these concerns.^[111] Unlike SMA yarns, little characterization of the textile structural effects on actuation behavior has been performed and rarely are parameters like loop length in knits or yarn densities in wovens noted. One can potentially assume that the lessons learned when incorporating SMA yarns into textiles would carry over into these systems; however, because a majority of these actuators are coiled, while SMAs are more commonly uncoiled in knits and wovens,^[88,329] the effects of coil friction and locking may need further investigation. Effects of passive yarns in these systems are also rarely considered. For example, passive weft yarns have commonly been used in woven architectures,^[91,313,315] but the bending stiffness of the weft yarns is not described in these articles. One may hypothesize that these yarns have low bending stiffness relative to the warp, but as seen in fluidic woven actuators,^[9] this area could benefit from more thorough characterization. Although the integrated textiles employ only simple architectures, and the nuanced effects of realized structures need to be studied further, these successful structuring steps shows promise for additional textile processing of these yarns.

4.3.4. Electronic Induced Absorption and Mass-Transfer Mechanisms

Electronic induced absorption-based or swelling actuation mechanisms create actuators in which the active yarn is designed to uptake another material or transfer material internally for motion upon application of an electronic stimulus. These materials typically expand upon a stimulus as opposed to thermally driven actuators (SMAs, SMPs), which contract. Some of these actuators employ a combination of active and passive areas into their design to program motion. One of the most common approaches is reversible electrochemically-induced ion absorption.

Some of the earliest work was conducted on CNTs, making them one of the most common materials classes in these actuating yarns. CNT yarns were developed in the early 2000s by drawing CNTs from a multi-walled CNT (MWCNT) forest

and hand spinning with motors.^[345] In CNT yarn actuators, a voltage is applied between a CNT yarn electrode and a counter electrode in an ionic solution. The suggested mechanism of actuation involves charge buildup that causes ions from solution to become attracted to the yarns, leading to ion insertion and intercalation. These ions and solvent cause the yarn volume to increase.^[346,347]

The conversion of this volumetric expansion to yarn motion is predominantly dictated by yarn architecture and boundary conditions. Chirality plays a large role in operation. When a yarn is unbalanced, meaning it contains twist of one chirality, when either constrained or unconstrained, torsional actuation in the form of untwist can occur.^[347] Similar to McKibben muscles (discussed in Section 4.2.1), CNT actuating yarns have a winding helical architecture. When this architecture is smaller than approximately 54° and the ends are constrained, the yarn additionally contracts when the volume increases.^[347–350] Furthermore, yarn architecture can improve tensile actuation. Coils, achieved through overtwist or winding around a mandrel, can improve tensile stroke tenfold in some systems because the torque generated through untwisting the yarn pulls adjacent coils together.^[348,351–353] Plying an overtwisted and coiled CNT yarn in an opposing direction creates a torque-balanced structure and allows for a self-contained structure that can contract without external tethering.^[349]

Most recently, designer yarn structures have been proposed to further improve actuation stroke and work. Kim and colleagues developed a three-level hierarchical yarn consisting of twist, plying, and coiling to optimize contraction stroke.^[354] Through their highly-architected structure they obtained a maximum tensile stroke of 15.1% for an applied stress of 36.4 MPa. Additionally, alternative materials systems have been explored, either to improve actuation performance or to increase manufacturability of electrochemically actuating yarns. Graphene has been introduced into to CNT yarns. Hyeon and colleagues used graphene specifically as a guest material to increase capacitance and improve actuation contraction, with a tensile stroke of approximately 19%.^[355] Qiao leveraged a CNT-reduced GO yarn to increase capacitance and enhance ion diffusion to optimize performance for low cost aqueous electrolytes.^[356] In addition to CNTs, polymeric and polymer-composite systems have been developed. Active yarns formed from organic conductors such as poly(3,4-ethylenedioxythiophene) (PEDOT) and polypyrrole (PPy) (PEDOT:PPy) applied to cellulosic fabrics and PET-CNT-PPy composites have been developed to actuate based on this ion-motion mechanism.^[353,357]

Recently, both the effects of alternative architectures as well as guest-host materials systems have been leveraged to improve actuating yarn performance. In 2019, Mu and colleagues created a new paradigm of a “sheath run artificial muscle”, wherein a twisted and coiled CNT yarn was coated with a polymer in a manner to prevent polymer infiltration into the base yarn.^[358] The polymer sheath acts as a returning spring, enabling repeatable, reversible actuation in several mechanisms based on the yarn-material system, including electrochemical actuation. A coiled CNT-nylon 6 yarn could provide a contractile actuation stroke of 14.3%, lifting a load for an applied stress of 36 MPa.

As these materials require an electrolyte bath and cycles are eventually limited by bath evaporation, they are somewhat

impractical for wearables.^[346] Some alternative strategies have been suggested. For CNT yarn actuators, the electrolyte solution has been replaced with paraffin wax to remove the need for a liquid bath and an additional electrode.^[348] Voltage could be applied to the yarn which would in turn expand the wax and contract the yarn. Polymer electrolyte gels have also been used. Lee and colleagues prepared a CNT artificial muscle and subsequently coated the yarn with a gel electrolyte to make an electrolyte muscle.^[349] Their solid state artificial muscle exhibited a maximum stroke of 11.6% for an applied stress of 12–30 MPa, which is slightly lower than the same muscle in a electrolyte bath which had a stroke of 16%. Actuators with other programmed motions have leveraged this approach. Wu and colleagues made a textile actuator in which a polymer electrolyte gel and ionic liquid were trapped within a knit fabric between two conductive ink layers.^[359] This actuator bends upon an applied voltage due to ion migration, could function in air, and demonstrated a maximum strain of 0.28% and a stress of 0.21 MPa using an input of 3 V at 0.1 Hz.

One specific class of gel-based actuating textiles that are gaining traction are plasticized poly(vinyl chloride) (PVC) gels, a type of ionic electroactive polymer. When these gels are placed between electrodes of specific geometries, the motion of ions deforms the gel with the application of an electric field (typically <400 V).^[360] This voltage is high when compared to some of the previously described strategies requiring ions to migrate within a yarn. Yet, when compared to dielectric elastomer actuators (to be discussed later), which rely on a similar architecture, PVC gel actuators demonstrate similar performance with lower voltages.

There are limited textile examples of these actuation strategies. Maziz and colleagues knit a 2 × 1 rib and wove a 4/4 twill from staple spun lyocell yarns and subsequently coated the fabric with PEDOT:PPy.^[357] Using an electrolyte bath, a counter electrode, and a reference electrode, they could drive ion migration and actuate the fabric, and they observed effects of the textile structure on performance. Including more functional woven yarns in the structure slightly improved actuation force and displacement, while using a knit structure greatly improved actuation strain. When knitting a 1 × 1 rib with spandex yarn as the core (instead of lyocell), the actuation strain was amplified to 3%. Lee and colleagues created a solid state CNT artificial muscle braid by forming an anode CNT braid, coating it with gel electrolyte, wrapping this with a cathode CNT braid (Figure 12a), and coating once more with gel.^[349] With an applied voltage of 5 V, the muscle contracted approximately 5% with an applied stress of 24 MPa. PVC gel textiles have been formed by weaving core-sheath plasticized PVC gel yarns as the warp (and cathodes) through aluminum tubes as the weft (and anodes).^[361] Upon applying a 600 V stimulus, a 53% total contraction strain was achieved.

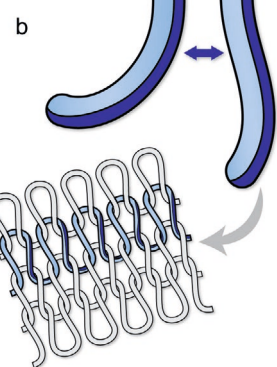
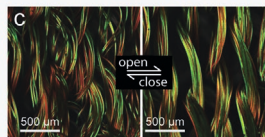
The majority of these mechanisms have been used for linear actuation, but other architectures are beginning to emerge.^[359] Originally, small actuation strains were achieved (≈1%); however, through the use of coils and hierarchical structuring, moderate actuation contraction strains of up to 16% have been realized.^[349] Furthermore, by using PVC gel actuating yarns in a textile-like structure, a contraction of 53% was possible.

active yarn actuators

electronic mass transfer



environmental mass transfer



dielectric elastomers

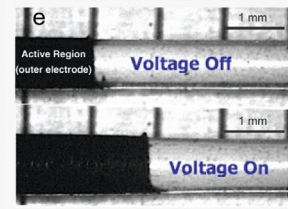


Figure 12. More active yarn actuators. a) CNT yarns are braided into a composite actuator through a maypole braiding process. Reproduced with permission.^[349] Copyright 2017, Wiley. b) Bimorph architectures have been used in actuating yarns to improve contraction and create bending motions. c) Knit bimorph fiber multifilament yarns expand and separate fiber spacing through humidity-induced actuation, changing the IR properties of the textile. Adapted with permission.^[349] Copyright 2019, AAAS. d) Textile composites with TPU layers and living cells act as bimorph actuators to open and close flaps in a garment for dynamic thermoregulation assistance. Reproduced with permission under the terms of the CC BY-NC 4.0 license.^[99] Copyright 2019, the authors, some rights reserved; exclusive licensee AAAS. e) Dielectric elastomer fibers expand under applied voltages. Reproduced with permission.^[362] Copyright 2007, Elsevier.

Actuation stresses can be relatively high. Loads resulting in stresses of 37 MPa have been lifted by these actuators.^[349] Typical actuation cycle speeds can fall within the 0.1–10 Hz range; higher speeds reduce the actuation stroke.^[349,359] These actuators can be driven by low voltages (typically <10 V except for PVC gel actuators) and gel electrolytes are replacing electrolyte baths, enabling more practical “solid state” actuators. Cost also may be a factor—these actuators are primarily formed from CNTs, which can be expensive, and although potentially lower cost conducting polymer implementations have been demonstrated as alternatives, their actuation strokes and forces have been thus far much lower.^[357]

4.3.5. Environmentally Induced Mass-Transfer Mechanisms

In addition to electrical stimuli, environmental changes can induce absorption and mass transfer mechanisms. Moisture driven—or hygroscopic—actuators are the prevalent actuator class using this mechanism. Actuating yarns swell in the presence of vapors or liquids based on their chemistries and drive textile shape-change.

Polymeric nanofibers have been leveraged for their high porosities and high surface area to volume ratios. Structured polyethylene oxide nanofibers with a passive polyimide layer created a bending actuator because the nanofiber region selectively swelled in the presence of humidity.^[212] The nanofiber structuring improved actuation time compared to films of the same polymer, while the linear morphology increased the overall amount of bending. Jiang and colleagues created an electrospun nonwoven bimorph actuator from a relatively passive layer of TPU and an acrylbenzophenone photo-crosslinker (APB), and an active layer from a thermoresponsive photo-crosslinkable copolymer of poly(*N*-isopropylacrylamide) and an acrylbenzophenone photo-crosslinker P(NIPAM-APB).^[363] Because of the unique properties of the P(NIPAM-APB) polymer and the relatively isotropic disorder of the nonwoven mats, when exposed to cold water the P(NIPAM-APB) swells slightly (7–8% increase in length and width) and the bimorph sees a slight bend, while when exposed to warm water the P(NIPAM-APB) contracts drastically (the mat becomes ≈40% of the area of its initial state), and the actuator undergoes an extreme bending motion in an opposing direction.

In addition to bimorph nanofiber mats, the bimorph architecture has been used in hygroscopically actuating textiles. Zhang and colleagues formed bimorph fibers (Figure 12b) with a hydrophobic cellulose triacetate component and a hydrophilic cellulose component, causing the fibers to actuate and change inter-fiber spacing (when bundled into a multifilament yarn) as a function of humidity (Figure 12c). By coating these fibers with CNTs, this spacing change can affect IR propagation because the intra-fiber length scales are comparable to IR radiation wavelengths, which can in turn modify IR transmittance through the textile.^[100] In addition to being used as coatings for modifying IR properties, CNT yarns themselves have also found applications as contracting yarns driven by environmental changes based on absorption of polar solvents and vapors.^[352]

Naturally derived and bio-hybrid materials also create moisture driven textile actuators. Silk is inherently hygroscopic and can absorb up to 40% moisture because silk fibers made from amino acids contain a large number of hydrophilic groups. Jia and colleagues leveraged this property in a yarn actuator where fibers from the *bombyx mori* silkworm were obtained and de-gummed.^[110] When exposed to water, the silk fibers predominantly expanded radially as opposed to axially. Because of this expansion modality, twisting single fibers and plying two twisted fibers together into yarns (in an opposing twist) increased actuation stroke. The fibers individually untwist because of their radial expansion when exposed to water molecules, causing the oppositely plied yarn to increase twist and contract with contraction strains up to 70%. Yin and colleagues further explored this mechanism by producing highly aligned nanofiber silk yarns through an electrospinning process and demonstrated that they could be driven to rotational actuation using sweat, although they observed lower contraction strains (3–8%).^[364] Liu and colleagues observed existing torsional behavior in untreated spider dragline silk fibers for multiple spider species, deducing these fibers must contain inherent molecular chirality (twist) in their proline-rich coils.^[365] This finding suggests another candidate

material with potentially improved response after additional hierarchical twisting is induced.

Integration into textiles is at an early stage. Jia and colleagues wove their silk muscle yarns into the warp of a plain weave using untwisted (and thus essentially non-contracting) fibers as the weft to create a uniaxially shape-changing textile.^[110] Mu and colleagues' previously discussed "sheath run artificial muscles" also find relevance here.^[358] Because these artificial muscles could be created with variable polymer systems (as opposed to CNTs), one such system structured into a weft knit textile saw reversible porosity change when exposed to water. Although not an active yarn, Wang and colleagues investigated using living *Bacillus subtilis* cells to create a biohybrid textile composite by coating thermoplastic polymer films with the cells. The cell layer contracted and expanded based on environmental moisture changes, bending these bimorph sheets^[99] (Figure 12d).

Environmental absorption textile actuators can achieve high contraction strains of up to 70% and can move loads with 18 MPa of applied stress at low contraction strains (≈1%), and at lower stresses (e.g., ≈15 kPa) can retain approximately 45% contraction.^[110] Because they rely on diffusion, moisture driven actuators are relatively slow. For example, average contraction rates of 1% s⁻¹ were reported in silk muscles and are on the high end for contractile moisture-driven actuators.^[110] Other solvent systems may be quicker—the majority of contractile stress of a solvent-driven actuator could be achieved in as little as 0.5 s^[352] (although a solvent droplet was directly applied to the actuator and it was not actuated by its ambient environment). The speeds of these actuators may not be a significant issue when used in certain wearable robot applications. In thermoregulation garments, the outcomes are temperature between the garment and skin and human comfort. For example, garments formed from textile-biohybrid hygroscopic actuators reduced the air temperature between the wearer and the garment by about 3 °C more than a passive control garment.^[99]

4.3.6. Dielectric Elastomer Actuator Yarns

Dielectric elastomer actuators (DEAs) are electroactive polymeric actuators that do not require any electrolyte bath for their operation, differing from electronically induced absorption mechanisms. In a DEA, a bias is applied between two electrodes with a dielectric in-between; the coulombic force causes the electrodes to compress the dielectric, which in turn causes the actuator to elongate perpendicularly to the applied field.^[366,367] This actuation method is promising for its rapid expansion and contraction speeds because it relies directly on electric fields and is not limited by absorption and diffusion. However, few implementations in fibers and textiles exist.

In 2007, Arora and colleagues reported on the successful development of fiber-based geometries for DEAs (Figure 12e). They formed DEA yarns through combining compliant electrodes of either sliver grease or an aqueous solution of calcium chloride, and they coated them with carbon-black-filled silicone using commercially available pre-strained silicone and polyurethane "fiber" tubes in microscale diameters (100–200 μm).^[362] For an individual polyurethane fiber, a maximum blocking force of 0.5 N was reached, while a maximum axial strain of

about 7% was obtained by a silicone fiber. The authors proposed that a next step would be to implement this mechanism in a scaled up fiber extrusion process in which continuous lengths of multi-material fibers are formed. They also suggested using modified DEA cross sections to achieve motions beyond axial and radial contraction and expansion, including bending.

Later, Cameron and colleagues explored this next step in fabrication by coextruding the core electrode from a graphite-based conductive grease along with a polyurethane dielectric layer through a melt spinning process and subsequently adding the exterior electrode through manual application; however, only small actuation strains (<2%) were possible.^[368] Kofod and colleagues improved upon actuation strain (<8%) by using dip coating to layer poly(styrene-*b*-(ethylene-*co*-butylene)-*b*-styrene) (SEBS)-carbon black composite electrodes and SEBS dielectrics upon a rubber scaffold.^[369] Their dip coating procedure enabled multi-layer actuating yarns, allowing for higher strains at lower voltages.

Although a fiber-based implementation has potential for wearables because DEA fibers could be knit, woven, or sewn into fabric, challenges remain in the fiber-based up-scaled manufacturing vision. Short lengths of fiber have been characterized,^[362,368,369] but translating these processes to long continuous lengths of fiber is non-trivial. The electrode and dielectric materials must be compatible to the same fiber formation process and to each other in terms of thermal, chemical, and viscoelastic properties to enable the production of contiguous DEA fibers without defects. Defects can prevent actuation due to dielectric breakdown and shorting of the electrodes, while causing potential safety risks.

Although not active-yarn-based, there are other alternative approaches recently explored to develop DEA textiles. Guo and colleagues chose a composite-manufacturing approach and produced a textile-elastomer composite hybrid DEA^[370] using commercially available conductive knit fabrics and elastomeric adhesives. They were able to achieve an electrode area expansion of 16.4% ($\approx 7.5\%$ and $\approx 9\%$ strains in the actuator x and y directions, respectively) at an applied voltage of 9 kV. The majority of displacement occurred within 1 second of applying the voltage. Xiang and colleagues built upon this work by comparing several commercially available fabrics and their performance as electrodes, opting for “ElectroLycra,” a silver-plated knit nylon spandex blend, based on its relative isotropy in strain between the warp and weft.^[371] In their resulting DEA they observed much less of an area change as a function of applied voltage than a DEA made with carbon grease electrodes (approximately 10% larger area compared to 100% larger area), but they did see a fast response time and less creep. They cut the textile composite into a kirigami structure to make a dynamic breathability material, potentially for thermoregulation assistance in wearables.

Although DEAs have high strains, high power densities, and can operate at high speeds,^[372] making them especially appealing for use in high-speed applications including haptics and communication, remaining challenges must be solved before they may see widespread implementation. The high voltages (typically >1 kV) required by DEAs pose a potential safety concern for wearers and create a need for miniaturization of the power electronics for portability. Developing DEAs

that require lower operating voltages through continuous fabrication methods with minimal defects may be necessary for wearable implementations.

4.3.7. Conclusions for Shape-Changing Yarn Actuators

Shape-changing yarn actuators offer a diverse set of materials-based actuation mechanisms, enabling a wide variety of stimuli to be used to actuate these systems, either through electronic or environmental means. As more of these materials are beginning to be incorporated into textile structures in order to direct forces and shape-change, more parameters relevant to textile-level implementations must be considered. For example, inter-yarn friction, bending stiffness, and yarn compressibility each play a key role in the tensile deformation of knits.^[373] And as discussed by Abel, active yarn motion within a textile is quite different from passive textile deformation,^[8,324] which has still not been thoroughly investigated for non-standard textile structures. Aside from the work on SMA knits, some of these properties have not traditionally been optimized, or even characterized, when developing active yarns. Research into these areas and materials optimization will need to coincide with textile integration and structural development.

In addition to understanding the textile-level deformations achieved by actuating yarns, a practical challenge remains in the ability to run these materials through textile machinery. Many active yarn materials such as coiled polymer actuators and SMAs have increased bending stiffness compared with that of typical spun apparel yarns. This bending stiffness can prevent textile processing. Earlier studies on knitting high bending stiffness yarns such as glass and Kevlar highlight that such materials can be knit, and several processing modifications that minimize simultaneous tensile and bending forces (such as yarn lubrication) can reduce yarn breakage, suggesting similar approaches could be employed for active yarns.^[374] For highly-architected yarns, such as CNT yarns and coiled polymer yarns, the addition of extreme amounts of twist and coils poses an additional challenge, when considering the potential for entanglement, snagging, and destruction of the engineered yarn structure (e.g., uncoiling). Passive “fancy yarns”^[175,176] with complex structures that contain outwardly protruding fibers, slubs, and coils have been successfully knit in standard knitting machines and woven in weaving looms,^[175,375,376] providing promising results when considering the implications for twisted and coiled active yarns. Precise preparation of the bobbin or cone that feeds the yarn into the machinery has been identified as a major factor in success.^[377] More work will need to be done to investigate if these successes will translate to active yarns, where the outcomes of structuring extend beyond aesthetic effects.

This overview of material-based mechanisms is by no means comprehensive of all soft actuators or artificial muscles; instead, it is specific to those implemented in fibers that have been demonstrated in textiles (e.g., that can be formed in lengths possible for textile structuring). Additional perspectives on active yarns and artificial muscles for robotics can be found in the following review articles:^[378] covers artificial muscles, while^[379] provides more literature on active fiber-based materials, and^[380] specifically details more information on active fibers used in textile

actuators. Last, a general overview on textile-based actuators which is mostly focused on the active materials approach has been written by Persson and colleagues.^[381]

5. Textile Sensors for Wearable Robots

Many sensors with relevance to wearable robotics are being developed, including yarn based electrodes for ion sensing,^[382] textile-based electrochemical sensors for analysis of sweat^[383] and other fluids,^[384] textile electrodes for analysis of electrical bio-signals from the wearer,^[385] and temperature and humidity sensors.^[386] Within the scope of this review paper, though, only mechanical strain and pressure sensors will be considered. In addition, the textile-based sensors discussed here will be classified into three categories based on how they are developed: fiber- and yarn-based sensors, textile-structure-based sensors, and textile composite sensors (Figure 13).

Several physical mechanisms are employed in textile sensors, including resistive, capacitive, optical, and triboelectric sensing mechanisms. Resistive sensors rely on repeatable modification of the distance and contact between conductive materials when a mechanical stimulus is applied. This change in conductor distance and contact as a function of the magnitude of the applied stimulus is reflected by a change in the measured resistance, and the sensor is restored to its initial resistance when the stimulus is removed.

Meanwhile, capacitive sensors are formed from two electrodes with a dielectric material sandwiched in between; the electrodes store charge separated by the dielectric, with the ratio of added charge to change in electric potential known as the capacitance. Most often, sensors are formed in a parallel plate architecture with capacitance described by the following equation:

$$C = \frac{k\epsilon_0 A}{d} \quad (1)$$

where C is capacitance, k is the relative permittivity of the dielectric, A is the overlapping area of the electrode plates, ϵ_0 is the permittivity of free space, and d is the dielectric thickness. Capacitive sensors are designed to take advantage of one, two, or all three of the variables that affect the capacitance value. The distance between the electrodes can change, the overlapping area of the electrodes can be modified, or the dielectric permittivity may be modified (e.g., it may allow air to escape, thereby creating a greater percent volume of non-air dielectric) as a function strain or compression.

Alternatively, optical sensors rely on the manipulation and subsequent detection of light passing through materials deformed by an applied stimulus. A common approach in textile-integrated optics is to use polymeric waveguides as sensing materials (which are at times intentionally lossy) and placing a light source on one end and a collector on the other. By stretching, pressing, or bending these waveguides, their optical properties change, altering the amount of light that is successfully transferred through the waveguide. Either this transmission alone or the transmission compared to its original intensity in an unstrained state, known as the intensity loss,

are reported. An optical sensor variation includes fiber Bragg grating sensors wherein a shift in the Bragg wavelength is measured.^[387]

Finally, triboelectric sensors rely on an imbalance of electric charge between two materials. When these materials come into contact, charge transfer occurs and equal opposing charges build up upon their surfaces. These charges create a potential, the flow of which can be measured when the triboelectric materials are connected to an external load. When the materials are released from contact, the generated charges neutralize and recombine, creating a potential (and consequently, a measured current) in the opposite direction.^[388] Commonly, the charge generation is used in textile devices for energy harvesting based on the wearer's motion, and both "voluntary" motions, such as stepping, as well as "involuntary motions," such as garment motion against the skin, have been exploited to generate friction between materials, and thus charge, in these systems.^[389,390] Recently, this charge generation has been exploited to create self-powered textile sensors for pressure, bending, and strain.^[391–393] At first these sensors were used as simple switches,^[394] yet through subsequent design of new architectures, they have been designed to measure loads and strains based on the currents generated.^[395]

Several factors are important for sensor performance, including linearity to applied strain, pressure, torque, or force (depending on the desired type of sensor), repeatability, range, hysteresis, bandwidth and response time, and sensitivity. The sensitivity of resistive and capacitive strain and pressure sensors is typically characterized by normalized metrics that enable comparisons. Researchers are also beginning to use similar metrics when evaluating triboelectric sensors. When considering strain sensor sensitivity, gauge factor (GF) is used:

$$GF = \frac{\Delta R/R_0}{\Delta L/L_0} \quad (2)$$

Where R and L are the instantaneous resistance and length, respectively, and R_0 and L_0 are the initial resistance and length. For capacitive sensors, the $\Delta R/R_0$ term can be substituted with $\Delta C/C_0$. GF can be negative or positive based on a sensor's specific mechanism. For example, the conductive particles in a resistive strain sensing yarn can be pulled apart, increasing resistance and leading to a positive GF. Conversely, conductive fibers within a conductive strain sensing yarn can be pulled together when stretching, resulting in a negative GF. Measurement electronics can capture either of these trends. The magnitude is often more important than the sign when determining GF.

When considering pressure sensors, the analog to GF is called the sensitivity. Sensitivity normalizes the change in sensor signal in response to a pressure, and can be evaluated as follows:

$$\text{Sensitivity} = \frac{\Delta R/R_0}{\text{Pressure (kPa)}} \quad (3)$$

Where R is instantaneous resistance and R_0 is initial resistance. Although any pressure unit can be used, in this review, we will use kPa as the preferred unit of pressure to maintain

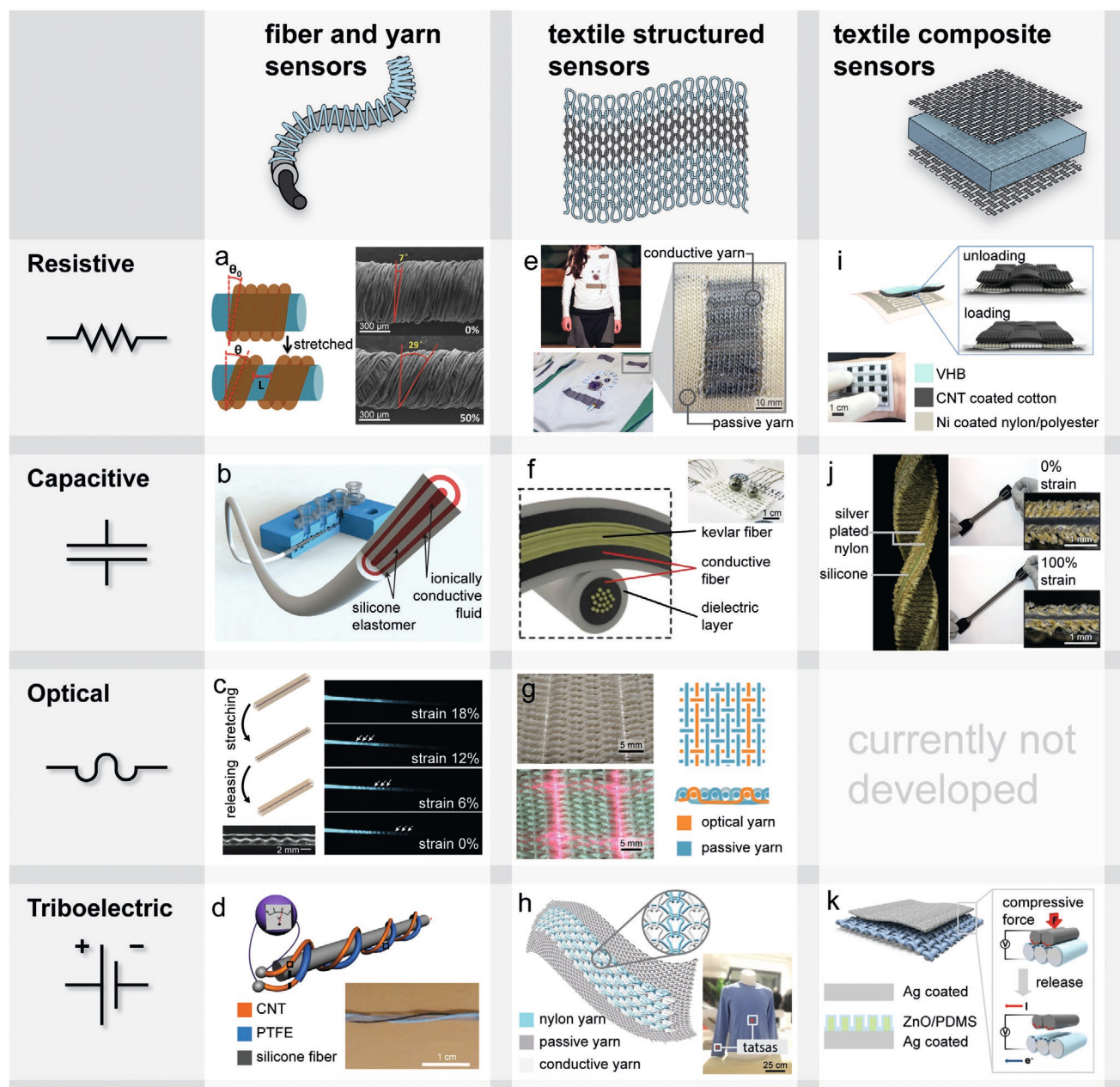


Figure 13. Textile-based sensors. a) Corespun yarn architectures create resistive strain sensors that vary resistance through changes cover yarn contact. Adapted with permission.^[172] Copyright 2015, Wiley. b) Coaxial multicore fiber printing produces stretchable dielectric and electrode layers for continuous strain sensing mono-filament yarns. Adapted with permission.^[170] Copyright 2015, Wiley. c) Thermal drawing techniques create stretchable monofilaments with complex internal architectures; the helical structure within these yarns is utilized in an unusual optical strain sensor based on helical straightening with applied strain. Adapted with permission.^[396] Copyright 2018, Wiley. d) Two intertwined yarns with different triboelectric properties are corespun around a stretchable core yarn to act as a self-powered strain sensor. Adapted with permission.^[392] Copyright Wiley, 2015. e) Changes in knit loop contact under strain cause conductive knits to act as strain sensors and 3D knitting techniques enable distributed sensor integration into a monolithic garment.^[10] Alternative photographs provided by authors and reproduced with permission. Copyright 2016, the authors. f) Variable contact between deformable conductive yarns in a woven textile can be made use of for capacitive pressure sensor arrays. Adapted with permission.^[397] Copyright 2015, Wiley. g) Pressure maps measure pressure and inform location based on networks of polymer optical fibers woven into a monolithic structure. Adapted under the terms of the CC BY 4.0 license.^[398] Copyright 2008, the authors. Published by MDPI. h) Knitting a conductive yarn and a nylon yarn side by side in a plating technique enables a triboelectric sensor from inter-yarn motion. Reproduced with permission under the terms of the CC BY-NC 4.0 license.^[395] Copyright 2020, the authors, some rights reserved; exclusive licensee AAAS. i) Composite pressure sensor based on piezoresistive CNT-coated woven. Adapted with permission.^[399] Copyright 2017, Wiley. j) Taking advantage of textile and elastomer properties creates a sensitive capacitive composite strain sensor. Adapted with permission.^[13] Copyright 2017, Wiley. k) By pairing two textiles with different triboelectric properties, a triboelectric composite that may act as a pressure sensor is formed. Reproduced with permission.^[394] Copyright 2015, American Chemical Society.

consistent comparisons. Similar to the approach used for GF, for capacitive sensors the $\Delta R/R_0$ term can be substituted with $\Delta C/C_0$, where C is capacitance. And akin to GF, the sensitivity metric can be positive or negative based on the sensor mechanism and behavior—compressing a resistive sensor may create more conductor contact, reducing resistance and resulting in a negative value, while compressing a parallel plate capacitive sensor can reduce dielectric thickness, thereby increase capacitance, causing sensitivity to be positive. Triboelectric sensors are beginning to be characterized in a similar manner, where the $\Delta R/R_0$ term is substituted for $\Delta V/V_0$ or $\Delta I/I_0$, where V is voltage and I is current. On the other hand, basic optical sensors are not usually described in this manner; either the transmission or the intensity loss (measured in dB) versus the applied pressure or strain is typically reported for these sensors. Two reasons for this anomaly may be: i) the field of optics is historically separate from electronics; and ii) because transmission and intensity loss (dB) are logarithmic, sensitivity values would “blow up” quickly. This discrepancy may signify a need for a simple metric to compare sensors across the board, regardless of mechanism.

These normalized values assist with quick comparisons between sensors and even enable such comparisons across sensors of different mechanisms, but they come with a caveat; they do not account for the range these sensitivity values span, often leading to misinterpretations. For example, sensors with exceptionally high GFs may only be linear over an extremely small range, with the remainder of the sensing range potentially nonlinear or not sensitive. It is important to consider the full story told by the data when evaluating textile-based and textile-integrated sensors.

In addition to general sensor performance metrics, some special considerations may be made when developing sensors for wearable robots. Strain sensors can be optimized for the relevant strains of human motion and actuator motion of the wearable robot (typically <100% strain). However, these sensors should be robust to extreme strains encountered during wear (imagine what might happen when snagging a jacket in a door and walking away). Similarly, the relevant ranges in detecting interfacial pressures between a person and a robot (e.g., pressure mapping in therapeutic compression robots), a robot and its environment (e.g., safety), and a person and their environment (e.g., insole sensors to detect gait) can guide sensor development. Some of these relevant guidelines are found in Section 2. As mentioned in the actuator section (Section 4), long term fatigue and washability are also of importance when considering sensors for robotic garments that can translate out of the lab. Sensor development has perhaps surpassed actuator research in characterizing and optimizing for these performance factors—cyclic tests measuring sensor readings over tens of thousands of cycles and are not uncommon. And while testing washability is not incredibly prevalent (approximately 15% for sensors reviewed), these types of tests are becoming more popular over time (Tables S7–S9, Supporting Information). At times, these tests only scratch the surface—for example, oftentimes in washability tests sensor baseline values are characterized, and performance under loading or strain is not reevaluated.

5.1. Fiber- and Yarn-Based Sensors

Fiber- and yarn-based sensors are discrete transducers that do not rely upon the interactions between neighboring yarns for sensor operation. These fibers and yarns perform successfully as sensors without being integrated into a textile (and many never make it to the textile stage). Sensors in fiber-based geometries enable the most manufacturing flexibility when programming a wearable robot—these sensors can be integrated into textile structures by weaving, knitting, braiding, sewing, and other fabrication techniques.

5.1.1. Fiber Formation for Monofilament Sensing Yarns

Fiber spinning techniques (e.g., wet spinning, melt extrusion, thermal drawing) create composite sensing yarns, enabling researchers to integrate new materials into a sensor. Fabrication process development can be non-trivial, and processing parameters, fiber architectures, and materials chemistries are often critical design parameters in fiber spinning techniques. These parameters can dictate simultaneous processability of the constituent materials, as well as deformation properties and adhesion in the finalized sensing yarns. A majority of fiber spinning techniques are developed to create essentially continuous lengths of sensing yarns, necessary for structuring into textiles at a later stage.

Some of the simplest sensors formed in this manner are conductive composite resistive sensors wherein conducting particles are introduced into a stretchable matrix. It is believed that these sensors rely on percolation and tunneling, where deforming the sensor macroscopically modifies the nanoscale tunneling distances between particles, thus modifying resistance. Bilotti and colleagues melt extruded a CNT-polyurethane (PU) composite fiber^[400] which acted as a resistive sensor with a strain range of 50%. They highlighted the effects of processing parameters—samples extruded at a higher temperature had lower sensitivity than those at a lower temperature.

Architectures of constituent materials in conductive composite sensors can affect performance as well. Lee and colleagues used a mix of monofilament spinning and coating mechanisms to create a silver nanowire (AgNW) composite strain sensor.^[401] They used a wet spinning method to produce an AgNW-poly(styrene-block-butadiene-block-styrene) (SBS) composite filament yarn and subsequently performed a cyclic process of dip coating with additional AgNWs paired with a solution-based reduction process to transform the AgNW into silver nanoparticles. Due to the effects of percolation theory and tunneling, this yarn could be used as a resistive sensor (GF=15 at 100% strain) and recovered up to 100% strain. They saw higher conductivities for AgNW embedded samples than those with silver nanoparticles and hypothesized that the AgNWs acted as bridges between gaps of the silver nanoparticles. Architecture can additionally affect durability. Resistive CNT/silicone-based strain sensing fibers with an integrated silicone elastomer sheath fabricated through a coaxial wet spinning technique could prevent shorting between sensing strands and protect the sensor during washing due to the sheath design.^[402] By tuning the CNT content of the sensor, the

strain sensitivity and range could be tuned; a sensor with 300% stretchability could achieve a maximum GF of 1378. Because of the external cladding, the baseline resistance increased by 15% after 10 cycles of washing—this change may be explained by the high permeability of silicone, enabling CNT leaching. In other electronic fibers, butyl rubber has been identified as a superior barrier material, although its stretchability is lower than some silicones.^[403]

Two-step formation processes can provide better control over sensing performance. The two-step approach consists of first spinning a fiber and subsequently modifying its architecture to create a sensor; this practice is most commonly utilized to create a hollow fiber sheath to be filled with a liquid as the active material for sensing. Zhu and colleagues used this technique by extruding SEBS (a thermoplastic elastomer) through a melt spinning process to form a hollow fiber, with fiber diameter modified by the spinning rate.^[171] They subsequently injected this hollow fiber with eutectic gallium-indium (EGaIn). Although designed primarily as stretchable conductors, these monofilaments undergo a resistance change when stretched due to a decrease in the conductor width coupled with an increase of the conductor path length. Others have since leveraged this strategy to intentionally produce sensors. Xi and colleagues developed a customized extrusion setup to create silicone microtubes to be filled with EGaIn to create strain sensors with a 120 μm diameter.^[404]

Coaxial extrusion techniques are also used to form core-sheath monofilament architectures relevant to capacitive and optical sensing without requiring an additional filling step, but the component material properties and interactions are more important in this case. Multicore-shell printing has been used to form coaxial capacitive sensing monofilaments consisting of alternating layers of silicone elastomer and ionically conducting liquid to act as a dielectric and electrodes, respectively^[170] (Figure 13b). When the yarn was stretched, the dielectric distance decreased, increasing capacitance. Strain could be sensed in a range up to 250% with a 0.348 GF and an overall extensible range of 700%. Leber and colleagues co-extruded two stretchable commercially available thermoplastic elastomers (TPEs) (Star Clear 1044 and Daikin T-530) with a vast difference in refractive index but relatively matched mechanical properties to respectively form the core and cladding of a stretchable optical fiber.^[405] Their resulting fiber could be stretched up to 545% before failure and saw transmission changes of approximately -40 dB with 300% applied strain and a 645 nm wavelength of light. This sensor was also able to detect bending and indenting. Coaxial fiber spinning can also produce resistive sensing yarns, such as those demonstrated by Seyedin and colleagues.^[406] By wet spinning a filament with a MXene/PU composite sheath and a PU core, a sensing yarn with strain ranges of $>150\%$ and GF of up to 12900 was achieved.

Building upon the structuring provided by coaxial extrusion techniques, thermal drawing processes have enabled researchers to impart additional geometric complexity within textile-scale monofilament fibers. In a thermal drawing fabrication process, a larger scale “preform,” typically consisting of multiple materials is created with other manufacturing processes, including molding, machining, and—more

recently—3D printing.^[407] This preform is then drawn (lengthened) under an increased temperature, shrinking its diameter drastically and forming long strands of monofilament fibers. Qu and colleagues used thermal drawing of preforms to create resistive, capacitive, and optical strain sensors.^[396] Their strain sensing optical monofilament includes a helical polycarbonate core in a SEBS copolymer cladding. The unique helical geometry straightens under strain, enabling output intensity to be increased when stretched (Figure 13c). To create resistive and capacitive sensors, they made hollow channels through these fibers and subsequently filled these channels with gallium, a liquid metal. Resistive sensors had a GF equal to 1.8 at 100% strain. These sensors were also sensitive to pressure, and a pressure sensitive fiber with an architecture that enables pressure location mapping and generalized detection of shear force direction was proposed. Leber and colleagues built upon this concept and used the thermal drawing process to create resistive pressure sensing fibers wherein the pressures and their generalized magnitudes could be localized.^[408] They created a unique architecture from SEBS as a deformable shell with highly structured internal geometries of carbon-black-loaded polyethylene as conductors. Depending on the amount of pressure applied, a corresponding number of conductors would come into contact with each other, enabling pressure sensing, while the position of the pressure input would reduce the total resistance linearly. Measuring both fiber ends enables two pressure points to be simultaneously detected.

Other mechanisms paired with thermal drawing have enabled localized pressure sensing within yarns. Yu and colleagues used thermal-drawing-based coextrusion to form a composite monofilament yarn from two copper conductors separated by a deformable SEBS layer, all of which were contained by a polycarbonate shell to strengthen the material stack for the drawing process.^[409] A high frequency signal is sent through these conductors and, when they are pressed, a difference in impedance resulting from a change in the distance between the two conductors can be measured. This impedance change reflects some of the incident pulse of the signal, and information from the reflection can be used to calculate a time domain which can help to reconstruct the position and magnitude of the pressure for two simultaneous locations. By modifying the materials in the system, simultaneous spatial and thermal measurements can be made.

Spinning sensing yarns often requires specialized equipment (e.g., screw extruders, thermal drawing towers, continuous coagulation bath setups) that can be expensive and challenging to operate, causing researchers to develop simplified methods of creating these materials. Zhao and colleagues explored using 3D printing and soft lithography in order to create stretchable lossy waveguides from a PU rubber core and a silicone composite sheath with very different refractive indices that were able to sense strain, bending, and pressure.^[410] Because of limitations in the molding process, near-continuous materials could not be produced. Other researchers have sought simplified continuous methods: For example, Li and colleagues fabricated CNT/PDMS composite sensing fibers by injecting a pre-crosslinked solution through screens with holes <500 μm in diameter^[411] and performing additional crosslinking to fully

cure. Their resulting resistive sensors showed high linearity, with the smallest diameter fibers (150 μm) having the highest GF of 2.08 and a strain range of 0–120%. These sensors also sensed temperature fluctuations and were tested for 20 000 cycles with only minimal degradation.

5.1.2. Yarn Spinning for Sensors

Yarn spinning techniques (Figure 7) may also simplify fabrication. Existing constituent yarns and fibers can be mechanically coupled into a sensing system without wet processing, can improve sensitivity by introducing additional hierarchy into the structure, and can enable sensing mechanisms not possible with only the constituent fibers.

For example, monofilament resistive sensing yarns can be formed into a capacitive sensing structure through yarn twisting. Cooper and colleagues plied two stretchable metal fibers with an EGaIn core and elastomer (Hytrel) sheath into a composite yarn structure for torsion and strain sensing.^[412] When the ends of the yarn are held constant and the yarn is twisted, a change in geometry between the two sub-yarns leads to an increase of capacitance. Furthermore, when twisted fibers are strained, an increase in contact area between the fibers causes the capacitance to increase, and strain can be measured. The twisted yarns also act as a capacitive touch sensor. Although touch sensing is needed in some use cases, this phenomenon additionally highlights that stray capacitance from the body may affect sensor readings in some implementations. Shang and colleagues used hierarchy to add durability by twisting CNT yarns.^[413] These yarns could act as force sensors, increasing resistance with applied tensile stress, as well as light and temperature sensors.

Corespinning (Figure 7) techniques couple multiple sub-yarns into one composite structure and are commonly used to introduce stretchability into inextensible materials for strain sensing. Huang and colleagues used a corespinning process to produce strain sensing yarns by wrapping a composite polyester-elastic core yarn with piezoresistive carbon-coated fibers.^[414] The piezoresistive fibers were loosely wrapped (spanning from 150–450 twists per meter) with no inter-coil interactions. As hypothesized because of this low-density architecture, there were no substantial effects on sensor sensitivity as a function of twists per inch. However, double wrapping the yarns in both clockwise and counterclockwise configurations resulted in a more linear sensor with lower sensitivity. Zhong and colleagues took advantage of corespinning for triboelectric strain sensors, wherein a CNT coated cotton yarn and a polytetrafluoroethylene (PTFE) coated cotton yarn were plied together and wrapped around a silicone core fiber^[392] (Figure 13d). Pulling the core causes contact between the exterior yarns, establishing the triboelectric effect, and current increased with applied strain, enabling triboelectric sensors with a range of 25% strain.

Aside from creating architectures required for sensing, corespinning has encased optical fibers in order to impart abrasion resistance, preventing cracks which scatter light,^[415] and to prepare them for future textile integration steps, such as weaving.^[416]

5.1.3. Coating for Sensing Yarns

Existing monofilament and spun yarns can be utilized as bases for sensors through coating processes. The interaction between the coating and yarn creates the sensing mechanism. Typically, a base yarn is selected as a passive scaffold for its mechanical properties, and functional, active materials (e.g., conductors) are subsequently coated onto this scaffold. Coated yarns can be some of the most facile textile sensors to produce, using processes as simple as dip coating off-the-shelf yarns. Conversely, illustrating the breadth of this technique, advanced materials manufacturing techniques like chemical vapor deposition (CVD) are also used.

Monofilament and multifilament elastomer yarns can form substrates for conductive materials to act as resistive strain sensors. Spandex and nylon 6 fibers have been used as relatively stretchable bases for CVD coating of PPY.^[417,418] SEM studies revealed that, when the yarns were strained, the formation of microcracks and their subsequent separation and reconnection resulted in strain-induced resistance variations.^[417] The contribution of crack geometry (length and width) is a good predictor of resistance, and models based on these geometric features can describe sensor performance.^[418] By using flexible and deformable, yet non-stretchable, base fibers and yarns, pressure sensors can be made in a similar manner.^[419]

Methods to improve conductor deposition and robustness have been explored for resistive sensor development. Wu and colleagues leveraged electrostatics and alternated coating a polyurethane rubber yarn with a conductive polymer composite formed from carbon black, cellulose nanocrystals (resulting in a negative charge), and positively charged chitosan as a mediator.^[420] Their resistive strain sensing yarn had a maximum GF of 70.6 and maximum strain range of 5%, and when washed with detergent, they observed a 23% change in baseline resistance. Zhang and colleagues investigated scaling up production and coated a TPU yarn in a continuous process by roll coating with a TPU-CNT composite film.^[421] The yarns acted as resistive strain sensors with GFs up to 4.3 for 10% strain, depending on CNT solution. Niu and colleagues utilized an adhesive-based layer by layer process and coated an existing stretchable polyurethane yarn by repeatedly dip coating the yarn with a polyvinyl alcohol (PVA) solution as adhesive and conductive reduced graphene oxide (rGO) nanosheets.^[422] A protective polydopamine layer was subsequently added by immersing the yarn in a dopamine solution. Through a microcrack separation and reconnection mechanism, the yarn acted as a resistive sensor with a notably high GF of 131.8 and a strain range of 90%. The coating enabled the yarns to be durable enough to undergo the textile structuring process and be integrated into a sensing fabric. Niu additionally performed fabric-level sensor characterization and discovered fabric had a lower GF of 25.3 at a 50% strain range, and performed washing simulation experiments.

Other coating techniques were designed to create additional hierarchy in structuring to impart sensing. Wang and colleagues prestrained their elastomer fiber, wrapped it with a CNT sheet, and released the prestrain to form a wrinkled hierarchical structure, a strategy used in surface engineering,^[423,424] forming a resistive strain sensor.^[425] By coating with a dielectric elastomer and repeating the prestrained wrapping process,

a capacitive sensor could also be realized. These hierarchical wrinkles allowed for extreme stretchability without sensor degradation due to cracked conductors. Interestingly, the coated base yarn or fiber does not need to remain in the final sensor. For example, Wang and colleagues created a resistive monofilament sensor by using twisted copper wires as a catalyst to grow graphene using CVD, and they then coated the graphene with polymethyl methacrylate (PMMA), used as a stabilizing adhesive, and etched the copper with ferric chloride, leaving a mostly hollow graphene/PMMA fiber.^[426] After subsequent removal of the PMMA with acetone, the remaining wrinkled graphene fibers were coated with PVA and could be used as sensors. The resulting sensors increased in resistance with applied strain due to the microcrack mechanism and had a GF of 5.02 under strains up to 16.3%, but remained sensitive to bending as well. The PVA coating also enabled the sensor to exhibit a similar response to strain and bending in varying relative humidities.

Triboelectric sensing yarns have also been formed through coating techniques. By coating a stainless steel thread with silicone, a single yarn can be used as a triboelectric sensor when leveraging the wearer's skin as the second material.^[427] These threads were sewn onto a stretchable base fabric where contact force could be measured because the voltage difference and the short circuit current increase with increased force. Although requiring more complex fabrication, layered structured yarns enable integrated triboelectric sensors that may operate without making contact with the wearer's skin. Sim and colleagues wrapped a PU fiber with silver coated nylon yarn as an inner electrode and positive triboelectric material, and then pre-strained this yarn before additionally wrapping it with a polyvinylidene fluoride-co-trifluoroethylene (PVDF-TrFE) nanofiber mat as a negative triboelectric material and a CNT sheet as a second electrode, enabling stretchability through wrinkling^[428] as discussed above. The output voltage increased with increased strain, and by integrating several of these yarns into a specifically engineered textile structure, the stretching direction could be differentiated. Dong and colleagues used a core-sheath method for triboelectric sensing by first winding both a silicone core and silicone tube with silver coated nylon yarns, coating the covered tube with silicone to keep the wound material in place, and then threading the core through the sheath tube to form one unified sensing yarn.^[429]

For monofilament optical sensors, a coating step adds a cladding layer with a different refractive index to prevent light scattering due to the presence of dust, oils, or eventual abrasion-induced roughness.^[243] Harnett and colleagues coated a low cost commercially available PU monofilament with a silicone elastomer cladding by pulling it through a syringe, allowing it to act as a stretchable sensing waveguide.^[243] As strain increased, the intensity at the output decreased. In subsequent iterations, a 3D printed sheath was devised so that the same core yarn could be used to sense bending in 3D printed scaffolds.^[430]

Yarn morphology has a large effect on the sensor behavior. The corespun architecture (Figure 7) has been leveraged when creating coated strain sensors—the stretchable elastomeric core allows for stretchable yarn that contains stiff yet flexible cover fibers. Such non-stretchable fibers make a great substrate to coat with conductive materials.

Simple techniques such as dip coating can deposit conductive materials to create resistive sensing yarns. Cheng and colleagues used a corespun yarn consisting of a PU core and polyester cover fibers, dip coated it with graphene oxide (GO), and subsequently reduced the GO to rGO for a resistive strain, bending, and torsion sensing yarn.^[172] When strained, the winding angle of the outer layer of coated PE cover fibers increased, forming gaps and reducing the contact area between the conductive coated polyester layers, leading to an increase in resistance (Figure 13a). The average GF was 10 within 1% strain and 3.7 within 50% strain. Because of the chiral twist of the cover fibers, when used as a torsion sensor (280 rad m^{-1} to 800 rad m^{-1}), clockwise and counterclockwise torsion could be distinguished; counterclockwise torsion increased resistance and clockwise torsion decreased resistance. Similarly, Wang and colleagues dip coated a corespun yarn with a PU core and cotton cover in a CNT solution.^[174] Separation of the winding fibers increased resistance with increasing strain. Based on the number of dip coating processes (leading to more material loading), the yarn properties could be modified. A yarn coated 12 times was able to be strained to 300% without sensor failure, while a yarn coated eight times could be strained to 150%. Their maximum GF was 0.65 for the yarn with 8 coatings over a range of <25% to approximately 150% strain.

Additional hierarchy within yarns has been used to improve sensor sensitivity and strain range. Chen and colleagues added additional material hierarchy to form a sensor by modifying a corespun yarn consisting of an elastic rubber latex core wound with polyurethane fibers.^[431] The yarn was pre-strained and coated with PVDF-TrFE nanofibers through electrospinning to act as a wrinkled layer and subsequently coated with AgNWs through a dip coating process as a conductive layer. PVDF-TrFE had a better long-term sensor stability and higher conductivity than other electrospun polymer sheets and could support a higher strain range than the native core-sheath yarn. When strained, the resistance increased, believed to be driven by flattening of wrinkles. When used as a resistive strain sensor, a maximum GF of 5.3 (for a 0–25% strain range) and a maximum strain range of 100% could be achieved. Gao and colleagues added hierarchy to improve stretchability through a twist and overtwist strategy, similar to the fabrication strategy seen in coiled polymer and CNT actuators. After preparing an aligned electrospun mat of PU fibers, they used spray deposition to coat their matrix with CNTs. Through twisting, the sheet was transformed into a yarn, and over twist allowed for a helical, spring-like yarn to be produced that could achieve recoverable extension of 900%, an approximate three-fold increase over the maximum stretchability of their original membrane, not accounting for recovery.^[432]

New material classes have also been explored for use in sensing yarns, leveraging the simplicity of dip coating processes. Uzun and colleagues explored the use of coating existing yarns with MXene coatings for use in composite sensors (to be discussed later).^[433] MXenes are a recently-developed class of highly conductive 2D materials with improved adhesion to substrates during coating due to their constituent functional groups and ability to employ charge-enhanced coating strategies. Building on the use of MXenes, Wang and colleagues developed a resistive strain sensing yarn through coating a

pre-strained PU-PET corespun yarn with MXene ink followed by oven curing.^[434] Strain detection ranged from 0.3% to 120%, and the yarn's GF was 0.67 for a range up to 120% strain. This construction also functioned as a humidity sensor.

Yarn architecture plays a large role in determining the behavior of coated sensors. Park and colleagues highlighted this effect by depositing graphene nanoplatelets onto i) a stretchable multifilament rubber yarn, ii) a corespun nylon covered rubber yarn, and iii) spun wool yarns, to make low cost stretchable resistive sensors.^[12] Multifilament rubber yarn sensing was driven by the microcrack mechanism, and straining the yarn increased resistance. The corespun nylon yarn lengthened and cover fibers were separated with strain, also increasing resistance. In contrast, resistance decreased when the wool yarn was strained due to increased contact between fibers and a reduction of the fiber crimp. These results show that tuning the yarn structure along with the coating materials and process, while not typically performed, may be an exciting direction.

5.1.4. Yarn-Based Sensor Conclusions

Yarn level textile sensors can be created using methods spanning from complex to remarkably simple. The yarn level architecture and some of these structuring techniques lend themselves to different sensing modalities. For example, one-step composite conductive elastomer extrusions can form resistive sensors, while triboelectric sensors typically benefit from multiple structuring steps. Moving forward, we should not lose sight of the system-level motivations for creating these sensing yarns. Although textile integration is often cited as a motivation for their development, most yarn-level designs have not been investigated past the yarn level.

Lessons from integration steps provide some initial insights on performance in programmed textile systems. Couching techniques have been used to attach monofilament strain sensors onto base fabrics without the use of textile formation equipment.^[243,323] In this process, a sewing machine is used to stitch an enclosing "cage" around the yarn without piercing through the sensor, thereby constraining it. This method can be modified based on sensor behavior. Soft strain sensors that were also responsive to pressure were attached by couching only at their edges to prevent mechanical cross-talk from adjacent threads.^[323]

When incorporating sensing yarns into fabrics, accommodations may need to be made in the textile structuring process. For example, when weaving a sensing yarn into a textile, Niu and colleagues chose a sateen weave because of the long floats in the structure. They proposed that the long floats and reduced interlacing between yarns would improve linearity of the sensor and reduce hysteresis, due to reduced friction.^[422] Even with these considerations, the sensor GF was reduced after integration. When using textile formation techniques, steps can be taken to prevent the damage of fragile yarns during the (sometimes violent) textile formation process. When forming a braided sensor, a conductive yarn was incorporated as an axial yarn that does not participate in the braiding movement and is instead surrounded by passive yarns.^[435] Considerations like these highlight an intuitive understanding of the

consequences of textile processing and structures on sensor performance; however, there remains a large gap in the literature on experimental evaluations and strategies to successfully integrate yarn-level sensors into textiles while maintaining (or even amplifying) their performance, as characterized in the standalone yarn stage.

5.2. Textile Structuring for Sensors

Textile-level sensors rely on their constituent textile structures to operate—that is, the interaction between yarns within the textile produces sensor output. This class of sensors is appealing because commercially available materials (most commonly, conductive yarns) can be used to form the sensors and machine automation can allow many distributed sensor regions to be produced within a monolithic textile structure. A potential trade-off arises when creating self-sensing actuators through these textile architectures; structures optimized for sensing may not be the ideal structures to program actuator motion. This concept is not a far-fetched possibility; researchers developing fluidic robots have already leveraged the ability of knit sensors to be structured into actuator geometries for self-sensing textile PAM actuators.^[272]

5.2.1. Stitched Sensors

Stitched sensors are some of the simplest textile-level sensors and have been used to form resistive, capacitive, and optical sensors. Early work by Gioberto and Dunne resulted in resistive sensors made from un-insulated conductive yarns sewn into looping architectures that typically lose contact when stretched, in turn increasing resistance. A resistive strain sensor was developed using silver-plated nylon yarn with the upper looper of a coverstitch machine (a type of sewing machine that produces stretchable looped seams) on a stretchable jersey knit substrate. This sensor had a highly nonlinear response and could be strained to approximately 19%.^[436] They expanded upon their initial design by incorporating a silver-plated nylon yarn as the bottom thread on the cover stitch machine (the bottom thread has more internal meanders than the top thread).^[437] By integrating this sensor at seams near the knee joint, they saw high correlations between sensor output and bending angle based on motion capture analysis. Because the yarn was not insulated for sensor function, bends caused by the stiff fabric at the joint could cause long-range shorting, potentially indicating self-intersecting folds in fabric. Further implementations explored the use of an overlock stitch in which a conductive yarn was placed in either the upper or lower looper, illustrating this method could carry over to other stretchable self-intersecting stitches.^[244]

In addition to resistive sensors, capacitive and optical sensors have been formed through stitching. Recently Zhang and colleagues used stitching to form a capacitive pressure sensor by layering two insulated conductive yarns upon each other using a basic lockstitch.^[438] This method enabled incorporation of sensors in arbitrary curved and linear shapes onto existing fabrics. Others have used stitching to pattern polymer optical

fibers (POFs) into textiles in engineered architectures to maximize changes in light transmission, and thus sensor sensitivity, under strain or bending. Rantala and colleagues created macro-bend sensing structures within fabrics by using a couching technique to couple a POF to a knitted elastic base textile.^[439] Upon stretching the fabric the shape of the coupled POF changed, altering its light leakage.

The wide variety of stitches, many of which are possible on a home sewing machine, opens up more opportunities to structure sensors.^[242] Stitched sensors are very simple to fabricate from existing materials with, perhaps, more accessible equipment than other textile formation methods. They are useful when coarse strain data or switches are required and could potentially act as additional reference sensors in wearable systems.

5.2.2. Woven Sensors

Woven textiles do not impart stretchability based on their structure alone, but their ability to structure multiple materials into a flexible architecture finds use in textile sensors. They enable the coupling of materials into sensor architectures not seen in the constituent yarns alone. Perhaps most excitingly, woven materials provide an opportunity to create distributed pressure sensing networks, or “sensing skins,” by leveraging the unique intersections between yarns in the structure—if the warp and weft yarns are each discrete yarns themselves, then each overlap point results in a unique combination that could be addressed through signal processing techniques. Several classes of sensors have been created using woven structures.

Woven structures dictate yarn location, which in turn affects sensor performance. Shaker and colleagues investigated the effects of woven structure on pressure switches.^[440] Single layer textiles shorted without applied pressure, while triple layer textile structures allowed yarns at the top and bottom layers to maintain an open circuit unless an external pressure was applied. Woven structuring could also enable arrays in resistive pressure sensing. By using elastic yarns “dyed” with AgNW electrodes and subsequently coated with piezoresistive elastomers, Ge and colleagues created specialty yarns that formed pressure-sensing circuits when paired.^[441] In a woven structure, each contact point between two yarns acted as a sensor responsive to pressure, strain, and flexion due to deformation of the piezoresistive layers, enabling arrays of multiple sensors within one textile.

The arrayed sensor approach is not only relevant to resistive textile sensors; the capacitive sensing mechanism also works synergistically with this technique. Yarns with conductive cores coated with dielectric shells can form capacitive sensors at each intersection point, where increased yarn contact and yarn deformation increase capacitance. Takamatsu and colleagues produced sensing textiles with this technique using (PEDOT:PSS) as their electrode and perfluoropolymer (Cytop) as their dielectric, using die-coating to produce continuous lengths of functional yarns for capacitive textile sensor integration.^[442] Using this architecture, Enokibori and colleagues produced a similar sensing structure and were able to incorporate their sensors into pressure-sensing mats in insoles for

gait detection.^[443] Lee and colleagues modified a kevlar fiber to produce a similar sensor, resulting in increased robustness and potentially ameliorating the degrading effects of repeated strain (Figure 13f). This sensor had a sensitivity of 0.21 kPa^{-1} over a range $<2 \text{ kPa}$.^[397] Chhetry and colleagues used Twaron as their base material, a para-aramid fiber similar to kevlar, in a pressure sensing woven for similar robustness reasons, but added a microporous dielectric to improve sensitivity.^[444] They coated Twaron with SBS, followed by AGNPs, using a silver precursor coating and subsequent reduction step to form electrodes, and finally added a microporous PDMS dielectric. By adding micropores to the dielectric, they saw improved sensitivity (0.278 kPa^{-1} at a range $<2 \text{ kPa}$) compared to that of a sensor with solid dielectric. Plain weave is not the only structure that can be used for capacitive sensors. Recently, Li and colleagues wove conductive yarns within an arrayed 3D pyramidal woven textile to achieve a pressure sensitivity of 0.045 kPa^{-1} for a range up to 10 kPa .^[445] Although this value is low, the work represents a first step in exploring alternative woven textile structuring.

Woven fabrics with POFs integrated into their structure have enabled similar arrays wherein pressures can be detected based on the response of integrated fibers, although the overlaps themselves do not create any unique sensing structures; instead, the transmission through several fibers is monitored to estimate load position^[398] (Figure 13g). The weaving process itself drastically affects how polymer optical fibers behave and can modify their sensing mechanism. For example, microbends from the undulating woven structure can cause light leakage, reducing transmission to a collector when sensing.^[415,446,447] Satin weaves (with longer floats) have produced a more linear decrease in transmitted light as textile length increased, while in plain weaves intensity decreased exponentially.^[448] In addition to standard POF yarns, fiber Bragg gratings have found use in acting as sensors and have additionally been structured into textiles, including braids.^[449]

Triboelectric pressure sensing textiles have also been produced through weaving by integrating multiple materials of different triboelectric properties into networks where they repeatedly make and break contact.^[393] This mechanism takes advantage of the loose mechanical coupling of the textile structure, enabling a monolithic material to exhibit a connect-and-release behavior. One advantage of triboelectric textile sensors (as well as the capacitive sensors previously discussed) is that, by design, a conductive network can be contained at the core of the yarn with surrounding insulating layers. This property can enable robust insulating coatings to act as sensing elements as well as protective materials for the conductive core, allowing improved machine washability.^[391]

5.2.3. Braided Sensors

Braided textile structures are able to effectively support both sensing and actuation. The yarn sliding motion within braided tubes has been leveraged for fluidic textile PAM actuators (discussed in Section 4.2.1). This yarn motion, unique to the braided structure, can be harnessed as a mechanism for sensing and has led to the formation of PAMs with integrated force and displacement (strain) sensing.

By treating insulated conductive winding yarns forming a braid as solenoids, the inductance can be quantified and used as a sensing metric.^[450] When a PAM composed of these yarns is inflated, the braid expands radially, modifying braid angle and causing the yarns to rotate and become more orthogonal to the lengthwise axis, altering inductance. Sensor sensitivity depends on initial braid angle; in one implementation the displacement sensitivity was found to be 0.069 H mm^{-1} for a 20° muscle and 0.072 H mm^{-1} for a 30° muscle. In following works, the effect of nearby ferromagnetic materials was evaluated, but minimal change was observed because a majority of the flux is concentrated within the inflated core of the actuator.^[451] When integrated into robotic manipulators and hinge joints, the contraction sensing provided by braided PAMs was used successfully in position-based closed-loop feedback control schemes.^[452]

5.2.4. Knit Sensors

Knit sensors represent a large sector of textile structured sensors. Because the looped knit structure enables stiff yarns to form stretchable fabrics, this textile formation method has been quite successful in forming strain sensors from conductive materials, either through knitting conductive yarns or coating knit textiles with conductors.

Interest in resistive knit strain sensors blossomed in the early 2000s and has since become a major strategy in textile sensor development. Most resistive knit sensors rely primarily on contacts,^[453–455] where the contact area of intersecting yarns in a knit structure governs the overall resistance. Piezoresistive materials have also been used,^[456] operating through a combination of the contact mechanism and their inherent material piezoresistivity. Using multi-material 3D knitting combined with intarsia knitting, distributed regions of knit sensors can be formed in garments.^[10,75,173,457] Materials such as stainless steel,^[10,454,458] carbon fibers,^[454] silver-plated nylons,^[10,459] and conducting polymers^[460] have been used for conductive elements in these knit sensors.

At times, yarns containing conductive materials have been optimized for the knitting process and sensor performance. Xie and colleagues highlighted the consequence of yarn construction when they compared a spun cotton-stainless steel yarn (where both steel and cotton components were mixed as fibers) with a multifilament silver-coated nylon yarn. The cotton-steel spun yarn exhibited a much higher GF (-20 compared to 0.05 for the coated nylon when stretched wale-wise), although it had two distinct sensing regimes. Moreover, the opposing signs of GF values highlight that the random fiber distribution of conductive and insulating fibers in spun yarn constructions were brought into contact with increased strain, while the silver-plated nylon loses contact with increased strain—meaning, intra-yarn motions can contribute to resistive knit sensor performance as well as inter-yarn contact^[10] (Figure 13e). Although the knit structure itself imparts a level of stretch to materials, highly elastic garments like yoga pants typically contain elastomers to allow additional stretch. By using hybrid elastomer-conductor yarns, researchers sought to improve the strain range of resistive knit sensors; corespun techniques once again

find relevance here,^[173,461] and in some cases have improved the sensitivity and range of strain sensors.^[461] To create stretchable sensing yarns, others have looked to wet-spinning constituent fibers, for example in the work by Seydin and colleagues.^[11,462] They also showed that plying more conductive PU/PEDOT:PSS fibers into their knit yarn resulted in a more sensitive sensor, while adding additional spandex had no improvement on sensitivity but did improve the stability of the sensor over repeated cycling.^[462] The stretchable fibers themselves had a positive GF, while the knit textile had a negative GF, highlighting once more the effects of knit construction on the sensing performance.^[11]

Aside from the yarns themselves, the knit structure, governed by knitting machine parameters, plays a major role in sensor behavior. When comparing the same conductive yarns knit into a 1×1 rib knit versus either an interlock knit or a knit structure with long floats, Qureshi and colleagues observed that the float and interlock structures had higher sensitivities than the rib, potentially because the rib was more loosely arranged than the others. However, they also pointed out that structures with long floats were highly irregular during sensing because of the freedom of the float motion.^[173]

The method of incorporating conductive materials into a knit structure in turn determines sensor behavior. Sensors made of primarily conductive yarns in their sensing regions often have increased contact between loops under strain and thus negative GF values,^[11] while single courses of knit conductors (i.e., one conductive stripe within a sea of insulating yarns) had positive GFs.^[459,463] Additionally, single course knit sensors formed with lower feeding tensions on the conductive yarns had slightly higher GFs due to the looser initial loop formation, leading to more initial contacts.^[459,463] Others looked at how conductive and non-conductive yarns plated (fed through the machine in parallel) within a jersey knit structure affect sensor performance. Seyedin and colleagues specifically highlighted that conductive stretchable fibers plated and knit with insulating polyester yarn performed differently based on how they were integrated.^[11] The structure that performed the best was one wherein they knit the conductor in a plain jersey structure and interlaced crossing passive polyester yarns as an inlay. However, when compared to the multifilament conductive fibers with a GF of approximately 1500 at 200% strain, all of the knit structures exhibited lower sensitivities, with the highest GF of any structure being approximately -0.95 at 50% strain.

To better understand and estimate how the knit structure imparts sensing, efforts in modeling knit strain sensors geometrically as resistance networks have been demonstrated. Many of these models neglect 3D effects and simplify the knit to a connected hexagonal or rectangular grid wherein inter-yarn contact points are nodes. Looking at a resistive jersey knit force sensor, this simplified model provided relatively good agreement when loaded in the warp direction. A positive offset was present, which the researchers believed was due to the 3D contacts in the actual sensor reducing the resistance.^[464] Applying a similar strategy to conductive jersey knits under biaxial elongation (i.e., both in the warp and weft direction) succeeded in determining the sensor resistance in a strain range up to 30% .^[465] Others looked to model machine parameters; for example, Wang and colleagues simulated how a jersey knit structure would affect strain sensitivity of a resistive knit strain

sensor as a function of initial loop length and knit stitch width. Smaller stitch widths and longer loop lengths were shown to enable more strain and provide higher strain sensitivity.^[466]

Thus far, we have spoken exclusively about conductive materials incorporated into knits as yarns; however, knit strain sensors can be made through coating or dyeing methods as well. Repeatedly coating nylon/PU plain jersey knit fabrics with GO sheets through a solution process has produced strain sensing fabrics that have GFs of 18.5 below 10% strain, when stretched in the wale direction.^[467] Other researchers have produced similar sensors by coating pre-strained knits with Ag nanoparticles, CNTs, and PPy.^[460,468]

Some new trends in 3D shaping resistive knit strain sensors have been demonstrated. Ou and colleagues used 3D weft knitting to produce several knit configurations for resistive and capacitive knit pressure and strain sensors.^[469] Most notably, they employed global shaping techniques to make a resistive knit strain sensor in which the contacting overlap area of several layered pockets is reduced upon material strain. This geometry enabled their resistive sensor to maintain a relatively linear output compared to knit-microstructure-based sensors, which are predominately nonlinear. As previously mentioned, Jamil and colleagues knit conductive fibers into a tube structure to be used as a self-sensing constraining layer for knitted PAM actuators, reducing the number of fabrication steps for an integrated robotic textile.^[272,277] Kim and colleagues leveraged spacer knit structures, wherein two fabric faces are separated by relatively linear yarns that are periodically interlaced into faces to join the material together (Figure 1i). When a spacer knit is coated with conductive materials, it can behave as a resistive pressure sensor due to increased contact between the initially separated layers and yarns.^[470]

Other researchers have explored leveraging the knit structure for different sensing mechanisms. In knit tubes, continuous pieces of yarn create courses in a spiral-like pattern. This helix of courses can be used for induction sensing, similar to that seen in the braided induction sensors previously discussed.^[453,471] Quite recently, Fan and colleagues produced a triboelectric knit pressure sensor through plating two yarn types together^[395] (Figure 13h). The first yarn was a corespun yarn consisting of a steel core and a terylene cover, and the secondary yarn was a spun nylon. These yarns were loosely mechanically coupled together through an interlocking full cardigan structure created on a flatbed knitting machine. Because of the opposing triboelectric properties of the yarns, when the yarns made and broke contact they could act as triboelectric pressure sensors, and the voltage change could be monitored. In a low-pressure region below 4 kPa, the sensors behaved linearly and had a sensitivity of 0.008 mV kPa⁻¹.

Knit sensor development highlights how material hierarchy in textiles—from the constituent material level to yarn and textile structures—impacts sensor performance. Most knit strain sensors are resistive and predominantly rely on material contact to operate. Methods that maximize the change in contact could potentially improve sensor sensitivity. The jersey knit structure has two distinct deformation regimes: 1) the curved loops of the knit stitches straighten (modifying contact), and 2) the yarn itself, now straightened, elongates (straining and compressing yarns).^[373] Potential future work may be in tuning the

constituent conductive yarns with knit structures to deform in manners matched with these regimes, in order to improve sensitivity and linearity.

5.2.5. Nonwoven Sensors

Although nonwovens are primarily incorporated as components into within yarn,^[428,431,472] or composite-level textile sensors,^[473,474] nonwovens can be used as textile sensors on their own. However, the nonwoven structure may be amenable to only some types of sensing. For example, a nonwoven resistive strain sensor formed by dip coating a nonwoven textile in GO solution and subsequently reducing had a low stretchability when used as a strain sensor, exhibiting only up to 3% strain, but had a moderate GF of ~71 at 1% strain.^[214] In this demonstration, the nonwoven could also function as a compressive force sensor, sensing up to 1 N. Although this material was thin (with a 150 μm thickness), it highlights that changes in its intra-fiber contacts can be leveraged for sensing. The use of thicker nonwoven materials, like batting (a nonwoven used for insulation and bulk), could potentially improve the pressure sensing performance of nonwoven sensors.

5.3. Composite Textile Sensors

Composite textile sensors are fabricated by layering and bonding existing textiles into sensors and the adding of non-textile materials, including elastomers, adhesives, and films, which are often necessary for operation. These sensors can take advantage of properties in materials not readily observed in textiles and are often able to be made using off-the-shelf materials without specialized textile formation equipment, making them amenable to researchers working on device development. Capacitive sensors are especially well-suited to this architecture; electrodes and dielectric materials can be stacked and bonded to form textile-based pressure and strain sensors, leading to implementations optimized for their use of low cost materials and ease of fabrication. Examples even include sensors formed from foam from Crocs (the shoes) bonded to textile electrodes to form pressure sensors^[475] as well as conductive fabric, plastic carbon composite films, and adhesive tapes stuck together.^[476] A downside to this approach lies in its requirement for bonding and adhering textiles together: delamination remains an issue in terms of durability, especially over long-term use, and yarn motion can be hindered by the addition of adhesive material, making the resulting textile less “textile-like” and instead more similar to a film.

Non-textile components can impart elasticity and durability to enable resistive sensing mechanisms. Zhang and colleagues formed a resistive strain sensor from carbonized plain weave cotton fabric through heating and subsequently encapsulating the fabric in silicone elastomer.^[477] Because the elastomer held the sensor structure intact, it was able to be strained and released repeatedly, even though the breaks in the yarn structure would not support a textile, nor would the woven structure impart the necessary elasticity on its own. Even so, the woven structure still contributed to sensor performance — sensors

with denser thread counts had higher sensitivities with smaller workable strain ranges. Similar processes have been used for other carbonized wovens^[478] and wovens coated with conductive inks.^[479]

Composite architectures can promote improved sensitivity. Atalay and colleagues demonstrated this advantage by producing a capacitive sensor from silver-plated nylon knit electrodes and a silicone elastomer dielectric in the form of a parallel plate capacitor^[13] (Figure 13j). While the elastomer dielectric enabled high deformation and reduced textile hysteresis, the low Poisson's ratio of the textiles enabled a larger electrode area change when strained, resulting in a sensor with a 1.23 GF and a range of 100% strain. Torato and colleagues built upon this design to create a sensor with an additional electrode and dielectric for shielding purposes.^[480] By modifying the dielectric and introducing air gaps in the original, three-layer design through a sacrificial material dissolving step during fabrication, the same composite textile architecture was used to form pressure sensors, where the air gap increased dielectric constant and compressibility.^[481] Atalay and colleagues observed effects of the textile electrode on sensor sensitivity—knit electrodes led to higher sensor sensitivities than wovens with the same dielectric construction. They hypothesized that the air gaps within the knit contributed to the total dielectric layer (in addition to the silicone). Wovens could potentially over-stabilize the structure, preventing deformation, while the stretchability of knits could allow dielectrics to deform more freely; further investigations on textile constructions in pressure sensing composites may uncover these mechanistic contributions. Later, Uzun and colleagues demonstrated high compressive strain sensitivity (GF = 6.02) in a pressure sensing fabric using MXene coated yarns knit into two electrodes and sandwiched around a rubber dielectric, illustrating the importance of exploring new materials.^[433]

The composite architecture is especially promising for leveraging the properties of nanomaterials introduced as nanofiber mats to improve sensitivity, either as electrodes or as the dielectric layer. Whereas, on their own, nanofiber matrices and other nonwovens can face robustness challenges, when employed as part of a composite, the addition of other materials strengthens the overall sensor.^[473] Li and colleagues built a composite capacitive pressure sensor and further imparted material functionality into their dielectric later.^[473] By using a nanofiber gel matrix of PVDF-co-hexafluoropropylene with bis(trifluoromethylsulfonyl) imide as an ionic component, an interfacial supercapacitive layer can be formed when in contact with an electrode, increasing capacitive sensor sensitivity to 114 nF kPa⁻¹. They leveraged the use of an electrospun nanofiber matrix for its porosity and high variation in surface area to support capacitance change. Aside from adding further structuring, electrospinning is an effective strategy to incorporate functional nanomaterials into fibers to alter dielectric and mechanical properties. Recently MXenes have once more found use because of their 2D nature as well as hydrophilicity and improved adhesion due to functional groups.^[482–484] Sharma and colleagues took advantage of the ability to electrospin MXene/PVDF-TrFE nanofiber scaffolds to increase dielectric constant and reduce the material compression modulus to enhance pressure sensitivity.^[485] Here MXene was specifically added to increase the dielectric constant, while

its 2D nature allowed for more uniform dispersion within the polymer matrix. With this approach, a sensitivity of 0.51 kPa⁻¹ could be achieved for a range of 0–1 kPa.

Meanwhile, Wu and colleagues improved performance with macroscale textile structures by using a highly porous mesh spacer knit construction as the dielectric.^[474] In a separate composite capacitive textile sensor formed by coating either side of a knit mesh spacer textile with conductive inks (CNTs and Ag paste), injecting elastomer between the faces to an led to an increase in sensitivity.^[486] The ability to pair multiple materials to improve sensitivity supports mechanisms beyond capacitive sensing as well. Seung and colleagues developed a triboelectric composite sensor made from a silver coated fabric and a silver fabric coated with zinc oxide nanowires followed by PDMS that exhibited force sensitivity and could be used as a switch in wearable devices^[394] (Figure 13k).

Composite architectures are also supportive of arrayed configurations. Meyer used embroidery to form electrodes and signal lines on sheets of insulating textile. By pairing these embroidered structures with a mesh spacer dielectric and an additional silver coated fabric shielding layer, an array of capacitive pressure sensors could be contained in one composite sheet.^[487] Parzer and colleagues took a similar approach with resistive sensing, sandwiching a piezoresistive fabric between two layers of knit fabrics containing linear electrode arrays in a crossed pattern.^[488] Liu took this process a step further, using processes such as electroless plating on textile substrates to create designer electrodes with high resolution^[399] (Figure 13i). When paired with piezoresistive distributed pressure sensing elements, this approach could allow for customizable designs for integration into wearable devices. To simplify the patterning process, removing wet chemistry, Sanchez and colleagues used a laser cutting strategy to produce arrays of composite capacitive pressure sensors with minimal manual alignment steps.^[259] Sundaran looked at scaling up the number of sensing nodes in arrays and integrated 548 low-cost composite resistive pressure sensors into a knit glove, enabling deep characterization on human grasping.^[489] Others used a composite strategy for multiple DOF sensors, like Viry and colleagues.^[490] In a parallel plate configuration with one upper textile electrode and four lower woven textile electrodes encased in silicone PDMS with an air-fluorosilicone dielectric, normal force could be sensed as usual, and the elastomer dielectric and encasement also enabled shear between textile electrodes, changing the coverage area of all four electrodes, and thus the capacitance, for shear detection.

One major question remains when considering composite textile sensors (and actuators): what is the cutoff point for classification as a textile-based component? At what point does a sensor stop being a textile sensor and start being something else entirely? Similar questions often arise in soft robotics: for example, how many rigid components can one include before the robot is no longer a soft robot? However, unlike the consideration of rigid components in soft robots, it appears the consequences of material and fabrication choices on the functionality of composite sensors may be more easily distilled out. Using large amounts of elastomers can produce strain sensors nominally incorporating textiles that otherwise would not operate, but these sensors are very unlike the fabrics in clothing they're

trying to emulate—for example, the drape and the breathability are lost. Although there would need to be agreement, a metric (e.g., something as simple as weight percent or volume percent) that can clarify how “textile” a component is could help guide the understanding of much of the work related to this field.

5.4. Conclusions for Textile Sensors

When considering textile-based sensing modalities relevant to wearable robots (especially strain and pressure), key differences arise between the architectural strategy and general sensor performance. When comparing between sensing yarns and fibers, textile-structure-based sensors, and composite sensors, architecture-based trends are apparent (Tables S7–S9, Supporting Information). Composite sensor designs are more likely to be leveraged for pressure sensing, while yarns are more likely to be developed to sense strain. Additionally, these architectures can affect the performance. Oftentimes strain sensing yarns are produced with extremely high GFs, but when integrated into textiles these values are reduced. On the other hand, composite sensors have some of the highest sensitivities as pressure sensors. Some hypotheses on these trends arise intuitively. For example, strain sensing yarns can stretch freely without the friction, geometric effects, or added stiffness resulting from being structured around neighboring yarns in a textile. Pressure sensing composites can be formed from thick stacks of materials which may enable relatively large pressure-induced displacements. The state of the field leads one to wonder: can these high GF yarns be translated to textile-structure-based sensors with equal or higher sensitivity? Could monolithic textile manufacturing techniques create pressure sensors that surpass current sensitivity limits?

In addition to textile architecture, the sensing mechanism plays a large role in determining performance. The simplicity of fabrication and readout electronics make the resistive mechanism an especially appealing choice for textile sensor development. The ability to design architectures that cause conducting elements to make and break connections allows for incredibly high GFs and sensitivities. Often this advantage comes with the caveat of highly non-linear behavior. Additionally, resistive sensors can be quite susceptible to environmental effects; moisture from the environment or the wearer’s sweat could seep into the textile matrix and lower resistance. Because some textile structure implementations, such as knit resistive strain sensors, rely on the sensors to be unencapsulated for operation, this susceptibility can pose a problem. Yarn based architectures are a promising approach to overcome this limitation because they can operate as stand-alone sensors, enabling encapsulation; however, as previously discussed, additional work on matching yarn level sensors to textile architecture needs to be done to meet yarn-level performance.

Capacitive sensors can produce an inherently linear response, but they typically have lower GFs and sensitivities than resistive sensors. Improvements to GF and sensitivity have been made through modification of the dielectric through the use of porous dielectrics, nanomaterials to increase dielectric constant, and iontronic design strategies to enable high baseline capacitance and improve sensitivity through dynamic

modification of the dielectric constant under stain and compression, suggesting that continuation of this direction will be fruitful. To improve sensitivity in strain sensors specifically, knit textile electrodes with reduced Poisson’s ratio have been employed,^[13] and highly structured knit electrodes have improved pressure response.^[481] The success of these strategies suggests that investigating the use of designer textile electrodes with further reduced or even negative Poisson’s ratios, as well as additional porosity, as discussed in Section 3, may find value. Other challenges faced by capacitive sensors include parasitic capacitance and complexity of readout electronics (compared to resistive sensors), which remain practical issues for integrating into wearable robots. Parasitic capacitance from the wearer’s body and their environment may arise, and previous work has shown shielding strategies can effectively reduce parasitic capacitance.^[15,480,487] Because of the added bulk and additional bonding steps, perhaps this design requirement may need to be taken into consideration earlier when developing textile based capacitive sensors that remain low profile and robust.

Although less common than other textile sensing modalities, optical sensors overcome some previously discussed challenges by being relatively immune to effects of electromagnetic interference in the environment or from the wearer. Waveguide materials with low coefficients of thermal expansion and temperature-dependent change in refractive index can be selected to ensure environmental stability, even when used in extreme environments.^[491] Typical optical fiber materials include glass and PMMA, creating challenges in textile integration due to yarn bending stiffness, as discussed in Section 4.3.7 for actuating yarns. Although these materials have been woven and discretely attached onto fabrics through stitching, knitting POFs had remained a challenge because of bending stiffness. Recent work in knitting POFs for light-up garments highlights that, by using weft knit structures with long floats that reduce the amount of areas with extreme curvatures, these materials can be successfully knit.^[492] An alternative approach is to use elastomeric materials to create optical fibers and waveguides that provide additional flexibility and stretchability.^[405,491,493] Challenges remain in miniaturizing and routing the electronics because both a light emitter and a photodetector are required at either end of the textile-integrated waveguide. Studies of semiconductor LEDs and photodetectors within fibers suggest both components may have the potential to be located within one integrated fiber in the future.^[494]

Triboelectric sensors are beginning to emerge as a promising class of textile sensors due to their self-powered nature. Earlier work highlighted the potential for sensing performance in recognizing motions of the body, such as tapping a finger or breathing. Full sensor characterization, relating electrical outputs to forces, pressures, and strains, has recently begun.^[395,427,428] Because triboelectric sensors rely on electrostatics for operation, challenges remain in that some are susceptible to effects from electromagnetic interference such as external errant charges as well as environmental effects such as humidity.^[392,395,427]

Regardless of sensor architecture, one major challenge is the multi-stimuli response of sensors. Although multi-stimuli responses (e.g., responsiveness to temperature and pressure, or bending and pressure, etc.) are often highlighted as features

in textile sensor research, for roboticists these are undesired effects. For accurate estimation of motion and interactions, the ability to decouple these signals is required. Engineering modifications can solve some problems; for example, including a temperature sensor in the device as a reference for a textile sensor that is sensitive to both strain and temperature can decouple the measurements. Not all fixes are as straightforward, especially when a sensor is sensitive to multiple physical deformation modes. There is a need for soft, flexible, and stretchable textile-based sensors that can clearly discriminate sensing modes. Fortunately, the hierarchical and anisotropic nature of textiles may be a part of the solution. For example, material anisotropy could lock stretch to one 2D direction, preventing undesired off-axis strains from occurring. Hierarchy could enable smaller sensing yarns to be integrated into larger sensing fabrics and sensing textile composites for multi-mode sensing.

The field of textile sensors is much more nuanced than the streamlined presentation in this review. For other perspectives related to this area of research, we recommend several other review papers. Zeng's review on fiber based wearable electronics is quite thorough and includes sensors and conductors.^[495] Seydin and colleagues provide a detailed review on textile strain sensors.^[496] Souri and colleagues provide a holistic review on wearable strain sensors and summarize some recent resistive textile strain sensors.^[497]

6. Textile Integration for Wearable Robots

Integration elements connect textile sensors and actuators to power and controls elements. They include conductors that act as power and signal lines, fluidic routing tubes, textile-integrated circuit boards, and connection strategies that often bridge hard and soft materials. Many clever engineering innovations enable textile-associated fabrication strategies to be leveraged to support integration.

Electronic signal lines and textile circuits allow for controller components to be connected with sensing and actuation elements, while remaining flexible and soft. Early work investigated using embroidery techniques and soldering to create textile circuits that remained flexible and could be coupled with traditional integrated circuit chips.^[498] An embroidery approach continues to be used for creating circuits, signal lines, and electrodes, such as those used to measure bio-signals.^[499] Embroidery can be highly automated; however, because yarns are stitched through the textile substrate, it can potentially lead to shorts when a double-layer textile circuit board is formed. Laser cutting and bonding conductive fabrics, as shown in **Figure 14a**,^[500] and screen printing upon thermal film substrates so as not to have inks penetrate the porous fabric network are amenable to double-sided fabric circuit boards.^[501]

Weaving can produce flexible fabric with integrated conductors, without any added height or stiffness from additional threads, films, or inks seen in embroidery, bonding, and printing processes. Jung and colleagues wove copper wires coated with silver and polyester to use as interconnects and removed the insulation via laser to solder to wires on a rigid printed circuit board.^[504] Google's "project jacquard"^[505] provided a holistic overview of the process of developing and

integration strategies

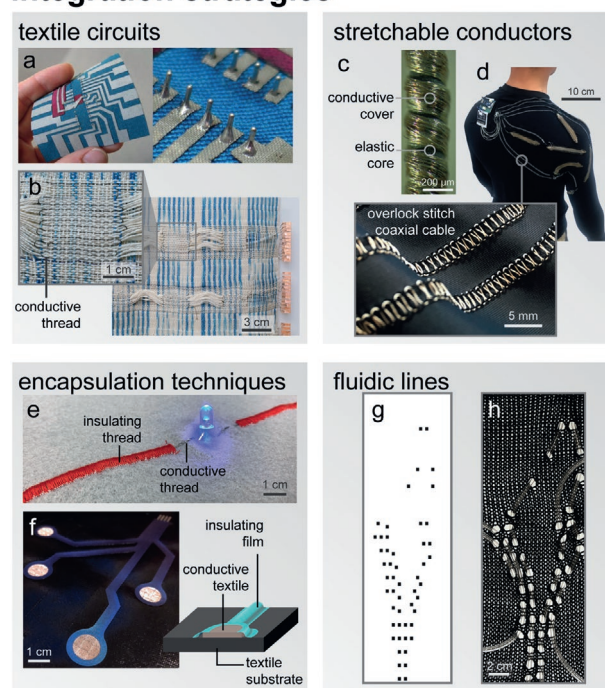


Figure 14. Textile-based integration strategies connect sensors and actuators to power and control elements. a) Textile circuit boards can be formed through bonding textile materials to insulating textile substrates, and in some cases have been supportive of soldering to more classical circuit elements. Reproduced with permission.^[500] Copyright 2007, Springer Nature: W.W. Norton & Company. b) Hand weaving techniques incorporated the conductors in a patterned manner, and can include pockets for sensor integration.^[502] Photographs provided by the authors and reproduced with permission. Copyright 2019, the authors. c) The geometric strategy of core-spinning enables stretchable conductors from inextensible silver wires. Reproduced with permission.^[503] Copyright 2011, Elsevier. d) Overlock stitching techniques create stretchable conductive signal lines from micro coaxial cables. Reproduced with permission.^[15] Copyright 2020, IEEE. e) Additional layers of insulating yarns created through embroidery techniques can encapsulate conductors. f) Thermal films can also enable encapsulation of textile conductors. Fluidic line routing can be directly integrated in constraining textile layers through knitting; the knit pattern in (g) produces the structure in (h) through a lace stitch. Reproduced with permission.^[290] Copyright 2016, eCAADe2016. eCAADe publications are Open Access.

engineering conductive yarns that would withstand weaving without short-circuiting, while remaining similar in physical feel to the yarns of traditional fabrics. Recent efforts in hand weaving by Devendorf and colleagues have led to integrated conductors within flexible textiles using a lab-scale loom (Figure 14b). Due to the high customizability, effects not commonly seen in machine-made wovens, like integrated conductive pockets for circuit elements such as pressure sensors and vias through layers, were realized.^[502]

In addition to flexibility, stretchability may be required of interconnects and conductors. Stretchable yarns can be manufactured by similar approaches to those used for sensing yarns, with conductors that exhibit minimal changes in conductivity when strained. Composite conductor-elastomer yarns have been employed^[506] as well as yarn-encapsulated liquid metals^[171]

and ionic conductors^[403] (which may reduce cost and potentially increase safety). Geometric approaches can also create stretchable connections from relatively stiff, yet flexible, conductors. Corespinning elastic yarns with conductors as cover yarns (Figure 14c), knitting, and using stretchable seaming techniques (Figure 14d) have been used.^[15,503,507] Knitting has enabled materials including insulated copper wires and carbon-coated nylon yarns to act as interconnects by plating the wires with additional passive yarns.^[507,508] When these passive yarns included stretchable materials like spandex filaments, interconnects could be stretched for 5,000 cycles with minimal change in conductivity.^[507] Knitting techniques can also support integration of non-textile components. For example, rigid sensors can be incorporated at floats, allowing them to remain linear while using knit stitches for the connectors,^[508] and processes like intarsia and plating enable stretchable connectors, electrodes, and sensing elements to be precisely patterned within a monolithic textile.^[75,173,457]

As previously mentioned, regarding actuators and sensors, washability remains an important question in wearable robots, especially when considering those with integrated electronics. Encapsulating conductive yarns appears to be an effective strategy to improve longevity. Ionic conducting fibers encapsulated with butyl rubber integrated into a sock remained mechanically and electrically stable for five washes.^[403] Other methods of encapsulation include using textile paint, heat-sealable films, or stitching to create washable conductors in textiles (Figure 14e,f).^[499,500] For example, adding a second insulating embroidered layer atop an embroidered conductor reduced conductivity change due to washing.^[499] Additionally, the density of embroidery affected the change in conductivity after washing—a “swing pattern” with more yarns stitched per area performed worse with washing, possibly because with more stitches and yarns there is a greater chance of yarn damage occurring.

At times, uncovered conductors are used because they are required for the mechanism employed to produce stretchability or sensing (e.g., knitted resistive strain sensors rely on contact between multiple conductive yarns for operation), or for a specific use case requiring exposed conductors (e.g., electrodes for EMG need to remain uncoated to make contact with the wearer's skin). The conductor material and its chemistry can contribute to failure modes in washing. Schwarz and colleagues showed that silver-coated winding yarns had less changes in conductivity after washing than copper or steel. Explanations include the fact that copper ions can undergo a chemical reaction with sodium carbonate ions in the washing solution, and that crevice corrosion occurs in the steel.^[503] Eskinadarian and colleagues saw that carbon-particle-coated conducting yarns with a low initial conductivity had a lower relative change in conductivity than silver yarns (although much higher than silver yarns when looking at absolute values). In their study, EDS spectroscopy confirmed the presence of sulfur, indicating the silver yarns had undergone a reaction that produces a silver sulfide tarnish which occurs in the presence of sulfur and humidity.^[76] For more on electronic fibers for textiles (and in addition to reviews mentioned in the sensing section), Lund and colleagues have prepared a review.^[509]

Aside from electronic conductors, integration strategies for fluidic lines and actuator placement have been explored.

Baranovskaya and colleagues integrated pneumatic line routing into their knitted inflatable actuators by threading it through single lace openings knit into the constraining textile (Figure 14g,h). This method is not without its challenges—these lace “holes” reduce stiffness, requiring modifications in the knit stitch patterns surrounding the routing area to compensate and provide the required stiffness for actuation.^[290] Fluidic actuators with integrated zippers have assisted with donning garments by allowing the actuator to be attached with the base garment already on the wearer and potentially enabling actuator removal for washing.^[16] As previously discussed, reconfigurable multi-actuator systems enable actuation profiles to be modified on the fly and could be translated to wearables for customizable actuation based on the wearer's needs.^[257,288]

Another important consideration is sensor integration methods, which have been shown to affect textile sensor performance. For example, when applying a knit resistive strain sensor to two regions of a glove, one where compressive strain dominated and one where tensile strain occurred, the area with compressive strain saw a greater change in measured strain based on the deformation from finger bending,^[510] highlighting how the location of sensor integration can effect sensitivity even for the same textile architectures and wearer motions. Others have sought to optimize sensor integration by investigating the minimal number of distributed sensors required to track multi-DOF motion of the body, comparing to video-based motion tracking system results as ground truths.^[15,511] In a shirt that uses textile sensors to estimate shoulder kinematics, machine learning algorithms helped the researchers down-select from eight to four sensors for motion tracking.^[15] Regardless of the sensor architecture and underlying mechanism, choice of location of integration and sensor network design could benefit from experiment-based studies when implemented into wearable robots.

7. Conclusion and Future Directions

A boom in wearable robotics is currently underway, and textiles are a compelling material platform for the development of constituent elements. Textile structures have found function in actuators, sensors, and integration components. Furthermore, because of the hierarchy of textiles, this field transcends scale: Nano- and microscale materials program mesoscale textile properties and motions for macroscale robotic garments. Spanning across robotic components (actuators, sensors, and integration strategies) and between these scales, the effects of material-integration-related interactions are beginning to be considered. We should not shy away from this complexity, but rather recognize this frontier as an exciting area to delve into, understand, and leverage.

Because of the unique intersection of textile engineering, materials science, and robotics required to develop programmed systems, one may expect convergent approaches in research. Yet, when considering the literature and the groups working on these areas, it is clear there is still a disconnect between those working in materials science and those focused on robotic device development. Roboticists are working from a top-down perspective—looking at the end application and

desired outcomes for the wearer, often using the most immediately available materials. Conversely, materials scientists are working from a bottom-up perspective—moving towards a material understanding and highlighting new properties of oftentimes novel material classes, with a more peripheral focus on device integration. Meanwhile, textile scientists seem to be largely isolated from either group. Stemming from these diverse perspectives, the open questions and problems researchers are working to solve are quite different. Similar to how roboticists have found value in collaborating with biologists when developing bio-inspired robots, this field of textile-based wearable robots may find some merit in more conversations between roboticists, materials scientists, and textile engineers.

There is hope! When textiles were first leveraged by materials scientists and roboticists, a general lack of nuance prevailed when considering the textile contribution to function. Less precision was used in describing and characterizing the textile and its sub-components. However, the recent literature is moving towards a more precise approach in considering textile contributions and describing their features. Yarn spinning techniques are being utilized in articles published in materials journals, knits and wovens are largely properly identified by roboticists, and active knit yarn architectures have found their way into high-profile publications such as *Science*.^[100] The work in this area is not yet complete, but an optimistic outlook would suggest that this collaborative attitude will prevail and provide enough information to parse out and understand material-level contributions to high-level device function.

In addition to an investment in precision in language, new methods of creating larger monolithic structures from textiles provide an exciting opportunity in the field. Material and structural placement may potentially assist with the growing trend of distributed actuation and sensing because of ease of fabrication. New fabrication techniques that are highly automated through lab-scale machinery open up the potential for device-in-the-loop schemes of iteration and fabrication, as well as performance characterization, wherein specific textile contributions can be more thoroughly experimentally tested and fundamentally understood.

Although not included in the scope of this review, we would like to highlight that, in addition to actuators, sensors, and integration, *control, energy storage, and power generation* are important future considerations when developing robotic garments. To replace rigid IC chips and printed circuit boards, textile transistors may enable simple digital logic to be integrated directly into fabrics for increased flexibility and comfort. Research in this area leverages the use of new materials paired with textile architectures including using the weave structure for masking steps in forming on-fiber organic thin film transistors,^[512] using yarn junctions in a woven structure for electrochemical transistors,^[513] and using yarn plying strategies to create an architecture to improve performance of fiber-based organic transistors.^[514]

To power devices, textile-based energy storage strategies can potentially replace rigid batteries, air-tanks, and compressors with soft and flexible integrated power sources. Textile-based supercapacitors and batteries have been developed^[515,516] with both fabric-level^[517,518] and yarn-level^[519,520] configurations. As discussed for other components in this review, the textile

microstructure at a yarn and textile level continues to hold great importance. For example, at a yarn level, coils have been used to impart stretchability,^[520] and at a textile structure level, knit architecture dictates supercapacitor performance, where knits with rib architectures (as opposed to jersey) and higher stitch densities had increased areal capacitance.^[518]

To increase energy capacity of wearable robots without the need to replace or recharge batteries or alternative energy sources (e.g., refilling a compressed air tank), while simultaneously developing more “green” devices, power generation from the wearer and their interactions with their environment has been proposed.^[521] Thermoelectric fabrics may generate energy from the temperature differential from the body to the outside environment.^[522,523] Textile-based piezoelectric^[524,525] and triboelectric energy harvesting could produce power from the wearer’s motion.^[389,390,526–528] Textile structure once more affects performance; when comparing different woven structures, a plain weave was shown to have a higher electrical output when compared to a twill and satin weave.^[529]

On the critical path toward textile-based robotic garments, these components may be less likely to be included in first-generation implementations. In the case of control and energy storage, components do not need to be distributed or intimately coupled with specific locations on the body, whereas actuators and sensors require this location-dependent integration. Meanwhile in the area of power generation, there is a lower technology readiness level—rigid mobile devices, such as cell phones, do not yet use such components. In the near future, using rigid batteries and microcontrollers and leveraging the ability to create flexible textile-based connections to integrate these components to distributed soft actuators and sensors may be a practical first step. Nevertheless, to make robotic garments that truly preserve the properties of our everyday clothing, without requiring any hard components, these control, energy storage, and power generation components will need to be integrated at the yarn and textile level. For more information on this area we suggest the following reviews.^[515,516,530]

It is an exciting time in developing textile-based wearable robots and their constituent materials. With more interdisciplinary work and understanding, a future of robots that are just as stretchable, soft, and conformable as our clothing may seem less like something out of the superhero, Sailor Moon, and science fiction universes and instead a likely future.

Supporting Information

Supporting Information is available from the Wiley Online Library or from the author.

Acknowledgements

V.S. would like to thank Rachael Granberry, Krithika Swaminathan, Clark Teeple, Dr. Dae-Young Lee, Dr. James Weaver, and Prof. George Whitesides for wonderful conversations that ultimately impacted the work. V.S. would also like to thank Dr. Oluwaseun Araromi for valuable feedback on the manuscript, Robyn Rosenberg for assistance with locating references, and Dr. Peter York for critical LaTeX advice. The authors would also like to thank all the authors and designers

they reached out to who took the time to clarify questions and provide images. V.S. acknowledges the support of the United States Department of Defense through the National Defense Science and Engineering Graduate (NDSEG) Fellowship Program and the National GEM Consortium through the GEM Fellowship. This research was partially supported by the National Science Foundation EFRI Program (Award Number EFMA-1830901) and the National Science Foundation EFRI Program (Award Number 1830896).

Conflict of Interest

The authors declare no conflict of interest.

Author Contribution

All authors conceived the scope and focus of the review. V.S. researched, read, and compiled articles and wrote the manuscript draft. All authors reviewed and edited the manuscript.

Keywords

smart textiles, soft robotics, textile actuators, textile sensors, wearable robots

Received: September 28, 2020

Revised: November 15, 2020

Published online: December 10, 2020

- [1] L. Kramar, *J. Coated Fabr.* **1998**, 28, 106.
- [2] S. Backer, *Text. Res. J.* **1948**, 18, 650.
- [3] B. Quinlivan, A. Asbeck, D. Wagner, T. Ranzani, S. Russo, C. Walsh, presented at the *ASME 2015 Int. Design Engineering Technical Conf. and Computers and Information in Engineering Conf.*, Boston, MA, August **2015**.
- [4] M. Xiloyannis, E. Annese, M. Canesi, A. Kodiyan, A. Bicchi, S. Micera, A. Ajoudani, L. Masia, *Front. Neurobot.* **2019**, 13, 39.
- [5] D. Popov, I. Gaponov, J. H. Ryu, *IEEE/ASME Trans. Mechatronics* **2017**, 22, 865.
- [6] L. Cappello, K. C. Galloway, S. Sanan, D. A. Wagner, R. Granberry, S. Engelhardt, F. L. Haufe, J. D. Peisner, C. J. Walsh, *Soft Rob.* **2018**, 5, 662.
- [7] C. M. Thalman, T. Hertzell, H. Lee, in *2020 3rd IEEE Int. Conf. on Soft Robotics (RoboSoft)*, IEEE, Piscataway, NJ, **2020**, pp. 801–807.
- [8] J. Abel, J. Luntz, D. Brei, *Smart Mater. Struct.* **2013**, 22, 12.
- [9] T. Hiramitsu, K. Suzumori, H. Nabae, G. Endo, in *2019 2nd IEEE Int. Conf. on Soft Robotics (RoboSoft)*, IEEE, Piscataway, NJ, **2019**, pp. 1–6.
- [10] J. Xie, H. Long, M. Miao, *Smart Mater. Struct.* **2016**, 25, 105008.
- [11] S. Seyedin, S. Moradi, C. Singh, J. M. Razal, *Appl. Mater. Today* **2018**, 11, 255.
- [12] J. J. Park, W. J. Hyun, S. C. Mun, Y. T. Park, O. O. Park, *ACS Appl. Mater. Interfaces* **2015**, 7, 6317.
- [13] A. Atalay, V. Sanchez, O. Atalay, D. M. Vogt, F. Haufe, R. J. Wood, C. J. Walsh, *Adv. Mater. Technol.* **2017**, 2, 1700136.
- [14] Y. M. Zhou, D. Wagner, K. Nuckols, R. Heimgartner, C. Correia, M. Clarke, D. Orzel, O. Neill, R. Solinsky, S. Paganoni, C. J. Walsh, *2019 Int. Conf. on Robotics and Automation (ICRA)* **2019**, pp. 9059–9065.
- [15] Y. Jin, C. M. Glover, H. Cho, O. A. Araromi, M. A. Graule, N. Li, R. J. Wood, C. J. Walsh, in *2020 IEEE Int. Conf. on Robotics and Automation (ICRA)*, IEEE, Piscataway, NJ, **2020**, pp. 4863–4869.
- [16] C. O'Neill, T. Proietti, K. Nuckols, M. E. Clarke, C. J. Hohimer, A. Cloutier, D. J. Lin, C. J. Walsh, *IEEE Rob. Autom. Lett.* **2020**, 5, 3899.
- [17] J. Chung, R. Heimgartner, C. T. Oneill, N. S. Phipps, C. J. Walsh, in *2018 7th IEEE Int. Conf. on Biomedical Robotics and Biomechanics (Biorob)*, IEEE, Piscataway, NJ **2018**, pp. 509–516.
- [18] K. Schmidt, J. E. Duarte, M. Grimmer, A. Sancho-Puchades, H. Wei, C. S. Easthope, R. Riener, *Front. Neurobot.* **2017**, 11, 57.
- [19] M. Xiloyannis, D. Chiaradia, A. Frisoli, L. Masia, *J. NeuroEng. Rehabil.* **2019**, 16, 29.
- [20] Y. Kadowaki, T. Noritsugu, M. Takaiwa, D. Sasaki, M. Kato, *J. Rob. Mechatronics* **2011**, 23, 281.
- [21] J. Lee, C. Steen, *Technical Sourcebook for Apparel Designers*, 3rd ed., Fairchild Books, New York **2019**.
- [22] C. M. Thalman, Q. P. Lam, P. H. Nguyen, S. Sridar, P. Polygerinos, in *IEEE Int. Conf. on Intelligent Robots and Systems*, IEEE, Piscataway, NJ **2018**, pp. 6965–6971.
- [23] A. Freudmann, Customers want customization, and companies are giving it to them, <https://www.nytimes.com/2020/03/18/business/customization-personalized-products.html?referringSource=articleShare> (accessed: June 2020).
- [24] S. P. Ashdown, *Int. J. Clothing Sci. Technol.* **1998**, 10, 324.
- [25] S. P. Ashdown, in *Improving Comfort in Clothing*, Woodhead Publishing Limited, **2011**, pp. 278–302.
- [26] L. N. Awad, J. Bae, K. O'Donnell, S. M. M. De Rossi, K. Hendron, L. H. Sloat, P. Kudzia, S. Allen, K. G. Holt, T. D. Ellis, C. J. Walsh, *Sci. Transl. Med.* **2017**, 9, 400.
- [27] J. Bae, S. M. Maria De Rossi, K. O'Donnell, K. L. Hendron, L. N. Awad, T. R. Teles Dos Santos, V. L. De Araujo, Y. Ding, K. G. Holt, T. D. Ellis, C. J. Walsh, in *2015 IEEE Int. Conf. on Rehabilitation Robotics (ICORR)*, IEEE, Piscataway, NJ **2015**, pp. 131–138.
- [28] M. Wehner, B. Quinlivan, P. M. Aubin, E. Martinez-Villalpando, M. Baumann, L. Stirling, K. Holt, R. Wood, C. Walsh, in *2013 IEEE Int. Conf. on Robotics and Automation*, IEEE, Piscataway, NJ **2013**, pp. 3362–3369.
- [29] C. M. Thalman, J. Hsu, L. Snyder, P. Polygerinos, in *2019 Int. Conf. on Robotics and Automation (ICRA)*, Montreal, QC, Canada, **2019**, pp. 8436–8442.
- [30] S. Sridar, P. H. Nguyen, M. Zhu, Q. P. Lam, P. Polygerinos, *2017 IEEE/RSJ Int. Conf. on Intelligent Robots and Systems (IROS)*, IEEE, Piscataway, NJ **2017**, pp. 3722–3727.
- [31] J. Kim, G. Lee, R. Heimgartner, D. A. Revi, N. Karavas, D. Nathanson, I. Galiana, A. Eckert-Erdheim, P. Murphy, D. Perry, N. Menard, D. K. Choe, P. Malcolm, C. J. Walsh, *Science* **2019**, 365, 668.
- [32] A. Veale, K. Staman, H. van der Kooij, *Soft Rob.* **2020**, <https://www.liebertpub.com/doi/abs/10.1089/soro.2019.0076>.
- [33] B. T. Quinlivan, S. Lee, P. M. Lee, D. M. Lee, M. G. Lee, C. S. Lee, N. K. Lee, D. Wagner, A. Asbeck, I. G. Asbeck, C. J. Walsh, *Sci. Rob.* **2017**, 2, 2.
- [34] R. C. Browning, J. R. Modica, R. Kram, A. Goswami, *Med. Sci. Sports Exercise* **2007**, 39, 515.
- [35] S. Jin, N. Iwamoto, K. Hashimoto, M. Yamamoto, *IEEE Trans. Neural Syst. Rehabil. Eng.* **2017**, 25, 1192.
- [36] Y. L. Park, B. R. Chen, N. O. Pérez-Arancibia, D. Young, L. Stirling, R. J. Wood, E. C. Goldfield, R. Nagpal, *Bioinspiration Biomimetics* **2014**, 9, 016007.
- [37] Y. Ding, I. Galiana, A. Asbeck, B. Quinlivan, S. M. M. De Rossi, C. Walsh, in *2014 IEEE Int. Conf. on Robotics and Automation (ICRA)*, IEEE, Piscataway, NJ **2014**, pp. 1327–1334.
- [38] Y. Li, M. Hashimoto, *Smart Mater. Struct.* **2017**, 26, 12.
- [39] L. Stirling, C.-h. Yu, J. Miller, E. Hawkes, R. Wood, E. Goldfield, R. Nagpal, *J. Mater. Eng. Perform.* **2011**, 20, 658.
- [40] S. Sridar, Z. Qiao, N. Muthukrishnan, W. Zhang, P. Polygerinos, *Front. Rob. AI* **2018**, 5, 44.

- [41] A. T. Asbeck, R. J. Dyer, A. F. Larusson, C. J. Walsh, in *2013 IEEE 13th Int. Conf. on Rehabilitation Robotics (ICORR)*, IEEE, Piscataway, NJ **2013**, pp. 1–8.
- [42] Y. Mengüç, Y. L. Park, H. Pei, D. Vogt, P. M. Aubin, E. Winchell, L. Fluke, L. Stirling, R. J. Wood, C. J. Walsh, *Int. J. Rob. Res.* **2014**, 33, 1748.
- [43] E. M. McCain, T. J. Dick, T. N. Giest, R. W. Nuckols, M. D. Lewek, K. R. Saul, G. S. Sawicki, *J. NeuroEng. Rehabil.* **2019**, 16, 57.
- [44] P. R. Cavanagh, *Foot Ankle Int.* **1987**, 7, 197.
- [45] M. D. Latt, H. B. Menz, V. S. Fung, S. R. Lord, *Exp. Brain Res.* **2008**, 184, 201.
- [46] J. Zhang, P. Fiers, K. A. Witte, R. W. Jackson, K. L. Poggensee, C. G. Atkeson, S. H. Collins, *Science* **2017**, 356, 1280.
- [47] Y. Ding, M. Kim, S. Kuindersma, C. J. Walsh, *Sci. Rob.* **2018**, 3, eaar5438.
- [48] P. R. Cavanagh, R. J. Gregor, *J. Biomech.* **1975**, 8, 337.
- [49] Y. C. Pai, M. W. Rogers, *Arch. Phys. Med. Rehabil.* **1991**, 72, 881.
- [50] L. Cappello, J. T. Meyer, K. C. Galloway, J. D. Peisner, R. Granberry, D. A. Wagner, S. Engelhardt, S. Paganoni, C. J. Walsh, *J. NeuroEng. Rehabil.* **2018**, 15, 59.
- [51] H. In, B. B. Kang, M. K. Sin, K. J. Cho, *IEEE Rob. Autom. Mag.* **2015**, 22, 97.
- [52] H. K. Yap, P. M. Khin, T. H. Koh, Y. Sun, X. Liang, J. H. Lim, C. H. Yeow, *IEEE Rob. Autom. Lett.* **2017**, 2, 1383.
- [53] Y. G. Kim, M. Xiloyannis, D. Accoto, L. Masia, in *2018 7th IEEE Int. Conf. on Biomedical Robotics and Biomechanics (Biorob)*, IEEE, Piscataway, NJ **2018**, pp. 324–329.
- [54] H. K. Yap, N. Kamaldin, J. H. Lim, F. A. Nasrallah, J. C. H. Goh, C. H. Yeow, *IEEE Trans. Neural Syst. Rehabil. Eng.* **2017**, 25, 782.
- [55] H. K. Yap, J. H. Lim, F. Nasrallah, F. Z. Low, J. C. Goh, R. C. Yeow, in *2015 IEEE Int. Conf. on Rehabilitation Robotics (ICORR)*, IEEE, Piscataway, NJ **2015**, pp. 735–740.
- [56] A. Stilli, A. Cremonini, M. Bianchi, A. Ridolfi, F. Gerii, F. Vannetti, H. A. Wurdemann, B. Allotta, K. Althoefer, *2018 IEEE Int. Conf. on Soft Robotics, RoboSoft 2018*, IEEE, Piscataway, NJ **2018**, pp. 579–584.
- [57] N. Li, T. Yang, P. Yu, J. Chang, L. Zhao, X. Zhao, I. H. Elhajj, N. Xi, L. Liu, *Bioinspir. Biomim.* **2018**, 13, 6.
- [58] H. Choi, B. B. Kang, B. K. Jung, K. J. Cho, *IEEE. Rob. Autom. Lett.* **2019**, 4, 4499.
- [59] T. Abe, S. Koizumi, H. Nabae, G. Endo, K. Suzumori, N. Sato, M. Adachi, F. Takamizawa, *IEEE. Rob. Autom. Lett.* **2019**, 4, 2532.
- [60] C. T. O'Neill, N. S. Phipps, L. Cappello, S. Paganoni, C. J. Walsh, in *2017 Int. Conf. on Rehabilitation Robotics (ICORR)*, IEEE, Piscataway, NJ **2017**, pp. 1672–1678.
- [61] I. Galiana, F. L. Hammond, R. D. Howe, M. B. Popovic, in *2012 IEEE/RSJ Int. Conf. on Intelligent Robots and Systems*, IEEE, Piscataway, NJ **2012**, pp. 317–322.
- [62] C. S. Simpson, A. M. Okamura, E. W. Hawkes, in *2017 IEEE Int. Conf. on Robotics and Automation (ICRA)*, IEEE, Piscataway, NJ **2017**, pp. 6651–6657.
- [63] R. F. Natividad, C. H. Yeow, in *2016 6th IEEE Int. Conf. on Biomedical Robotics and Biomechanics (BioRob)*, IEEE, Piscataway, NJ **2016**, pp. 989–993.
- [64] S. Moromugi, K. Kawakami, K. Nakamura, T. Sakamoto, T. Ishimatsu, in *2009 ICCAS-SICE*, IEEE, Piscataway, NJ **2009**, pp. 794–797.
- [65] H. K. Yap, J. H. Lim, F. Nasrallah, C. H. Yeow, *Front. Neurosci.* **2017**, 11, 547.
- [66] F. Connolly, D. A. Wagner, C. J. Walsh, K. Bertoldi, *Extreme Mech. Lett.* **2019**, 27, 52.
- [67] C. Correia, K. Nuckols, D. Wagner, Y. M. Zhou, M. Clarke, D. Orzel, R. Solinsky, S. Paganoni, C. J. Walsh, *IEEE Trans. Neural Syst. Rehabil. Eng.* **2020**, 28, 1407.
- [68] L. Ge, F. Chen, D. Wang, Y. Zhang, D. Han, T. Wang, G. Gu, *Soft Rob.* **2020**, 7, 5.
- [69] S. Lessard, P. Pansodtee, A. Robbins, J. M. Trombadore, S. Kurniawan, M. Teodorescu, *IEEE Trans. Neural Syst. Rehabil. Eng.* **2018**, 26, 1604.
- [70] M. Xiloyannis, L. Cappello, K. D. Binh, C. W. Antuvan, L. Masia, *J. Rehabil. Assistive Technol. Eng.* **2017**, 4, 205566831668031.
- [71] X. Chen, L. Gong, L. Wei, S.-c. Yeh, L. D. Xu, L. Zheng, Z. Zou, *IEEE Trans. Ind. Inf.* **2021**, 17, 94.
- [72] M. A. Delph, S. A. Fischer, P. W. Gauthier, C. H. Luna, E. A. Clancy, G. S. Fischer, in *2013 IEEE 13th Int. Conf. on Rehabilitation Robotics (ICORR)*, IEEE, Piscataway, NJ **2013**, pp. 1–7.
- [73] L. Gerez, J. Chen, M. Liarokapis, *IEEE. Rob. Autom. Lett.* **2019**, 4, 1.
- [74] J. M. Ochoa, D. G. Kamper, M. Listenberger, S. W. Lee, in *2011 IEEE Int. Conf. on Rehabilitation Robotics*, IEEE, Piscataway, NJ **2011**, pp. 1–5.
- [75] R. Paradiso, G. Loriga, N. Taccini, *IEEE Trans. Inf. Technol. Biomed.* **2005**, 9, 337.
- [76] L. Eskandarian, E. Lam, C. Rupnow, M. A. Meghraz, H. E. Naguib, *ACS Appl. Electron. Mater.* **2020**, 2, 1554.
- [77] K. Matheus, A. M. Dollar, in *2010 IEEE/RSJ Int. Conf. on Intelligent Robots and Systems*, IEEE, Piscataway, NJ **2010**, pp. 5020–5027.
- [78] N. Smaby, M. E. Johanson, B. Baker, D. E. Kenney, W. M. Murray, V. R. Hentz, *J. Rehabil. Res. Dev.* **2004**, 41, 215.
- [79] V. Mathiowetz, N. Kashman, G. Volland, K. Weber, M. Dowe, S. Rogers, *Arch. Phys. Med. Rehabil.* **1985**, 66, 69.
- [80] I. A. Murray, G. R. Johnson, *Clin. Biomech.* **2004**, 19, 586.
- [81] J. Rosen, J. C. Perry, N. Manning, S. Burns, B. Hannaford, *ICAR '05. Proc., 12th Int. Conf. on Advanced Robotics*, 2005, IEEE, Piscataway, NJ **2005**, pp. 532–539.
- [82] H. J. Freund, *Prog. Brain Res.* **1986**, 64, 287.
- [83] H. Zeng, Y. Zhao, *Sensors* **2011**, 11, 638.
- [84] P. Polygerinos, Z. Wang, K. C. Galloway, R. J. Wood, C. J. Walsh, *Rob. Auton. Syst.* **2015**, 73, 135.
- [85] P. Agarwal, J. Fox, Y. Yun, M. K. O'Malley, A. D. Deshpande, *Int. J. Rob. Res.* **2015**, 34, 1747.
- [86] J. M. Wiener, R. J. Hanley, R. Clark, J. F. Van Nostrand, *J. Gerontol.* **1990**, 45, 229.
- [87] B. J. Dudgeon, J. M. Hoffman, M. A. Ciol, A. Shumway-Cook, K. M. Yorkston, L. Chan, *Arch. Phys. Med. Rehabil.* **2008**, 89, 1256.
- [88] R. Granberry, K. Eschen, B. Holschuh, J. Abel, *Adv. Mater. Technol.* **2019**, 4, 1900548.
- [89] T. Helps, M. Taghavi, S. Manns, A. J. Turton, J. Rossiter, in *Towards Autonomous Robotic Systems: 19th Annual Conf., TAROS 2018*. Springer, Cham **2018**, pp. 79–90.
- [90] A. Y. Chen, C. Poh, C. Mallon, Cair Collective, <https://www.caircollective.com/introduction> (accessed: June 2020).
- [91] J. R. Steele, S. A. Gho, T. E. Campbell, C. J. Richards, S. Beirne, G. M. Spinks, G. G. Wallace, *J. Rehabil. Assistive Technol. Eng.* **2018**, 5, 205566831877590.
- [92] B. T. Holschuh, D. J. Newman, *Aerosp. Med. Hum. Perform.* **2016**, 87, 84.
- [93] L. Tessmer, C. Dunlap, B. Sparrman, S. Kernizan, J. Laucks, S. Tibbits, presented at the *ACM SIGGRAPH 2019 Emerging Technologies*, SIGGRAPH '19. Los Angeles, CA, July **2019**.
- [94] J. C. Cool, *Prosthet. Orthotics Int.* **1989**, 13, 90.
- [95] G. A. Holloway, C. H. Daly, D. Kennedy, J. Chimoskey, *J. Appl. Physiol.* **1976**, 40, 597.
- [96] Medical Compression Hosiery: Quality Assurance, RAL-GZ 387/1, German Institute for Quality Assurance, Sankt Augustin **2008**.
- [97] K. Stevens, M. Fuller, in *Textile-led Design for the Active Ageing Population*, Elsevier, New York, **2014**, pp. 117–138.
- [98] G. Havenith, *Exog. Dermatol.* **2002**, 1, 221.
- [99] W. Wang, L. Yao, C.-Y. Cheng, T. Zhang, H. Atsumi, L. Wang, G. Wang, O. Anilonyte, H. Steiner, J. Ou, K. Zhou, C. Wawrousek,

- K. Petrecca, A. M. Belcher, R. Karnik, X. Zhao, D. I. C. Wang, H. Ishii, *Sci. Adv.* **2017**, 3, 5.
- [100] X. A. Zhang, S. Yu, B. Xu, M. Li, Z. Peng, Y. Wang, S. Deng, X. Wu, Z. Wu, M. Ouyang, Y. H. Wang, *Science* **2019**, 363, 619.
- [101] Y. E. Ku, L. D. Montgomery, H. C. Lee, L. B. B. W. Webbon, *Mult. Sclerosis* **2000**, 79, 427.
- [102] C. Gao, K. Kuklane, F. Wang, I. Holmér, *Indoor Air* **2012**, 22, 523.
- [103] A. Meyer-Heim, M. Rothmaier, M. Weder, J. Kool, P. Schenk, J. Kesselring, *Mult. Sclerosis* **2007**, 13, 232.
- [104] S. A. Nunneley, *Space Life Sci.* **1970**, 2, 335.
- [105] Midwest Research Institute, Liquid Cooled Garments, Technical report, NASA **1975**.
- [106] G. Thilagavathi, N. Muthukumar, T. Kannaian, *J. Text. Eng. Fashion Technol.* **2017**, 1, 6.
- [107] L. Zhang, M. Baima, T. L. Andrew, *ACS Appl. Mater. Interfaces* **2017**, 9, 32299.
- [108] H. Park, S. K. Hwang, J. Y. Lee, J. Fan, Y. Jeong, *Int. J. Clothing Sci. Technol.* **2016**, 28, 254.
- [109] J. Tabor, K. Chatterjee, T. K. Ghosh, *Adv. Mater. Technol.* **2020**, 5, 1901155.
- [110] T. Jia, Y. Wang, Y. Dou, Y. Li, M. Jung de Andrade, R. Wang, S. Fang, J. Li, Z. Yu, R. Qiao, Z. Liu, Y. Cheng, Y. Su, M. Minary-Jolandan, R. H. Baughman, D. Qian, Z. Liu, *Adv. Funct. Mater.* **2019**, 29, 1808241.
- [111] M. Kanik, S. Orguc, G. Varnavides, J. Kim, T. Benavides, D. Gonzalez, T. Akintilo, C. C. Tasan, A. P. Chandrakasan, Y. Fink, P. Anikeeva, *Science* **2019**, 365, 145.
- [112] J. Berzowska, M. Coelho, in *Proc. - Int. Symp. on Wearable Computers, ISWC*, Vol. 2005, Association for Computing Machinery, New York, NY **2005**, pp. 82–85.
- [113] L. Albaugh, S. Hudson, L. Yao, in *Proc. of the 2019 CHI Conf. on Human Factors in Computing Systems*, CHI '19, Association for Computing Machinery, New York, NY **2019**, pp. 1–13.
- [114] M. Zhu, A. H. Memar, A. Gupta, M. Samad, P. Agarwal, Y. Visell, S. J. Keller, N. Colonnese, in *Proc. of the 2020 CHI Conf. on Human Factors in Computing Systems*, CHI '20, Association for Computing Machinery, New York, NY **2020**, pp. 1–12.
- [115] C. Pacchierotti, S. Sinclair, M. Solazzi, A. Frisoli, V. Hayward, D. Prattichizzo, *IEEE Trans. Haptics* **2017**, 10, 580.
- [116] S. Biswas, Y. Visell, *Adv. Mater. Technol.* **2019**, 4, 1900042.
- [117] T. Mitsuda, *2017 IEEE World Haptics Conf., WHC 2017*, IEEE, Piscataway, NJ **2017**, pp. 364–369.
- [118] E. M. Young, A. H. Memar, P. Agarwal, N. Colonnese, in *2019 IEEE World Haptics Conf. (WHC)*, IEEE, Piscataway, NJ **2019**, pp. 55–60.
- [119] F. Arafsha, K. M. Alam, A. E. Saddik, *2012 Int. Conf. on Innovations in Information Technology, IIT 2012*, IEEE, Piscataway, NJ **2012**, pp. 350–355.
- [120] R. W. Lindeman, R. Page, Y. Yanagida, J. L. Sibert, in *Proc. of the ACM Symp. on Virtual Reality Software and Technology, VRST '04*, Association for Computing Machinery, New York, NY **2004**, pp. 146–149.
- [121] A. Delazio, K. Nakagaki, R. L. Klatzky, S. E. Hudson, J. F. Lehman, A. P. Sample, in *Proc. of the 2018 CHI Conf. on Human Factors in Computing Systems*, CHI '18, Association for Computing Machinery, New York **2018**, pp. 1–12.
- [122] J. K. S. Teh, A. D. Cheok, R. L. Peiris, Y. Choi, V. Thuong, S. Lai, in *Proc. of the 7th Int. Conf. on Interaction Design and Children, IDC '08*, Association for Computing Machinery, New York, **2008**, pp. 250–257.
- [123] H. Pohl, P. Brandes, H. Ngo Quang, M. Rohs, in *Proc. of the 2017 CHI Conf. on Human Factors in Computing Systems*, CHI '17, Association for Computing Machinery, New York **2017**, pp. 5318–5330.
- [124] H. Pohl, F. Hoheisel, M. Rohs, in *Proc. of the 2017 CHI Conf. Extended Abstracts on Human Factors in Computing Systems*, CHI EA '17, Association for Computing Machinery, New York **2017**, pp. 1962–1969.
- [125] L. Bonanni, C. Vaucelle, J. Lieberman, O. Zuckerman, in *CHI '06 Extended Abstracts on Human Factors in Computing Systems*, CHI EA '06, Association for Computing Machinery, New York **2006**, pp. 580–585.
- [126] K. S. Hale, K. M. Stanney, *IEEE Computer Graphics and Applications* **2004**, 24, 33.
- [127] C. Rognon, V. Ramachandran, A. R. Wu, A. J. Ijspeert, D. Floreano, *IEEE Trans. Haptics* **2019**, 12, 375.
- [128] H. Zhao, A. M. Hussain, A. Israr, D. M. Vogt, M. Duduta, D. R. Clarke, R. J. Wood, *Soft Rob.* **2020**, 7, 451.
- [129] A. Gupta, A. A. R. Irudayaraj, R. Balakrishnan, in *Proc. of the 30th Annual ACM Symp. on User Interface Software and Technology*, UIST '17, Association for Computing Machinery, New York **2017**, pp. 109–117.
- [130] E. W. Foo, J. W. Lee, C. Compton, S. Ozbek, B. Holschuh, in *Proc. of the 23rd Int. Symp. on Wearable Computers, ISWC '19*, Association for Computing Machinery, New York **2019**, pp. 54–59.
- [131] E. W. Foo, J. W. Lee, S. Ozbek, C. Compton, B. Holschuh, in *Proc. of the 23rd Int. Symp. on Wearable Computers, ISWC '19*, Association for Computing Machinery, New York **2019**, pp. 267–273.
- [132] Z. McKinney, K. Heberer, B. N. Nowroozi, M. Greenberg, E. Fowler, W. Grundfest, in *2014 IEEE Haptics Symp. (HAPTICS)*, IEEE, Piscataway, NJ **2014**, pp. 135–140.
- [133] W. Wu, H. Culbertson, in *2019 IEEE World Haptics Conf. (WHC)*, IEEE, Piscataway, NJ **2019**, pp. 193–198.
- [134] P. M. Khin, J. H. Low, W. W. Lee, S. L. Kukreja, H. L. Ren, N. V. Thakor, C. H. Yeow, in *2016 6th IEEE Int. Conf. on Biomedical Robotics and Biomechanics (BioRob)*, IEEE, Piscataway, NJ **2016**, pp. 1272–1276.
- [135] D. A. Kontarinis, R. D. Howe, *Presence: Teleoperators Virtual Environ.* **1995**, 4, 387.
- [136] S. J. Lederman, R. L. Klatzky, *Atten., Percept., Psychophys.* **2009**, 71, 1439.
- [137] M. K. O'Malley, M. Goldfarb, *IEEE/ASME Trans. Mechatronics* **2002**, 7, 280.
- [138] M. K. O'Malley, in *Life Science Automation: Fundamentals and Applications*, Artech House Publishers, Norwood, MA **2007**, pp. 101–125.
- [139] M. C. Bloemen, W. M. van der Veer, M. M. Ulrich, P. P. van Zuijlen, F. B. Niessen, E. Middelkoop, *Burns* **2009**, 35, 463.
- [140] B. S. Atiyeh, A. M. El Khatib, S. A. Dibo, *Ann. Burns Fire Disasters* **2013**, 26, 205.
- [141] L. Macintyre, *Burns* **2007**, 33, 579.
- [142] L. Macintyre, M. Baird, *Burns* **2006**, 32, 10.
- [143] L. J. Olson, H. J. Moulton, *Occup. Ther. Int.* **2004**, 11, 52.
- [144] J. Case-Smith, L. L. Weaver, M. A. Fristad, *Autism* **2015**, 19, 133.
- [145] N. L. Vandenberg, *Am. J. Occup. Ther.* **2001**, 55, 621.
- [146] M. J. Brennan, L. T. Miller, *Cancer* **1998**, 83, 2821.
- [147] R. J. Morris, J. P. Woodcock, *Ann. Surg.* **2004**, 239, 162.
- [148] R. J. Morris, *J. Med. Eng. Technol.* **2008**, 32, 179.
- [149] CLOTS (Clots in Legs Or sTockings after Stroke) Trials Collaboration, *Lancet* **2013**, 382, 516.
- [150] K. T. Delis, G. Slimani, H. M. Hafez, A. N. Nicolaides, *Eur. J. Vasc. Endovasc. Surg.* **2000**, 19, 250.
- [151] A. Kordzadeh, A. Jonas, Y. P. Panayiotopoulos, *Case Rep. Clin. Med.* **2014**, 03, 513.
- [152] C. A. Cezar, E. T. Roche, H. H. Vandenberg, G. N. Duda, C. J. Walsh, D. J. Mooney, *Proc. Natl. Acad. Sci. USA* **2016**, 113, 1534.
- [153] J. D. Crane, D. I. Ogborn, C. Cupido, S. Melov, A. Hubbard, J. M. Bourgeois, M. A. Tarnopolsky, *Sci. Transl. Med.* **2012**, 4, 119ra13.
- [154] S. T. Yang, J. W. Ryu, S. H. Park, Y. B. Lee, S. H. Koo, Y. L. Park, G. Lee, *Smart Mater. Struct.* **2019**, 28, 11.
- [155] C. J. Payne, E. G. Hevia, N. Phipps, A. Atalay, O. Atalay, B. R. Seo, D. J. Mooney, C. J. Walsh, in *2018 IEEE Int. Conf. on Robotics and Automation (ICRA)*, IEEE, Piscataway, NJ **2018**, pp. 5459–5465.

- [156] D. J. Preston, H. J. Jiang, V. Sanchez, P. Rothenmund, J. Rawson, M. P. Nemitz, W.-K. Lee, Z. Suo, C. J. Walsh, G. M. Whitesides, *Sci. Rob.* **2019**, 4, eaaw5496.
- [157] M. Zhu, T. N. Do, E. Hawkes, Y. Visell, *Soft Rob.* **2020**, 7, 179.
- [158] J. C. Duvall, N. Schleif, L. E. Dunne, B. Holschuh, *J. Med. Devices* **2019**, 13, 021001.
- [159] B. Holschuh, E. Obropta, D. Newman, *IEEE/ASME Trans. Mechatronics* **2015**, 20, 1264.
- [160] C. Haas, T. A. Butterfield, Y. Zhao, X. Zhang, D. Jarjoura, T. M. Best, *Br. J. Sports Med.* **2013**, 47, 83.
- [161] T. L. Teng, K. T. Chou, *J. Med. Biol. Eng.* **2006**, 26, 155.
- [162] W. L. Olszewski, P. Jain, G. Ambujam, M. Zaleska, M. Cakala, T. Gradalski, *Lymphatic Res. Biol.* **2011**, 9, 77.
- [163] S. Zhao, R. Liu, C. Fei, D. Guan, *Sensors* **2019**, 19, 13.
- [164] S. Zhao, C. Ye, L. Jing, Z. Gong, J. Liu, J. Chen, C. C. Chan, S. Ruan, *IEEE Sens. J.* **2020**, 20, 12765.
- [165] M. D. Malone, P. L. Cisek, J. Comerota, B. Holland, I. G. Eid, A. J. Comerota, *J. Vasc. Surg.* **1999**, 29, 593.
- [166] R. Eisele, L. Kinzl, T. Koelsch, *JBJS* **2007**, 89, 1050.
- [167] H. Partsch, *Int. Wound J.* **2008**, 5, 389.
- [168] B. L. Hard, M.-H. Moncel, C. Kerfant, M. Le, N. Méléard, B. L. Hardy, M.-H. Moncel, C. Kerfant, M. Lebon, L. Bellot-Gurlet, N. Méléard, *Sci. Rep.* **2020**, 10, 4889.
- [169] E. Kvavadze, O. Bar-Yosef, A. Belfer-Cohen, E. Boaretto, N. Jakeli, Z. Matskevich, T. Meshveliani, *Science* **2009**, 325, 1359.
- [170] A. Frutiger, J. T. Muth, D. M. Vogt, Y. Mengüç, A. Campo, A. D. Valentine, C. J. Walsh, J. A. Lewis, *Adv. Mater.* **2015**, 27, 2440.
- [171] S. Zhu, J. H. So, R. Mays, S. Desai, W. R. Barnes, B. Pourdeyimi, M. D. Dickey, *Adv. Funct. Mater.* **2013**, 23, 2308.
- [172] Y. Cheng, R. Wang, J. Sun, L. Gao, *Adv. Mater.* **2015**, 27, 7365.
- [173] W. Qureshi, L. Guo, J. Peterson, L. Berglin, M. Skrifvars, presented at *Ambience'17*, Borås, Sweden, November **2011**.
- [174] Z. Wang, Y. Huang, J. Sun, Y. Huang, H. Hu, R. Jiang, W. Gai, G. Li, C. Zhi, *ACS Appl. Mater. Interfaces* **2016**, 8, 24837.
- [175] R. H. Gong, R. M. Wright, *Fancy Yarns: Their Manufacture and Application*, Elsevier, New York **2002**.
- [176] R. Wright, in *Specialist Yarn and Fabric Structures*, Woodhead Publishing Limited, Cambridge, UK **2011**, pp. 75–108.
- [177] E. Gohl, L. Vilensky, in *Textiles for Modern Living*, 5th ed., Addison Wesley Longman Australia Pty Limited, Melbourne, Australia **1993**, pp. 291–323.
- [178] Y. Chen, in *Specialist Yarn and Fabric Structures*, Woodhead Publishing Limited, Cambridge UK **2011**, pp. 118–140.
- [179] N. Ishmael, A. Fernando, S. Andrew, L. Waterton Taylor, *Res. J. Text. Apparel* **2017**, 21, 342.
- [180] M. R. N. , B. K. Behera, In *Advanced Textile Engineering Materials* (Eds: S. ul Islam, B. Butola), 1st ed., chapter 12, pp. 463–498. John Wiley & Sons, Inc., Hoboken, NJ **2018**.
- [181] A. Zulifqar, T. Hua, H. Hu, *Text. Res. J.* **2018**, 88, 2076.
- [182] H. Cao, A. Zulifqar, T. Hua, H. Hu, *Text. Res. J.* **2019**, 89, 2694.
- [183] H. Kamrul, A. Zulifqar, H. Hu, *Text. Res. J.* **2020**, 90, 410.
- [184] C. Ayranci, J. Carey, *Compos. Struct.* **2008**, 85, 43.
- [185] Y. Kyosev, *Braiding Technology for Textiles: Principles, Design and Processes*, Elsevier, New York **2014**.
- [186] G. W. Du, P. Popper, *J. Text. Inst.* **1994**, 85, 316.
- [187] R. M. Bruce, E. K. Lee, US20160345677A1, **2016**.
- [188] M.-A. Bueno, B. Camillieri, in *Structure and Mechanics of Textile Fibre Assemblies*, 2nd ed., Elsevier, New York **2019**, pp. 61–107, Ch. 3.
- [189] J. Underwood, *Ph.D. Thesis*, RMIT University, **2009**.
- [190] D. J. Spencer, *Knitting Technology: A Comprehensive Handbook and Practical Guide*, Woodhead Publishing, Cambridge, England **2001**.
- [191] J. McCann, L. Albaugh, V. Narayanan, A. Grow, W. Matusik, J. Mankoff, J. Hodgins, *ACM Trans. Graph.* **2016**, 35, 4.
- [192] R. V. Martinez, C. R. Fish, X. Chen, G. M. Whitesides, *Adv. Funct. Mater.* **2012**, 22, 1376.
- [193] S. Li, D. M. Vogt, D. Rus, R. J. Wood, *Proc. Natl. Acad. Sci. USA* **2017**, 114, 13132.
- [194] A. Rafsanjani, Y. Zhang, B. Liu, S. M. Rubinstein, K. Bertoldi, *Sci. Rob.* **2018**, 3, 15.
- [195] C. E. Knittel, D. S. Nicholas, R. M. Street, C. L. Schauer, G. Dion, *Fibers* **2015**, 3, 575.
- [196] A. Pavko-Cuden, D. Rant, in *Textiles for Advanced Applications*, Intech, London, UK **2017**, p. 13.
- [197] Y. Liu, H. Hu, J. K. C. Lam, S. Liu, *Text. Res. J.* **2010**, 80, 856.
- [198] F. Steffens, S. Rana, R. Figueiro, *Mater. Des.* **2016**, 106, 81.
- [199] H. Hu, Z. Wang, S. Liu, *Text. Res. J.* **2011**, 81, 1493.
- [200] K. Alderson, A. Alderson, S. Anand, V. Simkins, S. Nazare, N. Ravirala, *Phys. Status Solidi B* **2012**, 249, 1322.
- [201] A. Kaspar, L. Makatura, W. Matusik, in *Proc. of the 32nd Annual ACM Symp. on User Interface Software and Technology*, UIST '19. Association for Computing Machinery, New York **2019**, pp. 53–65.
- [202] Y. Igarashi, T. Igarashi, H. Suzuki, in *Eurographics 2008 - Short Papers* (Eds: K. Mania, E. Reinhard), European Association for Computer Graphics, Geneva, Switzerland **2008**.
- [203] J. Lin, V. Narayanan, J. McCann, in *Proc. of the 2nd ACM Symp. on Computational Fabrication*, SCF '18. Association for Computing Machinery, New York **2018**.
- [204] V. Narayanan, L. Albaugh, J. Hodgins, S. Coros, J. Mccann, *ACM Trans. Graph.* **2018**, 37, 3.
- [205] V. Narayanan, K. Wu, C. Yuksel, J. McCann, *ACM Trans. Graph.* **2019**, 38, 4.
- [206] K. Wu, H. Swan, C. Yuksel, *ACM Trans. Graph.* **2019**, 38, 10.
- [207] A. Kaspar, T.-H. Oh, L. Makatura, P. Kellnhofer, W. Matusik, in *Proc. of the 36th Int. Conf. on Machine Learning*, Vol. 97 (Eds: K. Chaudhuri, R. Salakhutdinov), PMLR Long Beach, CA, **2019**, pp. 3272–3281.
- [208] E. Gohl, L. Vilensky, in *Textile for Modern Living*, 5th ed., Addison Wesley Longman Australia Pty Limited, Melbourne, Australia **1993**, pp. 324–333.
- [209] N. R. Sinatra, T. Ranzani, J. J. Vlassak, K. K. Parker, R. J. Wood, *J. Micromech. Microeng.* **2018**, 28, aab373.
- [210] N. R. Sinatra, C. B. Teeple, D. M. Vogt, K. K. Parker, D. F. Gruber, R. J. Wood, *Sci. Rob.* **2019**, 4, eaax5425.
- [211] L. F. Deravi, N. R. Sinatra, C. O. Chantre, A. P. Nesmith, H. Yuan, S. K. Deravi, J. A. Goss, L. A. MacQueen, M. R. Badrossamy, G. M. Gonzalez, M. D. Phillips, K. K. Parker, *Macromol. Mater. Eng.* **2017**, 302, 1600404.
- [212] B. Shin, J. Ha, M. Lee, K. Park, G. H. Park, T. H. Choi, K. J. Cho, H. Y. Kim, *Sci. Rob.* **2018**, 3, 14.
- [213] N. K. Trejo, C. G. Reyes, V. Sanchez, D. Zhang, M. W. Frey, *Int. J. Fashion Des., Technol. Educ.* **2016**, 9, 192.
- [214] D. Du, P. Li, J. Ouyang, *J. Mater. Chem. C* **2016**, 4, 3224.
- [215] A. Hursa, T. Rolich, S. E. Ražić, *Text. Res. J.* **2009**, 79, 1588.
- [216] Ž. Penava, D. Š. Penava, Ž. Knežić, *Fibres Text. East. Eur.* **2014**, 104, 57.
- [217] L. Bao, M. Takatera, A. Shinohara, *Sen-i Gakkaishi* **1997**, 53, 20.
- [218] W. J. Hamburger, *J. Text. Inst., Proc.* **1949**, 40, P700.
- [219] H. Gabrijelčič, E. Cernoša, K. Dimitrovski, *Fibres Text. East. Eur.* **2008**, 16, 45.
- [220] T. Hussain, Z. A. Malik, A. Tanwari, *Indian J. Fibre Text. Res.* **2010**, 35, 243.
- [221] M. H. Seo, M. L. Realff, N. Pan, M. Boyce, P. Schwartz, S. Backer, *Text. Res. J.* **1993**, 63, 123.
- [222] Z. Jinyun, L. Yi, J. Lam, C. Xuyong, *Text. Res. J.* **2010**, 80, 1965.
- [223] E. Perumalsamy, J. C. Sakthivel, N. Anbumani, *Int. J. Clothing Sci. Technol.* **2014**, 26, 222.
- [224] D. B. Sitotaw, B. F. Adamu, *J. Eng.* **2017**, 2017, 4310782.
- [225] N. T. Akankwasa, W. Jun, Z. Yuze, M. Mushtaq, *Materialwiss. Werkstofftech.* **2014**, 45, 1039.
- [226] B. A. Mcgregor, R. Postle, *Text. Res. J.* **2008**, 78, 399.

- [227] C. C. Chu, *Ann. Surg.* **1981**, 193, 365.
- [228] A. Rawal, R. Kumar, H. Saraswat, *Text. Res. J.* **2012**, 82, 1703.
- [229] S. Omeroglu, *Fibres Text. East. Eur.* **2006**, 14, 53.
- [230] K. Hristov, E. Armstrong-Carroll, M. Dunn, C. Pastore, Y. Gowed, *Text. Res. J.* **2004**, 74, 20.
- [231] D. Brunnschweiler, *J. Text. Inst., Trans.* **1954**, 45, T55.
- [232] A. J. Schaff, A. A. Ogale, *Text. Res. J.* **1991**, 61, 386.
- [233] M. N. Silberstein, C. L. Pai, G. C. Rutledge, M. C. Boyce, *J. Mech. Phys. Solids* **2012**, 60, 295.
- [234] D. R. Petterson, *Ind. Eng. Chem.* **1959**, 51, 902.
- [235] S. Bais-Singh, B. C. Goswami, *J. Text. Inst.* **1995**, 86, 271.
- [236] S. Backer, D. R. Petterson, *Text. Res. J.* **1960**, 30, 704.
- [237] B. C. Goswami, J. Suryadevara, T. L. Vigo, *Text. Res. J.* **1984**, 54, 391.
- [238] S. Adanur, T. Liao, *Text. Res. J.* **1999**, 69, 816.
- [239] J. W. Hearle, P. J. Stevenson, *Text. Res. J.* **1963**, 33, 877.
- [240] M.-S. Choi, S. P. Ashdown, *Text. Res. J.* **2000**, 70, 1033.
- [241] D. Zhu, B. Mobasher, A. Vaidya, S. D. Rajan, *Compos. Sci. Technol.* **2013**, 74, 121.
- [242] D. H. Kincade, in *Sewn Product Quality: A Management Perspective*, 1st ed. (Ed: V. R. Anthony), Pearson, Upper Saddle River, NJ **2007**, pp. 177–228.
- [243] C. K. Harnett, H. Zhao, R. F. Shepherd, *Adv. Mater. Technol.* **2017**, 2, 1700087.
- [244] G. Gioberto, L. E. Dunne, *J. Text. Apparel, Technol. Manage.* **2013**, 8, 3.
- [245] N. D. Naclerio, E. W. Hawkes, *IEEE. Rob. Autom. Lett.* **2020**, 5, 3406.
- [246] J. Park, J. W. Yoo, H. W. Seo, Y. Lee, J. Suhr, H. Moon, J. C. Koo, H. R. Choi, R. Hunt, K. J. Kim, S. H. Kim, J. D. Nam, *Smart Mater. Struct.* **2017**, 26, 3.
- [247] M. D. Koerner, *M.Sc. Thesis*, Drexel University, **2017**.
- [248] C. Rognon, S. Mintchev, F. Dellagnola, A. Cherpillod, D. Atienza, D. Floreano, *IEEE. Rob. Autom. Lett.* **2018**, 3, 2362.
- [249] M. Xiloyannis, L. Cappello, D. B. Khanh, S.-C. Yen, L. Masia, in *2016 6th IEEE Int. Conf. on Biomedical Robotics and Biomechanics (BioRob)*, IEEE, Piscataway, NJ **2016**, pp. 1213–1219.
- [250] S. Lessard, P. Pansodtee, A. Robbins, L. B. Baltaxe-Admony, J. M. Trombadore, M. Teodorescu, A. Agogino, S. Kurniawan, in *2017 Int. Conf. on Rehabilitation Robotics (ICORR)*, IEEE, Piscataway, NJ **2017**, pp. 1633–1638.
- [251] A. T. Asbeck, K. Schmidt, C. J. Walsh, *Rob. Auton. Syst.* **2015**, 73, 102.
- [252] I. Gaponov, D. Popov, S. J. Lee, J. H. Ryu, *Int. J. Control, Autom. Syst.* **2017**, 15, 73.
- [253] A. T. Asbeck, S. M. De Rossi, K. G. Holt, C. J. Walsh, *Int. J. Rob. Res.* **2015**, 34, 744.
- [254] F. A. Panizzolo, I. Galiana, A. T. Asbeck, C. Sivi, K. Schmidt, K. G. Holt, C. J. Walsh, *J. NeuroEng. Rehabil.* **2016**, 13, 43.
- [255] E. J. Ball, M. A. Meller, J. B. Chipka, E. Garcia, *Smart Mater. Struct.* **2016**, 25, 11.
- [256] M. Bryant, M. A. Meller, E. Garcia, *Smart Mater. Struct.* **2014**, 23, 7.
- [257] R. F. Natividad, M. R. Del Rosario, P. C. Y. Chen, C. Yeow, in *2017 IEEE Int. Conf. on Robotics and Automation (ICRA)*, IEEE, Piscataway, NJ **2017**, pp. 6700–6705.
- [258] M. Wehner, M. T. Tolley, Y. Mengüç, Y. L. Park, A. Mozeika, Y. Ding, C. Onal, R. F. Shepherd, G. M. Whitesides, R. J. Wood, *Soft Rob.* **2014**, 1, 263.
- [259] V. Sanchez, C. J. Payne, D. J. Preston, J. T. Alvarez, J. C. Weaver, A. T. Atalay, M. Boyvat, D. M. Vogt, R. J. Wood, G. M. Whitesides, C. J. Walsh, *Adv. Mater. Technol.* **2020**, 5, 2000383.
- [260] H. Nabae, A. Kodaira, T. Horiuchi, K. Asaka, G. Endo, K. Suzumori, in *2019 IEEE/RSJ Int. Conf. on Intelligent Robots and Systems (IROS)*, IEEE, Piscataway, NJ **2019**, pp. 8287–8293.
- [261] F. Daerden, D. Lefeber, *Int. J. Fluid Power* **2001**, 2, 41.
- [262] C. P. Chou, B. Hannaford, *IEEE Trans. Rob. Autom.* **1996**, 12, 90.
- [263] H. Schulte, D. Adamski, J. Pearson, *Characteristics of the Braided Fluid Actuator*, Technical report, The University of Michigan Medical School, Ann Arbor, MI **1961**.
- [264] H. Schulte, *The Characteristics of the McKibben Artificial Muscle, The Application of External Power in Prosthetics and Orthotics*, Vol. 874, National Research Council **1961**, pp. 94–115.
- [265] G. Belforte, G. Eula, A. Ivanov, T. Raparelli, S. Siroli, *J. Text. Inst.* **2018**, 109, 757.
- [266] C. S. Kothera, M. Jangid, J. Sirohi, N. M. Wereley, *Journal of Mechanical Design, Transactions of the ASME* **2009**, 131, 0910101.
- [267] B. Tondy, *J. Intell. Mater. Syst. Struct.* **2012**, 23, 225.
- [268] W. Liu, C. R. Rahn, *J. Appl. Mech.* **2004**, 70, 853.
- [269] S. Davis, D. G. Caldwell, *Int. J. Rob. Res.* **2006**, 25, 359.
- [270] B. Tondy, P. Lopez, *IEEE Control Syst. Mag.* **2000**, 20, 15.
- [271] F. Daerden, D. Lefeber, *Eur. J. Mech. Environ. Eng.* **2002**, 47, 11.
- [272] B. Jamil, S. Lee, Y. Choi, *IEEE Access* **2019**, 7, 84770.
- [273] G. Belforte, G. Eula, A. Ivanov, A. L. Visan, *J. Text. Inst.* **2014**, 105, 356.
- [274] H. M. Paynter, *US 4,751,869* **1988**.
- [275] G. Belforte, G. Eula, S. Appendino, *J. Text. Inst.* **2012**, 103, 733.
- [276] G. Belforte, G. Eula, A. Ivanov, T. Raparelli, S. Siroli, in *Advances in Service and Industrial Robotics* (Eds: C. Ferraresi, G. Quaglia), Springer International Publishing, Cham, Switzerland **2018**, pp. 854–861.
- [277] B. Jamil, S. Lee, Y. Choi, in *2018 IEEE/RSJ Int. Conf. on Intelligent Robots and Systems (IROS)*, IEEE, Piscataway, NJ **2018**, pp. 1476–1481.
- [278] E. W. Hawkes, D. L. Christensen, A. M. Okamura, in *2016 IEEE Int. Conf. on Robotics and Automation (ICRA)*, IEEE, Piscataway, NJ **2016**, pp. 4022–4029.
- [279] E. H. Skorina, M. Luo, W. Y. Oo, W. Tao, F. Chen, S. Youssefian, N. Rahbar, C. D. Onal, *PLoS One* **2018**, 13, e0204637.
- [280] E. H. Skorina, M. Luo, C. D. Onal, *Front. Rob. AI* **2018**, 5, 83.
- [281] S. Fujimoto, T. Akagi, A. Yamamoto, in *MATEC Web of Conferences*, Vol 51. EDP Sciences, Les Ulis **2016**, p. 02010.
- [282] A. R. Mettam, *Inflatable Servo Actuators*, C. P. No. 671, Ministry of Aviation, Aeronautical Research Council, London **1964**.
- [283] R. Niiyama, X. Sun, C. Sung, B. An, D. Rus, S. Kim, *Soft Rob.* **2015**, 2, 59.
- [284] S. Park, J. Yi, D. Kim, Y. Lee, H. S. Koo, Y. Park, in *2019 2nd IEEE Int. Conf. on Soft Robotics (RoboSoft)*, IEEE, Piscataway, NJ **2019**, pp. 636–641.
- [285] D. Bigaud, C. Szostkiewicz, P. Hamelin, *Compos. Struct.* **2003**, 62, 129.
- [286] W. Adams, S. Sridar, C. M. Thalman, B. Copenhaver, H. Elsaad, P. Polygerinos, in *2018 IEEE Int. Conf. on Soft Robotics (RoboSoft)*, IEEE, Piscataway, NJ **2018**, pp. 321–326.
- [287] P. H. Nguyen, I. B. Imran Mohd, C. Sparks, F. L. Arellano, W. Zhang, P. Polygerinos, in *2019 Int. Conf. on Robotics and Automation (ICRA)*, IEEE, Piscataway, NJ **2019**, pp. 8429–8435.
- [288] R. Natividad, M. Del Rosario, P. C. Chen, C. H. Yeow, *Soft Rob.* **2018**, 5, 304.
- [289] J. Fang, J. Yuan, M. Wang, L. Xiao, J. Yang, Z. Lin, P. Xu, L. Hou, *Soft Rob.* **2020**, 7, 95.
- [290] Y. Baranovskaya, M. Prado, M. Dörstelmann, A. Menges, *Complexity Simplicity - Proc. of the 34th eCAADe Conf.* **2016**, 1, 571.
- [291] X. Liang, H. Cheong, Y. Sun, J. Guo, C. K. Chui, C. H. Yeow, *IEEE. Rob. Autom. Lett.* **2018**, 3, 2702.
- [292] P. M. Khin, H. K. Yap, M. H. Ang, C. Yeow, in *2017 IEEE/RSJ Int. Conf. on Intelligent Robots and Systems (IROS)*, IEEE, Piscataway, NJ **2017**, pp. 2744–2750.
- [293] J. H. Low, N. Cheng, P. M. Khin, N. V. Thakor, S. L. Kukreja, H. L. Ren, C. H. Yeow, in *2017 IEEE/RSJ Int. Conf. on Intelligent Robots and Systems (IROS)*, IEEE, Piscataway, NJ **2017**, pp. 1180–1186.
- [294] H. K. Yap, F. Sebastian, C. Wiedeman, C. Yeow, in *2017 Int. Conf. on Rehabilitation Robotics (ICORR)*, IEEE, Piscataway, NJ **2017**, pp. 1465–1470.

- [295] A. Stilli, H. A. Wurdemann, K. Althoefer, in *2014 IEEE/RSJ Int. Conf. on Intelligent Robots and Systems*, IEEE, Piscataway, NJ **2014**, pp. 2476–2481.
- [296] F. Maghooa, A. Stilli, Y. Noh, K. Althoefer, H. A. Wurdemann, in *2015 IEEE Int. Conf. on Robotics and Automation (ICRA)*, IEEE, Piscataway, NJ **2015**, pp. 2556–2561.
- [297] J. Nassour, *Sens. Actuators, A* **2019**, 291, 93.
- [298] J. Nassour, F. Hamker, in *2019 IEEE Int. Conf. on Cyborg and Bionic Systems (CBS)*, IEEE, Piscataway, NJ **2019**, pp. 60–65.
- [299] H. Al-Fahaam, S. Davis, S. Nefti-Meziani, in *2016 21st Int. Conf. on Methods and Models in Automation and Robotics (MMAR)*, IEEE, Piscataway, NJ **2016**, pp. 472–477.
- [300] H. Al-Fahaam, S. Davis, S. Nefti-Meziani, T. Theodoridis, *Intell. Serv. Rob.* **2018**, 11, 247.
- [301] A. Wang, S. Ahlquist, in *Proc. of the 36th Annual Conf. of the Association for Computer Aided Design in Architecture (ACADIA)*, ACADIA, Delaware **2016**, pp. 290–297.
- [302] S. Ahlquist, W. Mcgee, S. Sharmin, in *Acadia 2017 Disciplines & Disruption: Proc. of the 37th Annual Conf. of the Association for Computer Aided Design in Architecture*, ACADIA, Delaware **2017**, pp. 38–51.
- [303] A. Sadeghi, A. Mondini, B. Mazzolai, in *Wearable Robotics: Challenges and Trends. WeRob 2018. Biosystems & Biorobotics* (Eds: M. C. Carrozza, S. Micera, J. L. Pons), Springer International Publishing, Cham, Switzerland **2019**, pp. 49–52.
- [304] A. Al Maimani, A. Roudaut, in *Proc. of the 2017 CHI Conf. on Human Factors in Computing Systems*, CHI '17, Association for Computing Machinery, New York **2017**, pp. 2440–2448.
- [305] K. E. Gordon, G. S. Sawicki, D. P. Ferris, *J. Biomech.* **2006**, 39, 1832.
- [306] D. T. Goetz, D. K. Owusu-Antwi, H. Culbertson, in *2020 IEEE Haptics Symp. (HAPTICS)*, IEEE, Piscataway, NJ **2020**, pp. 643–649.
- [307] T. H. Chang, H. Nabae, G. Endo, K. Suzumori, K. Hatakeyama, S. Chida, Y. Shimada, *Proc. of the 2018 18th Int. Conf. on Mechatronics - Mechatronika, ME 2018*, IEEE, Piscataway, NJ **2019**.
- [308] Y. Funabara, in *2017 IEEE/SICE Int. Symp. on System Integration (SII)*, IEEE, Piscataway, NJ **2017**, pp. 356–361.
- [309] Y. Funabara, in *2018 IEEE/RSJ Int. Conf. on Intelligent Robots and Systems (IROS)*, IEEE, Piscataway, NJ **2018**, pp. 6992–6997.
- [310] S. Koizumi, S. Kurumaya, H. Nabae, G. Endo, K. Suzumori, *IEEE. Rob. Autom. Lett.* **2018**, 3, 3240.
- [311] S. Kurumaya, H. Nabae, G. Endo, K. Suzumori, *Soft Rob.* **2019**, 6, 250.
- [312] C. A. Weinberg, S. Cai, J. Schaffer, J. Abel, *Adv. Mater. Technol.* **2020**, 5, 1901146.
- [313] C. S. Haines, M. D. Lima, N. Li, G. M. Spinks, J. Foroughi, J. D. Madden, S. H. Kim, S. Fang, M. J. De Andrade, F. Goktepe, O. Goktepe, S. M. Mirvakili, S. Naficy, X. Lepro, J. Oh, M. E. Kozlov, S. J. Kim, X. Xu, B. J. Swedlove, G. G. Wallace, R. H. Baughman, *Science* **2014**, 343, 868.
- [314] C. S. Haines, N. Li, G. M. Spinks, A. E. Aliev, J. Di, R. H. Baughman, *Proc. Natl. Acad. Sci. USA* **2016**, 113, 11709.
- [315] S. Y. Yang, K. H. Cho, Y. Kim, K. Kim, J. H. Park, H. S. Jung, J. U. Ko, H. Moon, J. C. Koo, H. Rodrigue, J. W. Suk, J. Nam, H. R. Choi, in *2018 IEEE/RSJ Int. Conf. on Intelligent Robots and Systems (IROS)*, IEEE, Piscataway, NJ **2018**, pp. 5451–5456.
- [316] K. Eschen, J. Abel, R. Granberry, B. Holschuh, in *ASME 2018 Conf. on Smart Materials, Adaptive Structures and Intelligent Systems, SMASIS 2018*, Vol. 1, ASME, New York, NY **2018**, p. V001T04A002.
- [317] R. Granberry, J. Abel, B. Holschuh, in *Proc. of the 2017 ACM Int. Symp. on Wearable Computers, ISWC '17*, Association for Computing Machinery, New York, NY **2017**, pp. 186–191.
- [318] B. Holschuh, D. Newman, *Smart Mater. Struct.* **2015**, 24, 3.
- [319] J. M. Abel, P. Mane, B. Pascoe, J. Luntz, D. Brei, in *Active and Passive Smart Structures and Integrated Systems 2010*, SPIE, Bellingham, WA **2010**, p. 156.
- [320] J. A. Shaw, S. Kyriakides, *J. Mech. Phys. Solids* **1995**, 43, 1243.
- [321] S. Kim, E. Hawkes, K. Choy, M. Joldaz, J. Foley, R. Wood, in *2009 IEEE/RSJ Int. Conf. on Intelligent Robots and Systems*, IEEE, Piscataway, NY **2009**, pp. 2228–2234.
- [322] S. Seok, C. D. Onal, K. J. Cho, R. J. Wood, D. Rus, S. Kim, *IEEE/ASME Trans. Mechatronics* **2013**, 18, 1485.
- [323] M. Yuen, A. Cherian, J. C. Case, J. Seipel, R. K. Kramer, in *2014 IEEE/RSJ Int. Conf. on Intelligent Robots and Systems*, IEEE, Piscataway, NJ **2014**, pp. 580–586.
- [324] J. Abel, J. Luntz, D. Brei, *Proc. of the ASME Conf. on Smart Materials, Adaptive Structures and Intelligent Systems 2009, SMASIS2009*, ASME, New York, NY **2009**, p. 353.
- [325] J. M. Abel, *Ph.D. Thesis*, University of Michigan **2014**.
- [326] K. Eschen, J. Abel, *Smart Mater. Struct.* **2019**, 28, 2.
- [327] R. Granberry, B. Holschuh, J. Abel, in *Proc. of the ASME 2019 Conf. on Smart Materials, Adaptive Structures and Intelligent Systems*, ASME, New York, NY **2019**, p. V001T08A006.
- [328] M.-W. Han, M.-S. Kim, S.-H. Ahn, *Composites, Part B* **2020**, 198, 108170.
- [329] A. Skalitzy, D. Beale, A. Gurley, K. Kubik, in *Proc. of the ASME 2018 Conf. on Smart Materials, Adaptive Structures and Intelligent Systems. Volume 1: Development and Characterization of Multifunctional Materials; Modeling, Simulation, and Control of Adaptive Systems; Integrated System Desi*, ASME, New York, NY **2018**, p. V001T03A033.
- [330] A. Skalitzy, C. Petersen, A. Gurley, D. Beale, in *Proc. of the ASME 2019 Conf. on Smart Materials, Adaptive Structures and Intelligent Systems. ASME 2019 Conf. on Smart Materials, Adaptive Structures and Intelligent Systems*, **2019**, p. V001T02A008.
- [331] M.-W. Han, S.-H. Ahn, *Adv. Mater.* **2017**, 29, 1606580.
- [332] M. C. Yuen, R. A. Bilodeau, R. K. Kramer, *IEEE. Rob. Autom. Lett.* **2016**, 1, 708.
- [333] K. Eschen, J. Garcia-Barriocanal, J. Abel, *Materialia* **2020**, 11, 100684.
- [334] C. Liu, H. Qin, P. T. Mather, *J. Mater. Chem.* **2007**, 17, 1543.
- [335] W. M. Huang, Z. Ding, C. C. Wang, J. Wei, Y. Zhao, H. Purnawali, *Mater. Today* **2010**, 13, 54.
- [336] K. Takashima, J. Rossiter, T. Mukai, *Sens. Actuators, A* **2010**, 164, 116.
- [337] T. P. Chenal, J. C. Case, J. Paik, R. K. Kramer, in *2014 IEEE/RSJ Int. Conf. on Intelligent Robots and Systems*, IEEE, Piscataway, NJ **2014**, pp. 2827–2831.
- [338] G. Moretti, A. Cherubini, R. Vertechy, M. Fontana, *Proc. SPIE* **2015**, 9432, 94320P.
- [339] S. M. Mirvakili, A. Rafie Ravandi, I. W. Hunter, C. S. Haines, N. Li, J. Foroughi, S. Naficy, G. M. Spinks, R. H. Baughman, J. D. W. Madden, in *Electroactive Polymer Actuators and Devices (EAPAD) 2014*, SPIE, Bellingham, WA **2014**, p. 905601.
- [340] M. C. Yip, G. Niemeyer, in *2015 IEEE Int. Conf. on Robotics and Automation (ICRA)*, IEEE, Piscataway, NJ **2015**, pp. 2313–2318.
- [341] S. Y. Yang, K. H. Cho, Y. Kim, M. G. Song, H. S. Jung, J. W. Yoo, H. Moon, J. C. Koo, J. D. Nam, H. R. Choi, *Smart Mater. Struct.* **2017**, 26, 10.
- [342] J. Fan, G. Li, *RSC Adv.* **2017**, 7, 1127.
- [343] D. J. Roach, C. Yuan, X. Kuang, V. C. F. Li, P. Blake, M. L. Romero, I. Hammel, K. Yu, H. J. Qi, *ACS Appl. Mater. Interfaces* **2019**, 11, 19514.
- [344] J. Foroughi, G. M. Spinks, S. Aziz, A. Mirabedini, A. Jeiranikhameneh, G. G. Wallace, M. E. Kozlov, R. H. Baughman, *ACS Nano* **2016**, 10, 9129.
- [345] M. Zhang, K. R. Atkinson, R. H. Baughman, *Science* **2004**, 306, 1358.
- [346] T. Mirfakhrai, *Ph.D. Thesis*, The University of British Columbia **2009**.
- [347] J. Foroughi, G. M. Spinks, G. G. Wallace, J. Oh, M. E. Kozlov, S. Fang, T. Mirfakhrai, J. D. W. Madden, M. K. Shin, S. J. Kim, R. H. Baughman, *Science* **2011**, 334, 494.

- [348] M. D. Lima, N. Li, M. J. De Andrade, S. Fang, J. Oh, G. M. Spinks, M. E. Kozlov, C. S. Haines, D. Suh, J. Foroughi, S. J. Kim, Y. Chen, T. Ware, M. K. Shin, L. D. Machado, A. F. Fonseca, J. D. Madden, W. E. Voit, D. S. Galvão, R. H. Baughman, *Science* **2012**, 338, 928.
- [349] J. A. Lee, N. Li, C. S. Haines, K. J. Kim, X. Lepró, R. Ovalle-Robles, S. J. Kim, R. H. Baughman, *Adv. Mater.* **2017**, 29, 1700870.
- [350] K. Y. Chun, S. H. Kim, M. K. Shin, C. H. Kwon, J. Park, Y. T. Kim, G. M. Spinks, M. D. Lima, C. S. Haines, R. H. Baughman, S. J. Kim, *Nat. Commun.* **2014**, 5, 3322.
- [351] M. D. Lima, M. W. Hussain, G. M. Spinks, S. Naficy, D. Hagenasr, J. S. Bykova, D. Tolly, R. H. Baughman, *Small* **2015**, 11, 3113.
- [352] P. Chen, Y. Xu, S. He, X. Sun, S. Pan, J. Deng, D. Chen, H. Peng, *Nat. Nanotechnol.* **2015**, 10, 1077.
- [353] S. Aziz, J. G. Martinez, J. Foroughi, G. M. Spinks, E. W. Jager, *Macromol. Mater. Eng.* **2020**, 305, 2000421.
- [354] K. J. Kim, J. S. Hyeon, H. Kim, T. J. Mun, C. S. Haines, N. Li, R. H. Baughman, S. J. Kim, *ACS Appl. Mater. Interfaces* **2019**, 11, 13533.
- [355] J. S. Hyeon, J. W. Park, R. H. Baughman, S. J. Kim, *Sens. Actuators, B* **2019**, 286, 237.
- [356] J. Qiao, J. Di, S. Zhou, K. Jin, S. Zeng, N. Li, S. Fang, Y. Song, M. Li, R. H. Baughman, Q. Li, *Small* **2018**, 14, 1801883.
- [357] A. Maziz, A. Concas, A. Khaldi, J. Stålhund, N.-K. Persson, E. W. H. Jager, *Sci. Adv.* **2017**, 3, e1600327.
- [358] J. Mu, M. de Andrade, S. Fang, X. Wang, E. Gao, N. Li, S. H. Kim, H. Wang, C. Hou, Q. Zhang, M. Zhu, D. Qian, H. Lu, D. Kongahage, S. Talebian, J. Foroughi, G. Spinks, H. Kim, T. H. Ware, H. J. Sim, D. Y. Lee, Y. Jang, S. J. Kim, R. H. Baughman, *Science* **2019**, 365, 150.
- [359] Y. Wu, Y. Yang, C. Li, Y. Li, W. Chen, *Front. Bioeng. Biotechnol.* **2020**, 8, 212.
- [360] Y. Li, M. Guo, Y. Li, *J. Mater. Chem. C* **2019**, 7, 12991.
- [361] A. Furuse, M. Hashimoto, *Proc. SPIE* **2017**, 101631, 016327.
- [362] S. Arora, T. Ghosh, J. Muth, *Sens. Actuators, A* **2007**, 136, 321.
- [363] S. Jiang, F. Liu, A. Lerch, L. Ionov, S. Agarwal, *Adv. Mater.* **2015**, 27, 4865.
- [364] Z. Yin, S. Shi, X. Liang, M. Zhang, Q. Zheng, Y. Zhang, *Adv. Fiber Mater.* **2019**, 1, 197.
- [365] D. Liu, A. Tarakanova, C. C. Hsu, M. Yu, S. Zheng, L. Yu, J. Liu, Y. He, D. J. Dunstan, M. J. Buehler, *Sci. Adv.* **2019**, 5, 3.
- [366] A. O'Halloran, F. O'Malley, P. McHugh, *J. Appl. Phys.* **2008**, 104, 71101.
- [367] P. Brochu, Q. Pei, *Macromol. Rapid Commun.* **2010**, 31, 10.
- [368] C. G. Cameron, J. P. Szabo, S. Johnstone, J. Massey, J. Leidner, *Sens. Actuators, A* **2008**, 147, 286.
- [369] G. Kofod, H. Stoyanov, R. Gerhard, *Appl. Phys. A: Mater. Sci. Process.* **2011**, 102, 577.
- [370] J. Guo, C. Xiang, T. Helps, M. Taghavi, J. Rossiter, in *2018 IEEE Int. Conf. on Soft Robotics (RoboSoft)*, IEEE, Piscataway, NY **2018**, pp. 339–343.
- [371] C. Xiang, J. Guo, R. Sun, A. Hinitt, T. Helps, M. Taghavi, J. Rossiter, *Polymers* **2019**, 11, 7.
- [372] S. I. Rich, R. J. Wood, C. Majidi, *Nat. Electron.* **2018**, 1, 102.
- [373] S. Kawabata, In *Textile structural composites* (Eds: T.-W. Chou, F. K. Ko), Elsevier, New York **1989**, pp. 67–116.
- [374] K. W. Lau, T. Dias, *J. Text. Inst.* **1994**, 85, 173.
- [375] B. U. Nergis, C. Candan, *Text. Res. J.* **2006**, 76, 49.
- [376] R. Atef, R. Elbealy, A. A. Badr, R. A. Elkhalek, *J. Text. Sci. Eng.* **2018**, 8, 1000378.
- [377] K. E. Grabowska, I. L. Ciesielska, S. Vasile, *Autex Res. J.* **2009**, 9, 74.
- [378] J. Zhang, J. Sheng, C. T. O'Neill, C. Walsh, R. J. Wood, J. H. Ryu, J. P. Desai, M. C. Yip, *Rob. Auton. Syst.* **2019**, 75, 203.
- [379] G. V. Stoychev, L. Ionov, *ACS Appl. Mater. Interfaces* **2016**, 2016, 24281.
- [380] T. L. Buckner, R. Kramer-Bottiglio, *Multifunct. Mater.* **2018**, 1, 12001.
- [381] N.-K. Persson, J. G. Martinez, Y. Zhong, A. Maziz, E. W. H. Jager, *Adv. Mater. Technol.* **2018**, 3, 1700397.
- [382] M. P. Mousavi, A. Ainla, E. K. Tan, M. Abd El-Rahman, Y. Yoshida, L. Yuan, H. H. Sigurslid, N. Arkan, M. C. Yip, C. K. Abrahamsson, S. Homer-Vanniasinkam, G. M. Whitesides, *Lab Chip* **2018**, 18, 2279.
- [383] W. He, C. Wang, H. Wang, M. Jian, W. Lu, X. Liang, X. Zhang, F. Yang, Y. Zhang, *Sci. Adv.* **2019**, 5, eaax0649.
- [384] N. Coppedè, G. Tarabella, M. Villani, D. Calestani, S. Iannotta, A. Zappettini, *J. Mater. Chem. B* **2014**, 2, 5620.
- [385] S. Takamatsu, T. Lonjaret, D. Crisp, J. M. Badier, G. G. Malliaras, E. Ismailova, *Sci. Rep.* **2015**, 5, 15003.
- [386] R. Liu, S. Wang, T. T. Lao, *J. Eng. Fibers Fabr.* **2012**, 7, 50.
- [387] A. F. Da Silva, A. F. Gonçalves, P. M. Mendes, J. H. Correia, *IEEE Sens. J.* **2011**, 11, 2442.
- [388] F. R. Fan, Z. Q. Tian, Z. Lin Wang, *Nano Energy* **2012**, 1, 328.
- [389] X. Pu, L. Li, M. Liu, C. Jiang, C. Du, Z. Zhao, W. Hu, Z. L. Wang, *Adv. Mater.* **2016**, 28, 98.
- [390] J. Xiong, P. Cui, X. Chen, J. Wang, K. Parida, M.-F. Lin, P. S. Lee, *Nat. Commun.* **2018**, 9, 4280.
- [391] Z. Zhao, C. Yan, Z. Liu, X. Fu, L. M. Peng, Y. Hu, Z. Zheng, *Adv. Mater.* **2016**, 28, 10267.
- [392] J. Zhong, Q. Zhong, Q. Hu, N. Wu, W. Li, B. Wang, B. Hu, J. Zhou, *Adv. Funct. Mater.* **2015**, 25, 1798.
- [393] K. Dong, J. Deng, Y. Zi, Y. C. Wang, C. Xu, H. Zou, W. Ding, Y. Dai, B. Gu, B. Sun, Z. L. Wang, *Adv. Mater.* **2017**, 29, 1702648.
- [394] W. Seung, M. K. Gupta, K. Y. Lee, K. S. Shin, J. H. Lee, T. Y. Kim, S. Kim, J. Lin, J. H. Kim, S. W. Kim, *ACS Nano* **2015**, 9, 3501.
- [395] W. Fan, Q. He, K. Meng, X. Tan, Z. Zhou, G. Zhang, J. Yang, Z. L. Wang, *Sci. Adv.* **2020**, 6, eaay2840.
- [396] Y. Qu, T. Nguyen-Dang, A. G. Page, W. Yan, T. Das Gupta, G. M. Rotaru, R. M. Rossi, V. D. Favrod, N. Bartolomei, F. Sorin, *Adv. Mater.* **2018**, 30, 1707251.
- [397] J. Lee, H. Kwon, J. Seo, S. Shin, J. H. Koo, C. Pang, S. Son, J. H. Kim, Y. H. Jang, D. E. Kim, T. Lee, *Adv. Mater.* **2015**, 27, 2433.
- [398] M. Rothmaier, M. P. Luong, F. Clemens, *Sensors* **2008**, 8, 4318.
- [399] M. Liu, X. Pu, C. Jiang, T. Liu, X. Huang, L. Chen, C. Du, J. Sun, W. Hu, Z. L. Wang, *Adv. Mater.* **2017**, 29, 1703700.
- [400] E. Bilotti, R. Zhang, H. Deng, M. Baxendale, T. Peijs, *J. Mater. Chem.* **2010**, 20, 9449.
- [401] S. Lee, S. Shin, S. Lee, J. Seo, J. Lee, S. Son, H. J. Cho, H. Algadi, S. Al-Sayari, D. E. Kim, T. Lee, *Adv. Funct. Mater.* **2015**, 25, 3114.
- [402] Z. Tang, S. Jia, F. Wang, C. Bian, Y. Chen, Y. Wang, B. Li, *ACS Appl. Mater. Interfaces* **2018**, 10, 6624.
- [403] P. Le Floch, X. Yao, Q. Liu, Z. Wang, G. Nian, Y. Sun, L. Jia, Z. Suo, *ACS Appl. Mater. Interfaces* **2017**, 9, 25542.
- [404] W. Xi, J. C. Yeo, L. Yu, S. Zhang, C. T. Lim, *Adv. Mater. Technol.* **2017**, 2, 1700016.
- [405] A. Leber, B. Cholt, J. Sandt, N. Vogel, M. Kolle, *Adv. Funct. Mater.* **2019**, 29, 1802629.
- [406] S. Seyedin, S. Uzun, A. Levitt, B. Anasori, G. Dion, Y. Gogotsi, J. M. Razal, *Adv. Funct. Mater.* **2020**, 30, 1910504.
- [407] P. M. Toal, L. J. Holmes, R. X. Rodriguez, E. D. Wetzel, *Addit. Manuf.* **2017**, 16, 12.
- [408] A. Leber, A. G. Page, D. Yan, Y. Qu, S. Shadman, P. Reis, F. Sorin, *Adv. Funct. Mater.* **2020**, 30, 1904274.
- [409] L. Yu, S. Parker, H. Xuan, Y. Zhang, S. Jiang, M. Tousi, M. Manteghi, A. Wang, X. Jia, *Adv. Funct. Mater.* **2020**, 30, 1908915.
- [410] H. Zhao, K. O'Brien, S. Li, R. F. Shepherd, *Sci. Rob.* **2016**, 1, 1.
- [411] Y. Li, C. Zheng, S. Liu, L. Huang, T. Fang, J. X. Li, F. Xu, F. Li, *ACS Appl. Mater. Interfaces* **2020**, 12, 23764.
- [412] C. B. Cooper, K. Arutselvan, Y. Liu, D. Armstrong, Y. Lin, M. R. Khan, J. Genzer, M. D. Dickey, *Adv. Funct. Mater.* **2017**, 27, 1605630.
- [413] Y. Shang, Y. Li, X. He, S. Du, L. Zhang, E. Shi, S. Wu, Z. Li, P. Li, J. Wei, K. Wang, H. Zhu, D. Wu, A. Cao, *ACS Nano* **2013**, 7, 1446.
- [414] C. T. Huang, C. L. Shen, C. F. Tang, S. H. Chang, *Sens. Actuators, A* **2008**, 141, 396.

- [415] A. Masuda, T. Murakami, K. Honda, S. Yamaguchi, *J. Text. Eng.* **2006**, 52, 93.
- [416] Y. Koyama, M. Nishiyama, K. Watanabe, *IEEE Sens. J.* **2018**, 18, 6175.
- [417] P. Xue, X. M. Tao, H. Y. Tsang, *Appl. Surf. Sci.* **2007**, 253, 3387.
- [418] J. P. Wang, P. Xue, X. M. Tao, *Mater. Sci. Eng., A* **2011**, 528, 2863.
- [419] Y. Abdul Samad, K. Komatsu, D. Yamashita, Y. Li, L. Zheng, S. M. Alhassan, Y. Nakano, K. Liao, *Sens. Actuators, B* **2017**, 240, 1083.
- [420] X. Wu, Y. Han, X. Zhang, C. Lu, *ACS Appl. Mater. Interfaces* **2016**, 8, 9936.
- [421] R. Zhang, H. Deng, R. Valenca, J. Jin, Q. Fu, E. Bilotti, T. Peijs, *Sens. Actuators, A* **2012**, 179, 83.
- [422] B. Niu, T. Hua, H. Hu, B. Xu, X. Tian, K. Chan, S. Chen, *J. Mater. Chem. C* **2019**, 7, 14651.
- [423] W. K. Lee, C. J. Engel, M. D. Huntington, J. Hu, T. W. Odom, *Nano Lett.* **2015**, 15, 5624.
- [424] W. K. Lee, W. B. Jung, S. R. Nagel, T. W. Odom, *Nano Lett.* **2016**, 16, 3774.
- [425] H. Wang, Z. Liu, J. Ding, X. Lepró, S. Fang, N. Jiang, N. Yuan, R. Wang, Q. Yin, W. Lv, Z. Liu, M. Zhang, R. Ovalle-Robles, K. Inoue, S. Yin, R. H. Baughman, *Adv. Mater.* **2016**, 28, 4998.
- [426] X. Wang, Y. Qiu, W. Cao, P. Hu, *Chem. Mater.* **2015**, 27, 6969.
- [427] Y. C. Lai, J. Deng, S. L. Zhang, S. Niu, H. Guo, Z. L. Wang, *Adv. Funct. Mater.* **2017**, 27, 1604462.
- [428] H. J. Sim, C. Choi, S. H. Kim, K. M. Kim, C. J. Lee, Y. T. Kim, X. Lepró, R. H. Baughman, S. J. Kim, *Sci. Rep.* **2016**, 6, 35153.
- [429] K. Dong, J. Deng, W. Ding, A. C. Wang, P. Wang, C. Cheng, Y. C. Wang, L. Jin, B. Gu, B. Sun, Z. L. Wang, *Adv. Energy Mater.* **2018**, 8, 1801114.
- [430] P. A. Xu, A. K. Mishra, H. Bai, C. A. Aubin, L. Zullo, R. F. Shepherd, *Sci. Rob.* **2019**, 4, eaaw6304.
- [431] S. Chen, Z. Lou, D. Chen, K. Jiang, G. Shen, *Adv. Mater. Technol.* **2016**, 1, 1600136.
- [432] Y. Gao, F. Guo, P. Cao, J. Liu, D. Li, J. Wu, N. Wang, Y. Su, Y. Zhao, *ACS Nano* **2020**, 14, 3442.
- [433] S. Uzun, S. Seyedin, A. L. Stoltzfus, A. S. Levitt, M. Alhabeib, M. Anayee, C. J. Strobel, J. M. Razal, G. Dion, Y. Gogotsi, *Adv. Funct. Mater.* **2019**, 29, 1905015.
- [434] L. Wang, M. Tian, Y. Zhang, F. Sun, X. Qi, Y. Liu, L. Qu, *J. Mater. Sci.* **2020**, 55, 6187.
- [435] X. Ma, X. Cao, *Results Phys.* **2018**, 9, 231.
- [436] G. Gioberto, L. Dunne, in *2012 IEEE Int. Conf. on Systems, Man, and Cybernetics (SMC)*, IEEE, Piscataway, NY **2012**, pp. 3275–3280.
- [437] G. Gioberto, J. Coughlin, K. Bibeau, L. E. Dunne, in *Proc. of the 2013 Int. Symp. on Wearable Computers, ISWC '13*, Association for Computing Machinery, New York, NY **2013**, pp. 53–56.
- [438] Q. Zhang, Y. L. Wang, Y. Xia, T. V. Kirk, X. D. Chen, *ACS Sens.* **2020**, 5, 1535.
- [439] J. Rantala, J. Hännikäinen, J. Vanhala, *Pers. Ubiquitous Comput.* **2011**, 15, 85.
- [440] K. Shaker, Y. Nawab, M. U. Javaid, M. Umair, M. Maqsood, *Autex Res. J.* **2015**, 15, 148.
- [441] J. Ge, L. Sun, F. R. Zhang, Y. Zhang, L. A. Shi, H. Y. Zhao, H. W. Zhu, H. L. Jiang, S. H. Yu, *Adv. Mater.* **2016**, 28, 722.
- [442] S. Takamatsu, T. Kobayashi, N. Shibayama, K. Miyake, T. Itoh, *Sens. Actuators, A* **2012**, 184, 57.
- [443] Y. Enokibori, A. Suzuki, H. Mizuno, Y. Shimakami, K. Mase, in *Proc. of the 2013 ACM Conf. on Pervasive and Ubiquitous Computing Adjunct Publication*, UbiComp '13 Adjunct, Association for Computing Machinery, New York, NY **2013**, pp. 207–210.
- [444] A. Chhetry, H. Yoon, J. Y. Park, *J. Mater. Chem. C* **2017**, 5, 10068.
- [445] S. Li, R. Li, T. Chen, X. Xiao, *IEEE Sens. J.* **2020**, 20, 14436.
- [446] L. Ashok Kumar, C. Vigneswaran, T. Ramachandran, *J. Ind. Text.* **2010**, 39, 305.
- [447] X. Yang, Z. Chen, C. S. M. Elvin, L. H. Y. Janice, S. H. Ng, J. T. Teo, R. Wu, *IEEE Sens. J.* **2015**, 15, 757.
- [448] B. M. Quandt, M. S. Pfister, J. F. Lübbers, F. Spano, R. M. Rossi, G.-L. Bona, L. F. Boesel, *Biomed. Opt. Express* **2017**, 8, 4316.
- [449] K. Jung, T. J. Kang, *J. Compos. Mater.* **2007**, 41, 1499.
- [450] W. Felt, C. D. Remy, in *2014 IEEE/RSJ Int. Conf. on Intelligent Robots and Systems*, IEEE, Piscataway, NY **2014**, pp. 2821–2826.
- [451] W. Felt, K. Y. Chin, C. D. Remy, *IEEE/ASME Trans. Mechatronics* **2016**, 21, 1201.
- [452] W. Felt, K. Y. Chin, C. D. Remy, *Soft Rob.* **2017**, 4, 261.
- [453] M. Catrysse, R. Puers, C. Hertleer, L. Van Langenhove, H. Van Egmond, D. Matthys, *Sens. Actuators, A* **2004**, 114, 302.
- [454] H. Zhang, X. Tao, T. Yu, S. Wang, *Sens. Actuators, A* **2006**, 126, 129.
- [455] H. Zhang, *Meas. Sci. Technol.* **2015**, 26, 10.
- [456] E. P. Scilingo, F. Lorusi, A. Mazzoldi, D. D. Rossi, *IEEE Sens. J.* **2003**, 3, 460.
- [457] M. Pacelli, L. Caldani, R. Paradiso, *Annual Int. Conf. of the IEEE Engineering in Medicine and Biology - Proc.*, IEEE, Piscataway, NY **2006**, pp. 5358–5361.
- [458] M. Pacelli, G. Loriga, N. Taccini, R. Paradiso, in *2006 3rd IEEE/EMBS Int. Summer School on Medical Devices and Biosensors*, IEEE, Piscataway, NY **2006**, pp. 1–4.
- [459] O. Atalay, W. R. Kennon, *Sensors* **2014**, 14, 4712.
- [460] D. Hao, B. Xu, Z. Cai, *J. Mater. Sci.: Mater. Electron.* **2018**, 29, 9218.
- [461] L. Guo, L. Berglin, H. Mattila, *Text. Res. J.* **2012**, 82, 1937.
- [462] S. Seyedin, J. M. Razal, P. C. Innis, A. Jeiranikhameneh, S. Beirne, G. G. Wallace, *ACS Appl. Mater. Interfaces* **2015**, 7, 21150.
- [463] O. Atalay, W. Richard Kennon, M. Dawood Husain, *Sensors* **2013**, 13, 11114.
- [464] H. Zhang, X. Tao, S. Wang, T. Yu, *Text. Res. J.* **2005**, 75, 598.
- [465] J. Xie, H. Long, *Sens. Actuators, A* **2014**, 220, 118.
- [466] J. Wang, H. Long, S. Soltanian, P. Servati, F. ko, *Text. Res. J.* **2014**, 84, 200.
- [467] G. Cai, M. Yang, Z. Xu, J. Liu, B. Tang, X. Wang, *Chem. Eng. J.* **2017**, 325, 396.
- [468] M. Altaf, B. Rehman, A. Rehman, N. I. Sonil, S. Atiq, S. Riaz, S. Naseem, Z. Ullah, *J. Mater. Sci.: Mater. Electron.* **2020**, 31, 9870.
- [469] J. Ou, D. Oran, D. D. Haddad, J. Paradiso, H. Ishii, *3D Printing and Addit. Manuf.* **2019**, 6, 1.
- [470] K. Kim, M. Jung, S. Jeon, J. Bae, *Smart Mater. Struct.* **2019**, 28, 6.
- [471] R. Wijesiriwardana, *IEEE Sens. J.* **2006**, 6, 571.
- [472] K. Qi, Y. Zhou, K. Ou, Y. Dai, X. You, H. Wang, J. He, X. Qin, R. Wang, *Carbon* **2020**, 170, 464.
- [473] R. Li, Y. Si, Z. Zhu, Y. Guo, Y. Zhang, N. Pan, G. Sun, T. Pan, *Adv. Mater.* **2017**, 29, 36.
- [474] R. Wu, L. Ma, A. Patil, C. Hou, S. Zhu, X. Fan, H. Lin, W. Yu, W. Guo, X. Y. Liu, *ACS Appl. Mater. Interfaces* **2019**, 11, 33336.
- [475] T. Holleczeck, A. Rüegg, H. Harms, G. Tröster, in *SENSORS, 2010 IEEE*, IEEE, Piscataway, NJ **2010**, pp. 732–737.
- [476] F. Pizarro, P. Villavicencio, D. Yunge, M. Rodríguez, G. Hermosilla, A. Leiva, *Sensors* **2018**, 18, 4.
- [477] M. Zhang, C. Wang, H. Wang, M. Jian, X. Hao, Y. Zhang, *Adv. Funct. Mater.* **2017**, 27, 1604795.
- [478] C. Wang, K. Xia, M. Jian, H. Wang, M. Zhang, Y. Zhang, *J. Mater. Chem. C* **2017**, 5, 7604.
- [479] H. Souril, D. Bhattacharyya, *J. Mater. Chem. C* **2018**, 6, 10524.
- [480] M. Totaro, T. Poliero, A. Mondini, C. Lucarotti, G. Cairolì, J. Ortiz, L. Beccai, *Sensors* **2017**, 17, 10.
- [481] O. Atalay, A. Atalay, J. Gafford, C. Walsh, *Adv. Mater. Technol.* **2018**, 3, 1700237.
- [482] P. Sobolciak, A. Ali, M. K. Hassan, M. I. Helal, A. Tanvir, A. Popelka, M. A. Al-Maadeed, I. Krupa, K. A. Mahmoud, *PLoS One* **2017**, 12, 8.
- [483] W. Shao, M. Tebyetekerwa, I. Marriam, W. Li, Y. Wu, S. Peng, S. Ramakrishna, S. Yang, M. Zhu, *J. Power Sources* **2018**, 396, 683.

- [484] A. S. Levitt, M. Alhabeb, C. B. Hatter, A. Sarycheva, G. Dion, Y. Gogotsi, *J. Mater. Chem. A* **2019**, *7*, 269.
- [485] S. Sharma, A. Chhetry, M. Sharifuzzaman, H. Yoon, J. Y. Park, *ACS Appl. Mater. Interfaces* **2020**, *12*, 22212.
- [486] C. C. Vu, J. Kim, *Sens. Actuators, A* **2020**, *314*, 112029.
- [487] J. Meyer, *Ph.D. Thesis*, ETH Zurich, **2008**.
- [488] P. Parzer, K. Probst, T. Babic, C. Rendl, A. Vogl, A. Olwal, M. Haller, in *Proc. of the 2016 CHI Conf. Extended Abstracts on Human Factors in Computing Systems*, CHI EA '16, Association for Computing Machinery, New York **2016**, pp. 3754–3757.
- [489] S. Sundaram, P. Kellnhofer, Y. Li, J. Y. Zhu, A. Torralba, W. Matusik, *Nature* **2019**, *569*, 698.
- [490] L. Viry, A. Levi, M. Totaro, A. Mondini, V. Mattoli, B. Mazzolai, L. Beccai, *Adv. Mater.* **2014**, *26*, 2659.
- [491] C. B. Teeple, K. P. Becker, R. J. Wood, *IEEE Int. Conf. on Intelligent Robots and Systems*, IEEE, Piscataway, NJ **2018**, pp. 1621–1627.
- [492] A. Chen, J. Tan, P. Henry, X. Tao, *J. Text. Inst.* **2020**, *111*, 745.
- [493] J. Guo, B. Zhou, R. Zong, L. Pan, X. Li, X. Yu, C. Yang, L. Kong, Q. Dai, *ACS Appl. Mater. Interfaces* **2019**, *11*, 33589.
- [494] M. Rein, V. D. Favrod, C. Hou, T. Khudiyev, A. Stolyarov, J. Cox, C. C. Chung, C. Chhav, M. Ellis, J. Joannopoulos, Y. Fink, *Nature* **2018**, *560*, 214.
- [495] W. Zeng, L. Shu, Q. Li, S. Chen, F. Wang, X. M. Tao, *Adv. Mater.* **2014**, *26*, 5310.
- [496] S. Seyedin, P. Zhang, M. Naebe, S. Qin, J. Chen, X. Wang, J. M. Razal, *Mater. Horiz.* **2019**, *6*, 219.
- [497] H. Sourli, H. Banerjee, A. Jusufi, N. Radacsi, A. A. Stokes, I. Park, M. Sitti, M. Amjadi, *Adv. Intell. Syst.* **2020**, *2*, 2000039.
- [498] E. Post, M. Orth, P. Russo, N. Gershenfeld, *IBM Syst. J.* **2000**, *39*, 840.
- [499] A. Ankhili, S. U. Zaman, X. Tao, C. Cochrane, V. Koncar, D. Coulon, *IEEE Sens. J.* **2019**, *19*, 11995.
- [500] L. Buechley, M. Eisenberg, *Pers. Ubiquitous Comput.* **2009**, *13*, 133.
- [501] G. Paul, R. Torah, S. Beeby, J. Tudor, *Sens. Actuators, A* **2014**, *206*, 35.
- [502] L. Devendorf, C. Di Lauro, in *Proc. of the Thirteenth Int. Conf. on Tangible, Embedded, and Embodied Interaction*, TEI '19, Association for Computing Machinery, New York, NY **2019**, pp. 77–85.
- [503] A. Schwarz, I. Kazani, L. Cuny, C. Hertleer, F. Ghekiere, G. De Clercq, G. De Mey, L. Van Langenhove, *Mater. Des.* **2011**, *32*, 4247.
- [504] S. Jung, C. Lauterbach, M. Strasser, W. Weber, in *2003 IEEE Int. Solid-State Circuits Conf., 2003. Digest of Technical Papers, ISSCC*, IEEE, Piscataway, NJ **2003**, pp. 386–387.
- [505] I. Poupyrev, N.-W. Gong, S. Fukuhara, M. E. Karagozler, C. Schwesig, K. E. Robinson, in *Proc. of the 2016 CHI Conf. on Human Factors in Computing Systems*, CHI '16, Association for Computing Machinery, New York, NY **2016**, pp. 4216–4227.
- [506] Y. Lu, J. Jiang, S. Yoon, K. S. Kim, J. H. Kim, S. Park, S. H. Kim, L. Piao, *ACS Appl. Mater. Interfaces* **2018**, *10*, 2093.
- [507] Q. Li, X. Tao, *Text. Res. J.* **2011**, *81*, 1171.
- [508] A. Atalay, O. Atalay, M. D. Husain, A. Fernando, P. Potluri, *J. Ind. Text.* **2017**, *47*, 505.
- [509] A. Lund, N. M. van der Velden, N. K. Persson, M. M. Hamed, C. Müller, *Mater. Sci. Eng., R* **2018**, *126*, 1.
- [510] H. Ryu, S. Park, J. J. Park, J. Bae, *Smart Mater. Struct.* **2018**, *27*, 5.
- [511] J. L. Samper-Escudero, A. F. Contreras-González, M. Ferre, M. A. Sánchez-Urán, D. Pont-Esteban, *Soft Rob.* **2020**, *7*, 370.
- [512] J. B. Lee, V. Subramanian, *IEEE Trans. Electron Devices* **2005**, *52*, 269.
- [513] M. Hamed, R. Forchheimer, O. Inganäs, *Nat. Mater.* **2007**, *6*, 357.
- [514] S. J. Kim, H. Kim, J. Ahn, D. K. Hwang, H. Ju, M. C. Park, H. Yang, S. H. Kim, H. W. Jang, J. A. Lim, *Adv. Mater.* **2019**, *31*, 1900564.
- [515] K. Jost, G. Dion, Y. Gogotsi, *J. Mater. Chem. A* **2014**, *2*, 10776.
- [516] Q. Huang, D. Wang, Z. Zheng, *Adv. Energy Mater.* **2016**, *6*, 1600783.
- [517] S. Pang, Y. Gao, S. Choi, *Adv. Energy Mater.* **2018**, *8*, 1702261.
- [518] A. Levitt, D. Hegh, P. Phillips, S. Uzun, M. Anayee, J. M. Razal, Y. Gogotsi, G. Dion, *Mater. Today* **2020**, *34*, 17.
- [519] Q. Huang, D. Wang, H. Hu, J. Shang, J. Chang, C. Xie, Y. Yang, X. Lepró, R. H. Baughman, Z. Zheng, *Adv. Funct. Mater.* **2020**, *30*, 1910541.
- [520] C. Choi, S. H. Kim, H. J. Sim, J. A. Lee, A. Y. Choi, Y. T. Kim, X. Lepró, G. M. Spinks, R. H. Baughman, S. J. Kim, *Sci. Rep.* **2015**, *5*, 9387.
- [521] T. Starner, *IBM Syst. J.* **1996**, *35*, 3.
- [522] L. K. Allison, T. L. Andrew, *Adv. Mater. Technol.* **2019**, *4*, 1800615.
- [523] B. Russ, A. Glaudell, J. J. Urban, M. L. Chabiny, R. A. Segalman, *Nat. Rev. Mater.* **2016**, *1*, 10.
- [524] A. Lund, K. Rundqvist, E. Nilsson, L. Yu, B. Hagström, C. Müller, *npj Flexible Electron.* **2018**, *2*, 9.
- [525] M. Kim, Y. S. Wu, E. C. Kan, J. Fan, *Polymers* **2018**, *10*, 7.
- [526] S. Lee, W. Ko, Y. Oh, J. Lee, G. Baek, Y. Lee, J. Sohn, S. Cha, J. Kim, J. Park, J. Hong, *Nano Energy* **2015**, *12*, 410.
- [527] A. Y. Choi, C. J. Lee, J. Park, D. Kim, Y. T. Kim, *Sci. Rep.* **2017**, *7*, 45583.
- [528] A. Hazarika, B. K. Deka, C. Jeong, Y. B. Park, H. W. Park, *Adv. Funct. Mater.* **2019**, *29*, 1903144.
- [529] J. Chen, Y. Huang, N. Zhang, H. Zou, R. Liu, C. Tao, X. Fan, Z. L. Wang, *Nat. Energy* **2016**, *1*, 16138.
- [530] A. Levitt, J. Zhang, G. Dion, Y. Gogotsi, J. M. Razal, *Adv. Funct. Mater.* **2020**, *30*, 2000739.



Vanessa Sanchez is a Materials Science and Mechanical Engineering doctoral candidate at Harvard University, where she received her M.Sc. in 2020. She obtained her B.S. in Fiber Science from Cornell University in 2016 after studying Fashion Design at the Fashion Institute of Technology from 2011–2012. Her current research interests are new materials for smart textiles, knit structures for sensing and actuation, material-in-the-loop device design, and wearable soft robotics.



Conor J. Walsh is the Paul. A. Maeder Professor of Engineering and Applied Sciences at the Harvard John A. Paulson School of Engineering and Applied Sciences and an Adjunct Associate Professor in the Department of Physical Therapy and Athletic Training at BU. He received degrees in Mechanical and Manufacturing engineering from Trinity College in Dublin, Ireland, and M.S. and Ph.D. degrees in Mechanical Engineering from the MIT. He directs the Harvard Biodesign Lab, which brings together researchers from the engineering, industrial design, apparel, and clinical communities to develop disruptive soft wearable robotic technologies for augmenting and restoring human performance.



Robert J. Wood is the Charles River Professor in the Harvard John A. Paulson School of Engineering and Applied Sciences and a National Geographic Explorer. Wood completed his M.S. and Ph.D. in the Department of Electrical Engineering and Computer Sciences at the University of California, Berkeley. He founded the Harvard Microrobotics Lab which leverages expertise in multi-scale, multi-material fabrication for the development of biologically inspired, soft, and wearable robots. His research interests include new micro- and meso-scale manufacturing techniques, fluid mechanics of flapping wings, control of sensor-limited and computation-limited systems, active soft materials, wearable robots, and morphable soft robots.